REMOTE SENSING APPLICATION IN BIOMASS CROP PRODUCTION SYSTEMS IN OKLAHOMA

By

ANSERD JULIUS FOSTER

Bachelor of Science in Environmental Management
Systems
Louisiana State University
Baton Rouge, LA
2002

Master of Science in Agronomy
Louisiana State University
Baton Rouge, LA
2003

Submitted to the Faculty of the
Graduate College of the
Oklahoma State University
in partial fulfillment of
the requirements for
the Degree of
DOCTOR OF PHILOSOPHY
December, 2013

REMOTE SENSING APPLICATION IN BIOMASS

CROP PRODUCTION SYSTEMS IN OKLAHOMA

Dissertation Approved:

Vijaya Gopal Kakani

Dissertation Adviser

William Raun

Jagadeesh Mosali

Mark Gregory

.

ACKNOWLEDGEMENTS

First, I must give all the credit to my Lord and savior Jesus Christ for giving me the strength, knowledge and will to pursue and complete this degree program. I would also like to express my sincere appreciation to my mom, church family and friends that have given their prayers, time, knowledge, words of encouragement and experience towards the completion of this endeavor. Special appreciations are extended to Dr. Gopal Kakani my major advisor and Dr. Jagadeesh Mosali for granting me the opportunity to pursue my degree. I would also like to extend my appreciation to my committee members, Professors, Mark Gregory and William Raun for their willingness to serve and their valuable feedback and participation toward the completion of this dissertation. I also want to express my sincerest gratitude to Dr Jiangun Ge and the Geography Department at Oklahoma State (OSU) for the use of the Analytical Spectral Device (ASD). Special thanks to Jay Prater for his assistance in the field and most importantly for his willingness to share his knowledge and experiences in field work and life in general. Special thanks to Drs., Jeff Edwards, Brian Arnall, Daren Redfearn and Tyson Ochsner for their support and guidance. In addition, I express sincere appreciation to members of the bioenergy production team and student workers Alissa Fisher and Aryam Abraham for their assistance in data collection and sample analysis.

Name: ANSERD JULIUS FOSTER

Date of Degree: DECEMBER, 2013

Title of Study: REMOTE SENSING APPLICATION IN BIOMASS CROP PRODUCTION SYSTEMS IN OKLAHOMA

Major Field: CROP SCIENCE

Abstract:

This study was conducted to evaluate the combined effects of nitrogen and cropping systems on biomass yield and quality and to describe the spatial variation of biomass yield, soil carbon and nitrogen within a switchgrass field. Field plots at Stillwater and Woodward in Oklahoma consisting of five nitrogen treatments and three cropping systems were used for the nitrogen x cropping system study and an 8 ha switchgrass field at Chickasha, Oklahoma was used to describe the spatial variability at fine (2.5 m sampling distance) and coarse scale (10 m sampling distance). Remote sensing technique was used to monitor biomass yield and quality to better understand N requirement and usage for production. Semivariogram were used to evaluate spatial variability of the soil parameters and biomass yield. The results of this study showed that maximum yield was produced at both locations with less than 84 kg N ha^{-1} and high biomass sorghum has potential to produce biomass yield > 20 Mg ha^{-1} under normal conditions in Oklahoma. The study results also showed that perennial grass systems are more reliable sources of biomass yield, especially under adverse climatic conditions of Oklahoma. Final biomass yield of high biomass sorghum could be predicted using both broadband (aerial photograph) and narrowband (GreenSeeker) normalized difference vegetation index (NDVI) from July to close to harvest, while biomass yield in the perennial grass was best predicted during June to July. Comparing simple ratios and best narrowband indices with partial least square regression (PLSR) models suggested that while PLSR calibration models produced significantly lower error and higher r^2 for predicting biomass yield and N concentration within a growing season, the simple ratios and best narrowband indices were more stable and reliable when used for prediction across growing seasons. Spatial pattern in switchgrass field was described using both ground and aerial imagery. The NDVI computed from aerial imagery provided good precision at the fine scale in describing the spatial distribution of switchgrass yield. Remote sensing application in biomass production systems can greatly improve prediction models for predicting biomass yield and quality in feedstock materials with use of optimal hyperspectral narrowband.

TABLE OF CONTENTS

Chapter Page

LIST OF TABLES

Chapter II

Chapter III

Chapter IV

Table Page

Chapter V

Table Page

Chapter VI

LIST OF FIGURES

Chapter II

Chapter III

Figure Page

Chapter V

Figure Page

Chapter VI

CHAPTER I

INTRODUCTION

Background

Energy crops such as switchgrass (*Panicum virgatum* L.*)* and sorghum *(Sorghum bicolor* L.*)* have the potential to produce large quantity of biomass that is not currently available from forest land without disrupting the food supply. To develop such a biomass production system three important concepts, biomass yield, biomass quality and sustainable production or reliability, must be addressed. The challenges in developing sustainable biomass production systems are to characterize variation in biomass yield, quality and reliability in space and time to provide farmers with useful information for making management decisions. Recently, Wullschleger et al. (2010) identified growing season precipitation, annual temperature, N fertilizer and ecotype as the reasons for variation in biomass yield. In the Ozzano Dell'Emilia valley area in Spain, Di Virgilio et al. (2007) conducted a study using GIS and geostatistic methods to produce thematic maps of soil parameters and biomass yield to quantify the relationship between biomass yield spatial variation and soil parameters (nitrogen (N), phosphorous (P), soil moisture, soil texture and organic matter (OM)) in a small plot (5 ha) in 2004 and 2005. The maps produced from the study showed significant variability in the relationship between switchgrass biomass yield and nearly all the soil parameters. In the northern US location (Wisconsin), variation in switchgrass population for nine variables (biomass yield, survival, dry matter, lodging, maturity, plant height, holocellulose, lignin, and ash) was partly due to temperature and eco-region defined by soil type (Casler, 2005). Likewise, Schmer et al. (2010) reported switchgrass yield to vary across 10 locations in the Great Plains, North Dakota (Munich and Streeter), South Dakota (Bristol, Highmore, Huron and Ehtan) and Nebraska (Crofton, Atkinson, Douglas and Lawrence). Kiniry et al. (2005) simulating switchgrass yield using the ALMANAC (Agricultural Land Management Alternatives with Numerical Assessment Criteria) model for locations in three southern states, Texas (Dallas, Stephenville, and College Station), Arkansas (Hope) and Louisiana (Clinton) found that changing the runoff curve number used to determine potential runoff water from the soil by 15% increased the mean annual biomass from 1 to 31% depending on location. These findings suggest that weather factors are of paramount relevance for biomass yield variation.

Remote sensing, a process of acquiring information about an object by a device separated from it by some distance such as ground-based booms, aircraft, or satellite offers great opportunity for monitoring and providing information on variation in biomass yield, quality and reliability within a field and across fields. Barnes et al. (1996) outlined three applications for using remote sensing data in site specific agriculture. In the first application, multispectral images are used for detection of plant stresses (such as, pest, water stress and nutrient deficiency). In the second application, variation in spectral responses is correlated to specific variables such as soil properties. Once these site-specific relationships are developed, multispectral images can be translated directly to maps of fertilizer applications and yield variability. In the third application, multispectral data is converted to quantitative units such as vegetative indices (VIs) with physical meaning. Vegetation indices are computed as ratios, indices, and by forming linear combinations of spectral bands of two or more wavelengths (Jackson and Huete, 1991; Pinter et al., 2003). For example, the normalize difference vegetation index (NDVI), where red reflectance (R_{red}) and near-infrared reflectance (R_{nir}) are used (NDVI = $R_{nir} – R_{red}/ R_{nir} + R_{red}$) is a classic index that is widely used for modeling and estimation of crop biomass and N status. In addition to the use of VIs, few studies have explored the use of the full spectrum in estimating plant biomass [grasses and wheat, (Hansen and Schjoerring, 2003;Cho et al., 2007)], LAI [wheat (Hansen and Schjoerring, 2003)], N [wheat and rice, (Hansen and Schjoerring, 2003; Nguyen and Lee, 2006)] and chlorophyll [wheat, (Hansen and Schjoerring, 2003)] concentration using canopy reflectance measurements through partial least square regression (PLSR) methodology. These studies have also reported that PLSR improved the prediction of biomass yield and N concentration over that of the best vegetative indices. The VIs and full spectral canopy reflectance to assess crop yield potential for bioenergy crop production can play a significant role in providing reliable and consistent information about biomass yield and quality.

Aim

The overall aim of this research was to evaluate the potential of remote sensing applications to estimate variation in biomass yield and quality in different biomass crop production systems.

Objectives

The objectives of this dissertation are to:

1. Evaluate the effect of N fertilization on feedstock yield and quality of three bioenergy production systems.
2. Estimate biomass yield using narrowband and broadband NDVI collected at different times during the growing season.

3. Identify the optimal hyperspectral narrow-bands at leaf and canopy scale to discriminate N rates and to determine the ability of leaf and canopy scale hyperspectral reflectance data to discriminate N application rates.
4. Compare performance of PLSR (Partial Least Square Regression) and best narrow-band NDVI (Normalize difference vegetation index) linear regression models based on canopy hyperspectral reflectance data for predicting N concentration and end of season biomass yield in bioenergy crop production systems.
5. Estimate biomass composition (TN, ADF, NDF and ADL) in feedstock materials using linear regression of simple waveband ratios and PLS regression models with selected waveband approach.
6. Describe the spatial patterns of selected soil properties and biomass yield at fine and coarse scale in a switchgrass field to determine the appropriate sampling approach to enable the calculation of means with minimum variance.

REFERENCES

Barnes E.M., Moran M.S., Pinter J., P.J., Clarke T.R. 1996. Multispectral remote sensing and site-specific agriculture: Examples of current technology and future possibilities. pp. 843-854. *In* Proc. International Conference on Precision Agriculture, Minneapolis, MN. 23-26 June 1996. ASA-CSA-SSSA, Madison, WI.

Casler M. 2005. Ecotypic variation among switchgrass populations from the northern USA. Crop Science 45:388-398.

Cho M.A., Skidmore A., Corsi F., Van Wieren S.E., Sobhan I. 2007. Estimation of green grass/herb biomass from airborne hyperspectral imagery using spectral indices and partial least squares regression. International Journal of Applied Earth Observation and Geoinformation 9:414-424.

Di Virgilio N., Monti A., Venturi G. 2007. Spatial variability of switchgrass (*Panicum virgatum* L.) yield as related to soil parameters in a small field. Field Crops Research 101:232-239.

Hansen P., Schjoerring J. 2003. Reflectance measurement of canopy biomass and nitrogen status in wheat crops using normalized difference vegetation indices and partial least squares regression. Remote Sensing of Environment 86:542-553.

Jackson R.D., Huete A.R. 1991. Interpreting vegetation indices. Preventive Veterinary Medicine 11:185-200.

Kiniry J., Cassida K., Hussey M., Muir J., Ocumpaugh W., Read J., Reed R., Sanderson M., Venuto B., Williams J. 2005. Switchgrass simulation by the ALMANAC model at diverse sites in the southern US. Biomass and Bioenergy 29:419-425.

Nguyen H.T., Lee B.-W. 2006. Assessment of rice leaf growth and nitrogen status by hyperspectral canopy reflectance and partial least square regression. European Journal of Agronomy 24:349-356.

Pinter P.J., Hatfield J.L., Schepers J.S., Barnes E.M., Moran M.S., Daughtry C.S.T., Upchurch D.R. 2003. Remote sensing for crop management. Photogrammetric engineering and remote sensing 69:647-664.

Schmer M.R., Mitchell R.B., Vogel K.P., Schacht W.H., Marx D.B. 2010. Spatial and temporal effects on switchgrass stands and yield in the Great Plains. BioEnergy research 3:159-171.

Wullschleger S.D., Davis E.B., Borsuk M.E., Gunderson C.A., Lynd L.R. 2010. Biomass Production in Switchgrass across the United States: Database Description and Determinants of Yield. Agronomy Journal 102:1158-1168.

CHAPTER II

BIOMASS YIELD, QUALITY AND N RESPONSE OF THREE BIOENERGY CROP PRODUCTION SYSTEMS IN OKLAHOMA

ABSTRACT

Successful development of biofuels from feedstocks depends on the ability to produce high yields with acceptable quality using minimal inputs, particularly N fertilization. The objectives of this study were to evaluate the effect of N fertilization on feedstock yield and quality from three bioenergy production systems and to estimate biomass yield using narrowband and broadband NDVI collected a different times during the growing season. Variable biomass yield was generated by supplying N at different rates (winter legume (hairy vetch (*Vicia villosa* Roth) 2012 and crimson clover (*Trifolium incarnatum* L.) 2013), 0, 84,168, and 252 kg N ha^{-1}) in a field plot study at Stillwater, Oklahoma. Plots were planted with switchgrass "Alamo" (*Panicum, virgatum* L.), "ES 5200" high biomass sorghum (*Sorghum bicolor* L.) and mixed grasses ("Cheyenne" Indian grass (*Sorghastrum nutans* L.), "Kaw" big bluestem (*Andropogon gerardii* Vitman) and "Alamo" switchgrass) in a split plot design with three replications. Nitrogen was applied in the spring and biomass was harvested in fall after killing frost. . Biomass yield was a function of the environmental condition. The highest yields were achieved under normal condition in 2013. The high biomass sorghum producing 24 Mgha^{-1}, mixed grass 15.7 Mgha^{-1} at Stillwater and 6.8 Mgha^{-1} at Woodward and switchgrass 12.7 Mgha^{-1} at Stillwater and 7.2 Mgha^{-1} at Woodward. Applied N fertilizer significantly affect biomass yield in Woodward in

2012 and 2013, but combined with cropping system to affect yield at Stillwater in 2013. Feedstock cellulose and hemicellulose content varied with production system. Higher lignin, cellulose and hemicellulose content were observed in switchgrass and mixed grass systems, while high biomass sorghum had the highest N content in the biomass. Biomass yield of high biomass sorghum could be predicted with either narrowband (r^2=0.52) or broadband NDVI (r^2=0.60) spectral measurements collected early July. Predicting biomass yield in the perennial grasses was more challenging, but was best achieved with the narrowband NDVI when LAI was < 3. These results suggest that biomass yield and biomass quality were dependent on the crop species within the production systems.

INTRODUCTION

Successful development of a biofuels from feedstocks will be dependent on the ability to identify high yielding feedstock with acceptable quality (Xue et al., 2011). The US department of energy in the early 1990s identified switchgrass as the model bioenergy feedstock because of its high biomass yield and adaptability to diverse environmental conditions (McLaughlin and Walsh, 1998). Two other potential candidate feedstocks are mixed perennial grass systems and energy sorghum. Mixed grass systems have the potential to provide more stable long-term biomass yield (Jarchow and Liebman, 2012), while energy sorghum are annual crops with high water use efficiency, drought tolerance, low N requirement and very high biomass yield (Rooney et al., 2007; Maughan et al., 2012).

In the early years, studies of switchgrass focused on the use of the grass in mixed cropping systems with other native grasses. Studies and management of switchgrass in monoculture started in the 1970s (Balasko and Smith, 1971; Berg, 1971; Parrish, 2005). The monoculture production systems for switchgrass were largely for forage production, where the grass in general was either grazed or cut for hay. Similarly, energy production switchgrass is largely managed as monoculture (Sanderson et al., 1999; Muir et al., 2001; Vogel, 2002; Berdahl et al., 2005; Cassida et al., 2005). Several studies on switchgrass as a bioenergy feedstock were conducted across the USA including the Midwest (Vogel, 2002; Lemus, 2008; Kering et al., 2012), the south (Sanderson et al., 1999; Muir et al., 2001; Cassida et al., 2005) and northern great plains (Berdahl et al., 2005; Lee and Boe, 2005). These studies have concluded that switchgrass yield is dependent on the latitude of origin. Higher yields were observed in the lowland ecotype from southern latitudes in comparison to the cold tolerant upland ecotype from the northern latitudes. The enhanced ecosystem services (nutrient cycling, reduction in greenhouse gas emission and clean water) promoted to be provided by prairie vegetation has led to renewed interest of switchgrass mixed systems with other native grasses as an alternative bioenergy feedstock source (Tilman et al., 2006; Hill, 2007).

Prairies are native ecosystems comprising of four broad group of plants cool season (C_3) grasses, warm-season (C_4) grasses, leguminous forbs, and non-leguminous forbs (Kindscher and Wells, 1995; Craine et al., 2002). Increasing the dominance of warm season grasses has been reported to be correlated with increasing aboveground biomass (Adler et al., 2009; Jarchow et al., 2012) . In contrast, increasing the non-leguminous forbs was found to reduce the prairie biomass production (Kucharik et al., 2001). Jarchow and Liebman (2012) reported that fertilized and unfertilized mixtures of big bluestem (*Andropogon gerardi* Vitman), switchgrass (*Panicum virgatum* L.), and Indiangrass [*Sorghastrum nutans* (L.) Nash] produced as much total biomass as corn. They also found corn biomass yield to decrease over the 3-yr period of the study whereas yields of the fertilized grass mixtures were stable and the yield of the unfertilized mixtures increased to equal that of the fertilized.

Sorghum is a grass species that is widely dispersed throughout Africa, India and Australia (Price et al., 2005; Dillon et al., 2007). The recent genetic characterization of a regulatory system that modulates photoperiod sensitivity and flowering time in sorghum has led to the development of highly photoperiod sensitive, late flowering energy sorghum hybrids that exhibit long duration of vegetative growth and high biomass accumulation (Rooney et al., 2007). Therefore, for much of the Great Plains these varieties are unlikely to produce a head before a hard freeze kills the plant (Marsalis et al., 2010). These photoperiod sensitive energy sorghum have been reported to produced yields of 40 Mg DM ha^{-1} in a study at El Reno, OK (Venuto and Kindiger, 2008), 24.0

Mg DM ha^{-1} in Bushland, TX (McCollum et al., 2005), 35.1 Mg DM ha^{-1} in College Station, TX (Miller and McBee, 1993) and 30.1 Mg DM ha^{-1}in Illinois (Maughan et al., 2012).

Management practices for bioenergy production include fertilization in spring and annual harvest at the end of the growing season. It is well documented that perennial grasses remobilize nutrients from the aboveground materials, thus nutrient removal is dependent on the harvest timing. It is recommended that harvesting perennial grasses in the early winter after a killing frost reduces mineral concentrations in biomass producing a more desirable feedstock for direct combustion and thermochemical conversion systems and optimizes biomass yields and stand (Adler et al., 2006; Sanderson et al., 2006; Mitchell et al., 2008; Heaton et al., 2010; Guretzky et al., 2011). Studies evaluating N fertilization in bioenergy production systems for biomass have produced varied results, partly due to difference in management practices and site to site variation. Numerous studies were conducted or currently ongoing to evaluate N response in bioenergy crops, switchgrass (Vogel, 2002; Thomason, 2004; Lemus, 2008; Kering et al., 2012) and most recently in biomass sorghum (Marsalis et al., 2010; Maughan et al., 2012) and mixed grasses (Jarchow et al., 2012). In switchgrass studies, highest yields were obtained with varied rate of N fertilizer. For example, Lemus et al. (2008) obtained the highest yield with 112 kg N ha^{-1} in Iowa, Vogel et al. (2002) with 120 kg N ha^{-1} in Nebraska and Thomason et al. (2004) with 448 kg N ha^{-1} in Oklahoma. In biomass sorghum, the highest yields were reported with 224 kg N ha^{-1} (Maughan et al., 2012) in Illinois and 108 kg N ha^{-1} in Texas under limited irrigation (Tamang et al., 2011). Few studies have evaluated the effect of N fertilization on warm season mixtures for bioenergy. Jarchow and Liebman (2012) reported that fertilization increased yield of mixtures over unfertilized, but became more similar to the unfertilized over time.

Nitrogen fertilization of bioenergy crops not only affects the yield, but also biofuel quality. Studies have reported that with increasing N applied, cellulose, lignin and nitrogen content increased, while hemicellulose and ash content decreased (Lemus, 2008; Waramit et al., 2011). Biomass that has high lignin and cellulose and low N content is considered to be more suitable for co-firing, while high cellulose, N content and non-structural carbohydrate content (sugar and starches) is desirable for biofuel production using microbial and enzymatic conversion (Sanderson et al., 1996; Labbé et al., 2008). The nutrient content and energy density and other bioenergy related quality characteristics vary widely among biomass feedstock source (Cherney et al., 1988; Sanderson et al., 1996; Labbé et al., 2008; Lemus, 2008; Pauly and Keegstra, 2008; Waramit et al., 2011).

The cost of nitrogen fertilization, which is one of the most unsettling concerns for farmers, is guaranteed to play a major in the decision to include bioenergy crops into their conventional system. Information on nitrogen fertilization recommendation for bioenergy crops such as switchgrass and sorghum is useful to aid farmers' decision. Tradition approach for determining N recommendation involves soil sampling obtained before planting, pre-plant soil testing, or early spring in the case of perennial grasses. In most cropping systems, growing condition and soil N levels are dynamic and are generally not accounted for when making recommendation based on pre-plant soil testing and early season sampling. In season monitoring of the plant N status can provide information about the soil N status with regards to the current growing condition that could guide N management decision improving the precision of N recommendation. Several studies have reported success from using sensor based technology that measures plant reflectance to accurately predict crop physiological variables such as above ground forage biomass (Tucker, 1979; Mutanga and Skidmore, 2004; Fava et al., 2009; Numata,

2012) and plant N status (Hansen and Schjoerring, 2003; Xue et al., 2004; Zhu et al., 2007; Yao et al., 2010; Foster et al., 2012).

Vegetation indices (VIs) are computed from mathematical combination of wavebands in different region in the spectrum to minimize the influence on solar irradiance, canopy architecture and soil background in the measurement of plant reflectance information (Haboudane et al., 2002; Pinter et al., 2003; Zarco-Tejada et al., 2004; Hatfield et al., 2008). The most commonly used vegetation index is the normalize difference index (NDVI). The NDVI defined as (R_{NIR}–R_{RED}/R_{NIR}+R_{RED}) takes advantage of reflectance in both NIR and red region reducing measurement variability due to soil type, sunlight intensity and angle of sunlight incidence (Lusch, 1999). The NDVI has been reported to be strongly correlated with biomass when the leaf area index (LAI) is less than 3 (Weiser et al., 1986; Serrano et al., 2000; Flynn et al., 2008). The NDVI can be computed either using broad wavebands (50-100 nm scale) from the Landsat Thematic mapper satellite using the TM-spectrometer ™, or narrow wavebands (<10 nm scale) from field-based spectroradiometers such as GreenSeeker, ASD, and crop scan. In principle, vegetation index computed from average spectral information over broad waveband widths results in loss of critical information available in specific narrow wavebands (Blackburn, 1998; Thenkabail et al., 2000).

The objectives of this field study were to evaluate the effects of N fertilization on biomass yield and quality and to compare biomass yield prediction model of narrowband NDVI and broadband NDVI.

MATERIALS AND METHODS

Study Locations and Experimental Design

The experiment was carried out at two research sites in Oklahoma from 2010 through 2012. One location was at the USDA rangeland research facility in the city of Woodward (36.42˚N, 99.414˚W) and the other at the Oklahoma State Agronomy Farm Research facility (EFAW) (36.130˚N, 97.104˚W). At both locations, pure grass stands of switchgrass ‘Alamo”, a mixture of big bluestem, Indiangrass and switchgrass in a 50-25-25 mix and high biomass sorghum was seeded using a no-till drill planter. Switchgrass was seeded at a rate of 3.5 kg ha^{-1} pure live seed, sorghum at 8.5 kg ha^{-1} pure live seeds and mixture at 3.5 kg ha^{-1} pure live seed. Stand appraisal using visual observation was done in April in Stillwater and May in Woodward in 2011, 2012 and 2013. The experimental design was a split block randomized design with three replications at each location. Each replication included five plots randomly assigned to nitrogen fertility treatments of 0, 84, 168, and 252 $kgNha^{-1}$ applied to generate varying yield potential. In the split plot design, species was the main plot and fertilizer treatment was the subplot. The site characteristics and management practices performed are summarized in Table 2.1. No fertilizer was applied in the establishment year of 2010. Nitrogen was applied as UAN on 4 June 2011 in energy sorghum and perennial grasses and on April 2012 in perennial grasses and June 2012 in energy sorghum. Sevin (Carbaryl [1-naphthyl N-methylcarbamate]) was applied for grasshopper control at the Stillwater location. Plots were 9 m wide and 9 m long at Stillwater and 7.6 m wide and 9 m long at Woodward. Soil samples were collected from each plot before fertilization at both Stillwater and Woodward sites in the 2012 and 2013 growing seasons. Soil fertility characteristics are summarized in Table 2.2.

Field Data Collection

Biomass Yield

Plots were harvested for total seasonal yield after the first killing frost. Table 2.1 summarizes the harvest date and area for the two sites. Plots were cut to stubble height of 10-15cm with a John Deere 630 moco pull type swather (Deere and Company, Moline, IL, USA) and baled with a John Deere 568 round baler (Deere and Company, Moline, IL, USA) into round bales which were individual weighed at Stillwater. At Woodward, each plot was harvested with a swift machine forage harvester (Swift Current, Saskatchewan, Canada). Subsamples from each N treatment were collected weighted and dried for dry matter and quality determination.

Canopy NDVI

Color aerial photographs of the entire experimental plots (Fig 2.1) were taken from an airplane on cloud free days at both Stillwater and Woodward locations. The digitized and geo-reference images were provided by Geovantage (Peabody, MA, USA). The NDVI was computed for each image using the raster calculator in ArcGIS (ESRI). Mean NDVI was estimated for each plot by overlaying the plot boundaries and averaging the NDVI for each pixel within the plot boundary. Canopy NDVI readings were also collected using a GreenSeeker (Ukiah, CA) NDVI hand unit from an area of about 3 to 4 m^2 by holding sensor approximately 0.6-1.0 m above the canopy and walking at the same speed in each plot. Table 2.3 summarizes the sampling dates for NDVI measurements from aerial photograph and GreenSeeker sensor at both locations. The GreenSeeker handheld optical reflectance sensor uses active radiation from red (650 ± 10 nm) and near infrared (770 ± 15 nm) band independent of solar radiations

(Freeman et al., 2007). The device uses built-in software to calculate NDVI directly. The NDVI is computed according to the formula.

$$\text{NDVI} = \frac{\rho\text{NIR} - \rho\text{Red}}{\rho\text{NIR} + \rho\text{Red}} \qquad 1$$

Where: ρNIR is the fraction of emitted NIR radiation returned from the sensed area (reflectance)/ or NIR band in photograph, and ρRed is the fraction of emitted red radiation returned from the sensed area (reflectance)/ red band in photograph. The GreenSeeker NDVI is referred to as a narrowband NDVI as it is computed using average of less than fifty (< 50 nm) wavebands, while the aerial photograph is referred to as a broadband NDVI as it is computed using wavebands average across greater than fifty (> 50 nm) wavebands. Throughout this paper the GreenSeeker NDVI will be referred to as narrowband NDVI and the aerial photograph NDVI as broadband NDVI.

Leaf Area Index

Leaf area index readings were taken about the center point of the plots with the Li-Cor LAI 2000 leaf canopy analyzer. Average LAI was determined by the leaf canopy analyzer through measuring the light attenuation difference between the three above canopy and nine below canopy readings. The differences in light attenuation resulted from either the absorption or reflection of incident light by the vegetation. Using the attenuation values obtained, a standard attenuation coefficient was used automatically within the instrument to derive an output resulting in LAI value (Harmoney et al., 1997).

Biomass Quality Analysis

The biomass quality was determine by measuring concentrations of the cell wall constituents, neutral detergent fiber (NDF), acid detergent fiber (ADF), acid detergent lignin (ADL), and total nitrogen (TN) content. In 2011, the NDF, ADF, and ADL measurements were determined based on wet chemistry and total N content with the combustion method using a Leco elemental analyzer (Leco TruSpec CHN, St. Joseph, MI, USA). Regression equations developed using the 2011 season data based on near-infra-red spectroscopy calibration with the laboratory measurement were used to estimate the TN, ADF, NDF, and ADL in the 2012 and 2013 seasons (Foster et al., 2013). Samples were scanned using an Analytical Spectral Device (ASD) with spectral range of 350 -2500 nm. Hemicellulose was calculated as NDF-ADF and cellulose as ADF-ADL. Validation was performed for each biomass quality parameter with an independent dataset for the 2012 (TN: r^2 =0.84 and RMSE = 0.30 %; NDF: r^2 =0.10 and RMSE = 4.0 %; ADF: r^2 =0.12 and RMSE = 3.5 %; and ADL: r^2 =0.23 and RMSE = 1.0 %) and 2013 (TN: r^2 =0.95 and RMSE = 0.20 %; NDF: r^2 =0.48 and RMSE = 5.3 %; ADF: r^2 =0.41 and RMSE = 6.2 %; and ADL: r^2 =0.40 and RMSE = 1.3 %).

Statistical Analysis

The data was analyzed separately for each location and year using a split plot design with species as the whole plot and N rates as the subplot. The PROC GLM procedure in SAS (SAS, 2009) was performed to determine the main effects and interactions of N rate and species. Significance was determined at the $p < 0.05$ level. The PDIFF feature of the LSMEANS procedure was used to compare means. Analysis using the GLM model procedure was also conducted to determine main effects and interactions of N rate and species on biomass quality (hemicellulose, cellulose and TN). Single degree of freedom contrast was used to test linear and quadratic effects of N rate on biomass yield and quality parameters. Regression analysis was performed using PROC REG procedure to determine the relationship between in-season narrowband NDVI and broadband and harvestable biomass. All regression analysis was performed separately for the perennial grasses at Woodward and for the perennial grasses and high biomass sorghum at Stillwater.

RESULTS

Growing Condition

The growing condition for Woodward and Stillwater from 2010-2013 was dominantly dry with all four years reporting precipitation lower than the 30 year average and a 1-5 °C higher average temperature throughout the growing seasons (Table 2.4). Precipitation was on average slightly above the 30-year average in the 2010 growing season, but was below for the other three growing seasons (16-56%). The 2012 season had above normal precipitation in March and April, but was dry for the period of May to July. Precipitation was above normal for the months of April, May and July at Stillwater and for July and August at Woodard in the 2013 season. Warmer temperature during March of 2012 resulted in the perennial grasses breaking dormancy and growth started in late March. In contrast, cooler temperatures in the 2011 and 2013 seasons in March result in perennial grasses breaking dormancy and starting growth in April. In general, growing conditions during the months of May, June and July for the 2011 and 2012 seasons were below normal precipitation (>50%) and 1-5˚C above normal temperature. The growing conditions of the 2010 and 2013 seasons were with slightly above to normal precipitation and 1-2˚C below the normal temperature.

Satisfactory stands were maintained at both locations in the perennial grass systems for the three seasons data was collected based on annual visual appraisals. Dry condition affected biomass production throughout the three production seasons reported within this paper. At the Stillwater location, biomass yields were not only restricted by drought, but were also reduced due to grasshopper infestation in July of the 2011 season. Perennial grass systems were more severely affected by the grasshopper that reduced yield by upwards of 40-50%. At the Woodward location, dry condition affected crop growth more severely compared to Stillwater. Hence, no harvestable biomass was obtained for the high biomass sorghum for both the 2011 and 2012 season at Woodward. To address the challenge of weather condition and grasshopper infestation that occurred in 2011 management practices for the subsequent years included fertilizing of perennial grass at or within weeks after greening up and earlier planting of sorghum and a July spraying of sevin insecticide (at Stillwater) for grasshopper control (Table 2.1). The goal of the earlier planting (sorghum) and fertilizing (switchgrass and sorghum) was to maximize growth under the cool and moist condition in the months of May and June.

Biomass Yield

Stillwater

The biomass yield obtained during each growing season was a function of the growing environment. The 2011 growing season was the second year of establishment for switchgrass. Biomass yield of 2011 growing season was independently affected by the nitrogen treatments (P=0.03). Whereby, the highest yield (5.5 Mg ha^{-1}) was achieved without fertilizer, but it was not significantly different from applied N fertilizer rates of 84 and 168 kg N ha^{-1} (Table 2.5). In contrast, application of 252 kg N ha^{-1} was over 2 Mg ha^{-1} lower than the yield achieved without fertilizer. Cropping system and the combined effect of N treatment and cropping system did not affect the biomass yield. Moreover, the CV value greater than 30 is an indication of the variation in the stand density. The perennial grasses were significantly affected by grasshopper in late July which affected the stand density. In subsequent years sevin insecticide was applied in late July to control the grasshoppers.

In the 2012 growing season, cropping system, nitrogen treatment did not affect the biomass yield independently or in combination (Table 2.5). The average dry matter yield of 2012 (7.3 Mg ha^{-1}) more than doubled that of the 2011 (2.4 Mg ha^{-1}) season. In the 2013 growing season, cropping system and N treatment combined to affect the biomass yield (Table 2.5). The highest biomass yield was produced by the high biomass sorghum with the 84 kg N ha^{-1}, but did not differ from the 252 kg N ha^{-1}. The highest switchgrass yield was achieved from the 252 kg N ha^{-1} and mixed grass from the 168 kg N ha^{-1}, but was the same as that of the 84 kg N ha^{-1} for both cropping system (Fig 2.2). High biomass sorghum was more productive compared to the switchgrass and mixed grass, producing the same amount of biomass for the legume and unfertilized to that of the heavily fertilized switchgrass and mixed grass systems. Likewise, the unfertilized mixed grass system produced more biomass than the heavily fertilized mixed grass system. In switchgrass, biomass yield of the fertilized (168 kg N ha^{-1}= 13 Mg ha^{-1}) was not significantly different from that of the legume treatment (12 Mg ha^{-1}), but differed from the 84 kg N ha^{-1} (16 Mg ha^{-1}) and the 252 kg N ha^{-1}(16 Mg ha^{-1}). Soil N concentration before fertilization did not significantly affect the biomass yield (Table 2.2). Therefore, these results indicate that applied N increased biomass compared to the unfertilized, particularly in the monoculture crop production systems.

Woodward

The dry and hot condition was more severe in Woodward than in Stillwater for both the 2011 and 2012 growing seasons. The condition was so severe that the high biomass sorghum crop failed in both seasons at this location. While growing condition was adequate in the 2013 season the high biomass sorghum with applied N was severely lodged that it was impossible to harvest the biomass. Therefore, no harvestable biomass yield for the high biomass sorghum will be reported for Woodward in this study. The perennial grass system was also affected by the environmental condition, but was more robust and produced harvestable biomass in all three years of the study. In the 2011 season the second year after establishment, biomass yield was not affected by cropping system, N treatment or the combined effect (Table 2.5). Application of N increased biomass yield in the 2012 and 2013 seasons compared to the legume and unfertilized (Table 2.5), but was similar for all three rates of applied N. Biomass yield of 2013 approximately doubled that of the 2012 season. However, in 2012 the 84 kg N ha^{-1} was similar to the unfertilized and again was similar to the legume treatment in 2013. Cropping system and the combine effect of N treatment and cropping system did not affect the biomass yield. Likewise, soil N concentration before fertilization did not affect biomass yield (Table 2.2).

Biomass Quality

Stillwater

Cell wall components, cellulose, hemicellulose, and lignin, were found to be very stable across the years, but N concentration varied from year to year. High biomass sorghum consistently had lower hemicellulose, cellulose and lignin concentration in the biomass compared to the perennial grass systems (Table 2.6). Nitrogen concentration in the biomass increased with increased rate of N application, but N concentration was similar with 252 and 168 kg N ha^{-1}, 168 and 84 kg N ha^{-1}, and with 84 kg N ha^{-1}, legume and unfertilized in the 2011 season (Table 2.6). In the 2012 season, N concentration in the biomass was not affected by the applied N. These results indicate that in a high yielding environment applied N seems to have less effect on increasing biomass N concentration.

Woodward

Similar to Stillwater, cell wall component was stable across years, but N concentration varied. Hemicellulose, cellulose and lignin concentrations in biomass were similar for switchgrass and mixed grass system (Table 2.6). Variation in these cell wall components from year to year was less than 5%. Statistical significance was observed for the cellulose concentration in the mixed grass and switchgrass in 2013, but this difference was not of practical significance (about 1%). Likewise, applied N of 252 kg N ha^{-1} resulted in a 1% lower hemicellulose concentration compared to the other N treatments. Nitrogen concentration was greater with applied N than the legume treatment, but surprisingly was similar to the unfertilized in the 2011 season. However, in the 2012 season N concentration again was greater with the applied N, but significantly higher than the legume and unfertilized treatments. So clearly, applied N increased N concentration in the biomass compared to the unfertilized, but applying greater than the 82 kg N ha^{-1} offered no benefit with respect to increasing biomass N concentration.

Nitrogen Response

Biomass yield did not respond to the applied N fertilizer at either location in 2011, but did respond to applied N at Woodward in 2012 and 2013 and at Stillwater in 2013 (Table 2.5). A quadratic relationship described the response to N at Woodward in 2012 ($P < 0.05$) and 2013 ($P < 0.001$). Nitrogen response at Stillwater was linear for the high biomass sorghum ($P<0.01$)

and switchgrass ($P<0.01$). In Woodward, biomass yield increased up to 168 kg N ha^{-1}, while in Stillwater applied N increased biomass yield up to 252 kg N ha^{-1}. However, the increase in biomass with greater than the 84 kgNha^{-1} was not significant.

The response of N concentration in biomass to the applied N rates could be explained by a linear relationship in 2011 at Stillwater and in 2013 at both locations, but no relationship was observed in 2012 (Table 2.6).

Estimating Biomass yield

A moderately strong relationship (r^2=0.65) was observed between the 2 July narrowband and broadband NDVI readings for the perennial grasses and a strong correlation (r^2 = 0.95) for the high biomass sorghum (Fig 2.3) at the Stillwater location. At Woodward, narrowband and broadband were strongly correlated (r^2 =0.70 - 0.85) across all three sampling periods. Figure 2 shows the relationship between the narrowband and broadband NDVI for the 26 August and 8 September sampling, respectively. Prediction model for biomass yield was similar for the narrowband and broadband NDVI in perennial grass system at Stillwater at the 2 July sampling date (Table 2.7). Prediction of perennial grass biomass yield using the narrowband NDVI collected on 21 June (r^2=0.38) and 2 July (r^2=0.43) reported similar r^2 to that of the broadband NDVI on 8 September (r^2=0.37). In high biomass sorghum, broadband NDVI was more strongly correlated (r^2=0.60-0.73) with biomass yield closer to harvest, but similar prediction was observed for the narrowband and broadband NDVI for the July sampling date (Table 2.7). At Woodward, biomass prediction models using the broadband NDVI were stable with r^2=0.42, 0.40 and 0.45 for the 2 July, 11 August and 8 September sampling dates, respectively. In contrast, model predictability increased for narrowband NDVI with sampling date of 23 June, 24 July and 24 August with r^2 of 0.25, 0.55 and 0.61, respectively.

DISCUSSION

Biomass Yield

Biomass yield, quality and reliability or persistence are three concepts that are important to the development of a successful bioenergy feedstock production system. This study was conducted over three years with contrasting environmental conditions that greatly influenced these three concepts in relation to the bioenergy production systems and management. In each year of the study, biomass yield at the Stillwater location almost doubled that of Woodward location for the perennial grasses. One difference between these two sites is the amount of precipitation (Table 2.4). Clearly, the amount of biomass yield produced at each sites is related to the amount of precipitation. Wullschleger et al., (2010) also reported switchgrass yield to vary due to temperature and precipitation. They observed yield to increase with increase temperature up to a point and then decrease and lower yield with low precipitation during the growing season. Precipitation is the only one factor contributing to soil available moisture and thus the timing and size of rainfall event during critical portion of the growing season is most important for high biomass yield production (Sanderson et al., 1999; Wullschleger et al., 2010). In this study, the highest yields (6-25 Mg ha^{-1}) were produced in 2013 followed by 2012(2-8 Mg ha^{-1}) and 2011 (1-3 Mg ha^{-1}). The 2011 and 2012 growing seasons received less than 50% of the 30 year average season during the critical growing periods of April to September, with exception of April of 2012 in Woodward (Table 2.4). In both these years, June and July were extremely dry and hot with temperatures 2-3 ˚C above normal. In contrast, 2013 received above normal precipitation during the period of March-August and cool temperature 1-2 ˚C below normal. Clearly, high yields were associated with high precipitation in April to August in combination with cool temperature. Likewise, Sanderson et al. (1999) also reported an association of high switchgrass yield with years of high precipitation in April to September at five locations in east Texas, and Muir et al. (2001) also correlated yield with March to August precipitation at Stephenville, TX.

Harvestable biomass from the high biomass sorghum was unsuccessful at Woodward in all three years of the study. Extreme dry condition during the May to June period of 2011 and 2012 resulted in total failure in establishment, while favorable growth condition led to extreme lodging of more than 90% in each plot, except for the unfertilized and legume treatments in 2013.

Management in terms of N fertilization and cropping systems also plays a role in the productivity of these systems. Greater response to N fertilization was observed in the drier location in Woodward. A quadratic response to the applied N was found in Woodward in both 2012 and 2013, whereby biomass yield increased with application of N up to the 168 kg N ha^{-1} and then decrease with addition N application.

In Stillwater, N application did not affect biomass yield in 2011 and 2012, but interacted with cropping system to affect the biomass yield in 2013. In 2011, N treatment significantly affected the biomass yield, whereby the unfertilized treatment produced significantly higher biomass yield that the highest applied fertilized rate. This is a confirmation of the extreme dry condition during the 2011season and not necessarily an indication of the N response within the production systems. In 2012, N application did produce more biomass compared to the unfertilized, but the difference was not significant. With favorable condition for crop growth in 2013, N treatments and cropping systems interacted to affect biomass yield. The highest biomass yield (32.7 Mg ha^{-1}) was produced by the high biomass sorghum fertilized with the 84 $kgNha^{-1}$. Similarly, highest switchgrass yield (16 Mg ha^{-1}) was obtained with 252 kg N ha^{-1}, but did not differ significantly ($P < 0.05$) from the 16Mg ha^{-1} obtained with the 84 kg N ha^{-1}. Mixed grass yield was highest with the 168 kg N ha^{-1}, but again did not differ from the 15 Mg ha^{-1} obtained with the 84 kg N ha^{-1}. In the high biomass sorghum and switchgrass production systems, biomass yield was significantly higher with applied N compared to the unfertilized, but biomass from applied N was similar to the unfertilized and legume treatment in the mixed grass system (Fig 2.2). These results contradict the finding of Griffith et al. (2011) for the perennial grasses that unfertilized C_4 grass monocultures produced more harvestable biomass than unfertilized mixtures containing multiple functional groups, but regarding the perennial verses the annual these results confirm Griffith et al. (2011) findings. Likewise, the non-responsiveness to N fertilizer in the mixed grass system was also reported by with Jaschow and Liebman (2012). Biomass yield is an important attribute for any production system, and no doubt that the right cropping system that is capable of producing high yield is essential for success. These results demonstrate that precipitation is a key factor that influences biomass yield. Benefits of high biomass yield from management variables such as N fertilization and cropping systems were also found to be dependent on environmental factor such as precipitation and temperature. The high biomass sorghum has potential for producing large amount of biomass yield with minimal amount of N fertilizer under favorable condition. However, failure in Woodward in 2011 and 2012 and similar productivity to the perennial grass systems in adverse condition at Stillwater are strong indications for concerns in terms of reliability.

Biomass Quality

The second concept of biomass quality is important, particularly because the conversion of biomass to bioenergy is dependent on the material composition. Biomass materials that are high in lignin and cellulose and low in N concentration are considered more desirable for thermochemical conversion, while those with high cellulose, N concentration and non-structural carbohydrate content (sugar and starches) are suitable for biofuel production using microbial and enzymatic conversion (Sanderson et al., 1996; Labbé et al., 2008). Nitrogen is an important nutrient for plant growth and biomass production, but high N concentration in biomass can inhibit deoxygenation activity in the catalytic pyrolysis conversion process (Wilson et al., 2013). According to Wilson et al. (2012) high N content in feedstock is one of the many challenges to overcome with upgrading conversion technologies. Nitrogen concentration of biomass was not affected by applied N at Stillwater in 2012, but did in 2011. In 2011, biomass yield with applied N was similar to the unfertilized and legume treatment. This was attributed to the severe dry condition during the growing season. At Woodward, N concentration did not differ among the applied N rates from 2011 to 2013. Overall, N concentration increased with applied N compared to the unfertilized, but increased fertilizer rate did not significantly increase N concentration in the biomass These results were contrary to those reported by Lemus et al. (2008) that found increased in N concentration in switchgrass with increased rate of N in Iowa.

Cellulose, hemicellulose and lignin were not affected by N treatments at either location. Biomass quality was more affected by the cropping systems. Higher N concentration and lower lignin, hemicellulose and cellulose were observed in the high biomass sorghum compared to the perennial grasses. Moreover, quality parameters such as lignin, cellulose and hemicellulose were fairly stable from year to year for each cropping system. For the perennial grasses, biomass quality varied by about 5% for the mixed grasses and switchgrass throughout the entire period of the study. The low N concentration <3% (Kumar et al., 2009) and small variability in lignin, hemicellulose and cellulose due to management are strong indications that these material are suitable for conversion to biofuel using the thermochemical conversion approach.

Estimating Biomass Yield

To effectively plan year round operation for bio-refineries, efficient and reliable methods for estimating harvestable biomass are warranted. Profitability of these refineries will be dependent on the ability to maintain a reliable supply of feedstock material (Schmer et al., 2010). In this study, biomass yield prediction models using plant reflectance measurement from a hand held GreenSeeker sensor (narrowband NDVI) and aerial photograph (broadband NDVI) were compared. GreenSeeker measurements were obtained early in the season while aerial photograph were obtained late in the seasons (Table 2.4). Because GreenSeeker will need to be attached to tractor for large scale operations, measurements were collected early and frequently during the season. To minimize cost and maximize benefits, aerial photographs were collected late in the season at the time of greatest potential for estimating the final harvestable biomass yield. The goal was to provide producers as well as refineries with realistic options for in season estimation of biomass yield. Strong correlation ($r^2 > 0.6$) was observed between the narrowband and broadband NDVI for the 2 July sampling date for the Stillwater and for all three sampling period at Woodward. The strong correlation observed was attributed to the lower LAI at sampling for Stillwater and Woodward. Leaf area index for Stillwater was below 4 for the perennial grasses and below 3 for the high biomass sorghum during the 2 July sampling, but increased for the subsequent sampling to >4 in the perennial grass system. At Woodward, LAI remained below 3.5 for the entire sampling period. It is well documented that NDVI saturate at high biomass or LAI in several studies (Tucker, 1979; Mutanga and Skidmore, 2004). According to (Kumar et al., 2002) the reason for the saturation problem is that LAI greater than 3 (>3) the amount of red light at about 600-680 nm that can be absorbed by leaves reaches a peak while NIR reflectance continues to increase due to multiple scattering effects. The disparity between the red adsorption and NIR reflectance results in slight change in the NDVI and the result is a poor relationship with biomass (Mutanga and Skidmore, 2004; Cho et al., 2007). Therefore, the strongest relationship between biomass yields and the narrowband or broadband NDVI occurred during sampling times when LAI was on average below 3.5. In addition, biomass prediction in perennial grass systems are more challenging compared to the annual biomass sorghum, because of the high vegetation density and the presence of non-photosynthetic vegetation that masks spectral responses in the red and NIR (Numata, 2012). Therefore, the ability to better predict the biomass in the high biomass sorghum was not surprising.

In field variability is an important criterion in comparing the prediction models of the two NDVI sources. The GreenSeeker sampling area is a subset of the entire plot compared to the entire plot area captured by the aerial photograph. Therefore, variation between the narrowband and broadband NDVI could also be attributed to inherent plot variability. However, at large scale where multiple GreenSeeker sensors could be mounted on a tractor to increase coverage area to of the aerial photograph, reducing the inherent plot variability.

CONCLUSIONS

Minimal N fertilizer (< 84 kg N ha^{-1}) is required by these bioenergy crop production systems to produce maximum biomass yield, but the perennial grasses may be more reliable sources of biomass, particularly in dry conditions. Biomass quality differed between the high biomass sorghum and perennial grass systems. The high biomass sorghum had higher N and lower lignin, hemicellulose and cellulose concentration compared to the perennial grasses. Cell wall components such as lignin, cellulose and hemicellulose were not affected by management, but N concentration in biomass increased with applied N compared to the unfertilized and legume treatments. But, N concentration did not differed among the applied N treatments.

In general, narrowband NDVI has been reported to improve biomass prediction, however the results of this study indicates that biomass prediction was similar for narrowband and broadband NDVI, but was greatly affected by the cropping system. Narrowband and broadband NDVI performed poorly in perennial grass systems with LAI >3, but narrowband performed better at LAI (2-3). In high biomass sorghum, narrowband and broadband performed similarly for measurements collected at the same time. Early July sample was found to appropriate for collecting spectral reflectance of high biomass sorghum using the GreenSeeker or aerial photograph, while NDVI was only appropriate for estimating biomass in perennial grasses with LAI < 3. However, spectral reflectance of high biomass sorghum using aerial photograph could be collected as late as September.

REFERENCES

Adler P.R., Sanderson M.A., Weimer P.J., Vogel K.P. 2009. Plant species composition and biofuel yields of conservation grasslands. Ecological Applications 19:2202-2209.

Adler P.R., Sanderson M.A., Boateng A.A., Weimer P.I., Jung H.J.G. 2006. Biomass yield and biofuel quality of switchgrass harvested in fall or spring. Agronomy Journal 98:1518-1525.

Balasko J., Smith D. 1971. Influence of temperature and nitrogen fertilization on the growth and composition of switchgrass (*Panicum virgatum* L.) and timothy (*Phleum pratense* L.) at anthesis. Agronomy Journal 63:853-857.

Berdahl J.D., Frank A.B., Krupinsky J.M., Carr P.M., Hanson J.D., Johnson H.A. 2005. Biomass yield, phenology, and survival of diverse switchgrass cultivars and experimental strains in western North Dakota. Agronomy Journal 97:549-555.

Berg C. 1971. Forage yield of switchgrass (*Panicum virgatum*) in Pennsylvania. Agronomy Journal 63:785-786.

Blackburn G.A. 1998. Quantifying chlorophylls and caroteniods at leaf and canopy scales: An evaluation of some hyperspectral approaches. Remote Sensing of Environment 66:273-285.

Cassida K.A., Muir J.P., Hussey M.A., Read J.C., Venuto B.C., Ocumpaugh W.R. 2005. Biomass Yield and Stand Characteristics of Switchgrass in South Central U.S. Environments. Crop Sci. 45:673-681.

Cherney J.H., Axtell J.D., Hassen M.M., Anliker K.S. 1988. Forage Quality Characterization of a Chemically Induced Brown-Midrib Mutant in Pearl Millet. Crop Sci. 28:783-787.

Cho M.A., Skidmore A., Corsi F., Van Wieren S.E., Sobhan I. 2007. Estimation of green grass/herb biomass from airborne hyperspectral imagery using spectral indices and partial least squares regression. International Journal of Applied Earth Observation and Geoinformation 9:414-424.

Craine J., Tilman D., Wedin D., Reich P., Tjoelker M., Knops J. 2002. Functional traits, productivity and effects on nitrogen cycling of 33 grassland species. Functional Ecology 16:563-574.

Dillon S.L., Shapter F.M., Henry R.J., Cordeiro G., Izquierdo L., Lee L.S. 2007. Domestication to crop improvement: genetic resources for Sorghum and Saccharum (Andropogoneae). Annals of Botany 100:975-989.

Fava F., Colombo R., Bocchi S., Meroni M., Sitzia M., Fois N., Zucca C. 2009. Identification of hyperspectral vegetation indices for Mediterranean pasture characterization. International Journal of Applied Earth Observation and Geoinformation 11:233-243.

Flynn E.S., Dougherty C.T., Wendroth O. 2008. Assessment Of Pasture Biomass With The Normalized Difference Vegetation Index From Active Ground-based Sensors. Agron. J. 100:114-121.

Foster A.J., Kakani V.G., Ge J., Mosali J. 2012. Discrimination of Switchgrass Cultivars and Nitrogen Treatments Using Pigment Profiles and Hyperspectral Leaf Reflectance Data. Remote Sensing 4:2576-2594.

Foster A., Kakani V., Ge J., Mosali J. 2013. Rapid Assessment of Bioenergy Feedstock Quality by Near Infrared Reflectance Spectroscopy. Agronomy Journal 105:1-11.

Freeman K.W., Martin K.L., Teal R.K., Raun W.R., Girma K., Arnall D.B., Mullen R.W. 2007. By-Plant Prediction of Corn Forage Biomass and Nitrogen Uptake at Various Growth

Stages Using Remote Sensing and Plant Height [electronic resource]. Agronomy Journal 99:530-536.

Griffith A.P., Epplin F.M., Fuhlendorf S.D., Gillen R. 2011. A comparison of perennial polycultures and monocultures for producing biomass for biorefinery feedstock. Agronomy Journal 103:617-627.

Guretzky J.A., Biermacher J.T., Cook B.J., Kering M.K., Mosali J. 2011. Switchgrass for forage and bioenergy: harvest and nitrogen rate effects on biomass yields and nutrient composition. Plant and soil 339:69-81.

Haboudane D., Miller J.R., Tremblay N., Zarco-Tejada P.J., Dextraze L. 2002. Integrated narrow-band vegetation indices for prediction of crop chlorophyll content for application to precision agriculture. Remote Sensing of Environment 81:416-426.

Hansen P., Schjoerring J. 2003. Reflectance measurement of canopy biomass and nitrogen status in wheat crops using normalized difference vegetation indices and partial least squares regression. Remote Sensing of Environment 86:542-553.

Harmoney K.R., Brummer E.C., Russell J.R., Moore K.J., George J.R. 1997. Determination of pasture biomass using four indirect methods. Agronomy Journal 89:665-672.

Hatfield J., Gitelson A.A., Schepers J.S., Walthall C. 2008. Application of spectral remote sensing for agronomic decisions. Agronomy Journal 100:S-117-S-131.

Heaton E.A., Dohleman F.G., Miguez A.F., Juvik J.A., Lozovaya V., Widholm J., Zabotina O.A., McIsaac G.F., David M.B., Voigt T.B., Boersma N.N., Long S.P. 2010. Miscanthus: A Promising Biomass Crop. p. 75-137. *In*: J. C. Kader and M. Delseny (Eds.), Advances in Botanical Research, Vol 56.

Hill J. 2007. Environmental costs and benefits of transportation biofuel production from food- and lignocellulose-based energy crops. A review. Agronomy for Sustainable Development 27:1-12.

Jarchow M.E., Liebman M. 2012. Nutrient enrichment reduces complementarity and increases priority effects in prairies managed for bioenergy. Biomass & Bioenergy 36:381-389.

Jarchow M.E., Liebman M., Rawat V., Anex R.P. 2012. Functional group and fertilization affect the composition and bioenergy yields of prairie plants. Global Change Biology Bioenergy 4:671-679.

Kering M.K., Butler T.J., Biermacher J.T., Guretzky J.A. 2012. Biomass Yield and Nutrient Removal Rates of Perennial Grasses under Nitrogen Fertilization. BioEnergy research 5:61-70.

Kindscher K., Wells P.V. 1995. Prairie plant guilds: a multivariate analysis of prairie species based on ecological and morphological traits. Vegetatio 117:29-50.

Kucharik C.J., Brye K.R., Norman J.M., Foley J.A., Gower S.T., Bundy L.G. 2001. Measurements and modeling of carbon and nitrogen cycling in agroecosystems of southern Wisconsin: Potential for SOC sequestration during the next 50 years. Ecosystems 4:237-258.

Kumar A., Jones D.D., Hanna M.A. 2009. Thermochemical biomass gasification: a review of the current status of the technology. Energies 2:556-581.

Kumar L., Schmidt K., Dury S., Skidmore A. 2002. Imaging spectrometry and vegetation science. p. 111-155. *In*: S. M. d. J. F. van der Meer (Ed.), Imaging spectrometry, Kluwer Academic Publishing, Dordrecht, The Netherlands.

Labbé N., X.P. Ye, J. A. Franklin, A. R. Womac, D. D. Tyler, Rials T.G. 2008. Analysis of switchgrass characteristics using near infrared spectroscopy. BioRes. 3:1329-1348.

Lee D., Boe A. 2005. Biomass production of switchgrass in central South Dakota. Crop Science 45:2583-2590.

Lemus R., D.J. Parrish, and O. Abaye. 2008. Nitrogen-use dynamics in switchgrass grown for biomass. Bioenerg. Res. 1:153-162.

Lusch D.P. 1999. Introduction to environmental remote sensing Center for Remote Sensing and GIS Michigan State University East Lansing.

Marsalis M., Angadi S., Contreras-Govea F. 2010. Dry matter yield and nutritive value of corn, forage sorghum, and BMR forage sorghum at different plant populations and nitrogen rates. Field Crops Research 116:52-57.

Maughan M., Voigt T., Parrish A., Bollero G., Rooney W., Lee D.K. 2012. Forage and Energy Sorghum Responses to Nitrogen Fertilization in Central and Southern Illinois. Agronomy Journal 104:1032-1040.

McCollum T., McCuistion K., Bean B. 2005. Brown midrib and photoperiod sensitive forage sorghums. p. 36-46.*In*:Plains Nutrition Council Spring Conference. AREC 05-20. The Agriculture Program, The Texas A&M Univ. System, College Station.

McLaughlin S., Walsh M. 1998. Evaluating environmental consequences of producing herbaceous crops for bioenergy. Biomass and Bioenergy 14:317-324.

Mitchell R., Vogel K.P., Sarath G. 2008. Managing and enhancing switchgrass as a bioenergy feedstock. Biofuels, Bioproducts and Biorefining 2:530-539.

Muir J.P., Sanderson M.A., Ocumpaugh W.R., Jones R.M., Reed R.L. 2001. Biomass production of 'Alamo' switchgrass in response to nitrogen, phosphorus, and row spacing. Agronomy Journal 93:896-901.

Mutanga O., Skidmore A.K. 2004. Hyperspectral band depth analysis for a better estimation of grass biomass (*Cenchrus ciliaris*) measured under controlled laboratory conditions. International Journal of Applied Earth Observation and Geoinformation 5:87-96.

Numata I. 2012. Characterization on Pastures Using Field and Imaging Spectrometers. p. 207-226. *In*: P. S. Thenkabail, J.G. Lyon, and A. Huete (Ed.), Hyperspectral Remote Sensing of Vegetation, CRC Press, Boca Raton, FL.

Parrish D.J.a.J.H.F. 2005. The biology and agronomy of switchgrass for biofuels Critical Reviews in Plant Sciences 24:423-459.

Pauly M., Keegstra K. 2008. Cell-wall carbohydrates and their modification as a resource for biofuels. The Plant Journal 54:559-568.

Pinter P.J., Hatfield J.L., Schepers J.S., Barnes E.M., Moran M.S., Daughtry C.S.T., Upchurch D.R. 2003. Remote sensing for crop management. Photogrammetric engineering and remote sensing 69:647-664.

Price H.J., Dillon S.L., Hodnett G., Rooney W.L., Ross L., Johnston J.S. 2005. Genome evolution in the genus Sorghum (Poaceae). Annals of Botany 95:219-227.

Rooney W.L., Blumenthal J., Bean B., Mullet J.E. 2007. Designing sorghum as a dedicated bioenergy feedstock. Biofuels, Bioproducts and Biorefining 1:147-157.

Sanderson M.A., Read J.C., Reed R.L. 1999. Harvest management of switchgrass for biomass feedstock and forage production. Agronomy Journal 91:5-10.

Sanderson M.A., Agblevor F., Collins M., Johnson D.K. 1996. Compositional analysis of biomass feedstocks by near infrared reflectance spectroscopy. Biomass & Bioenergy 11:365-370.

Sanderson M.A., Adler P.R., Boateng A.A., Casler M.D., Sarath G. 2006. Switchgrass as a biofuels feedstock in the USA. Canadian Journal of Plant Science 86:1315-1325.

SAS. 2009. SAS User's Guide, SAS Institute Inc., Cary, North Carolina.

Schmer M.R., Schacht W.H., Marx D.B., Mitchell R.B., Vogel K.P. 2010. Efficient Methods of Estimating Switchgrass Biomass Supplies BioEnergy research 3:243-250.

Serrano L., Filella I., Penuelas J. 2000. Remote sensing of biomass and yield of winter wheat under different nitrogen supplies. Crop Science 40:723-731.

Tamang P., Bronson K., Malapati A., Schwartz R., Johnson J., Moore-Kucera J. 2011. Nitrogen requirements for ethanol production from sweet and photoperiod sensitive sorghums in the southern high plains. Agronomy Journal 103:431-440.

Thenkabail P.S., Smith R.B., De Pauw E. 2000. Hyperspectral vegetation indices and their relationships with agricultural crop characteristics. Remote Sensing of Environment 71:158-182.

Thomason W.E., W.R., Raun, G.V., Johnson, C.M. Taliaferro, K.W., Freeman, K.J., Wynn, and R.W. Mullen. 2004. Switchgrass response to harvest frequency and time and rate of applied nitrogen. J. Plant Nutr. 27:1199-1226.

Tilman D., Hill J., Lehman C. 2006. Carbon-negative biofuels from low-input high-diversity grassland biomass. Science 314:1598-1600.

Tucker C.J. 1979. Red and photographic infrared linear combinations for monitoring vegetation. Remote Sensing of Environment 8:127-150.

Venuto B., Kindiger B. 2008. Forage and biomass feedstock production from hybrid forage sorghum and sorghum–sudangrass hybrids. Grassland Science 54:189-196.

Vogel K.P., J.J. Brejda, D.T. Walters, and D.R. Buxton. 2002. Switchgrass biomass production in the Midwest USA: Harvest and nitrogen management. Agron. J. 94:413-420.

Waramit N., Moore K.J., Heggenstaller A.H. 2011. Composition of native warm-season grasses for bioenergy production in response to nitrogen fertilization rate and harvest date. Agronomy Journal 103:655-662.

Weiser R.L., Asrar G., Miller G.P., Kanemasu E.T. 1986. Assessing grassland biophysical characteristics from spectral measurements. Remote Sensing of Environment 20:141-152.

Wilson D.M., Dalluge D.L., Rover M., Heaton E.A., Brown R.C. 2013. Crop management impacts biofuel quality: influence of switchgrass harvest time on yield, nitrogen and ash of fast pyrolysis products. BioEnergy research 6:103-113.

Wullschleger S.D., Davis E.B., Borsuk M.E., Gunderson C.A., Lynd L.R. 2010. Biomass Production in Switchgrass across the United States: Database Description and Determinants of Yield. Agronomy Journal 102:1158-1168.

Xue L., Cao W., Luo W., Dai T., Zhu Y. 2004. Monitoring leaf nitrogen status in rice with canopy spectral reflectance. Agronomy Journal 96:135-142.

Xue Q., Nyren P.E., Wang G., Eriksmoen E., Bradbury G., Halverson M., Aberle E., Nichols K., Liebig M. 2011. Biomass composition of perennial grasses for biofuel production in North Dakota, USA. Biofuels 2:515-528.

Yao X., Zhu Y., Tian Y.C., Feng W., Cao W.X. 2010. Exploring hyperspectral bands and estimation indices for leaf nitrogen accumulation in wheat. International Journal of Applied Earth Observation and Geoinformation 12:89-100.

Zarco-Tejada P.J., Miller J., Morales A., Berjón A., Agüera J. 2004. Hyperspectral indices and model simulation for chlorophyll estimation in open-canopy tree crops. Remote Sensing of Environment 90:463-476.

Zhu Y., Zhou D., Yao X., Tian Y., Cao W. 2007. Quantitative relationships of leaf nitrogen status to canopy spectral reflectance in rice. Crop and Pasture Science 58:1077-1085.

Table 2.1. Site characteristics, cultural practice, harvest date and sampling intervals for parameters evaluated in the study.

	Site Characteristics	
	Stillwater	Woodward
Location	36.130 °N 97.104 °W	36.42°N , 99.414°W
Soil texture	Easpur loam (Fine-loamy, mixed, superactive, thermic Fluventic Haplustolls)	Carey silt loam (Fine-silty, mixed, superactive, thermic Typic Argiustolls)
Plot size	9 m x 9 m	7.6 m x 9 m
	Cultural practice	
Planting	Switchgrass and mix grass was planted on 12 May 2010; high biomass sorghum 5 May 2011;16 April 2012 and 29 April 2013; Legumes; Hairy vetch on 23 February 2011 and 4 March 2013; Crimson clover on 27 February 2012	Switchgrass and mix grass was planted on 24 May 2010; high biomass sorghum on 3 May 2011, 9 April 2012 and 10 May 2013; Legumes; Hairy vetch on 3 March 2011 and 15 March 2013; Crimson clover on 15 March 2012
Fertilizing	All plots except legume treatments were fertilized on 23 May 2011, switchgrass and mixed grass on 19 April 2012 and 30 April 2013; high biomass sorghum on 4 May 2012 and 7 June 2013	All plots except legume treatments fertilized on 9 June 2011, 3 May 2012 and 11 June 2013
Spraying	30 July 2012 and 23 July 2013 sprayed Sevin insecticide for grasshopper control at rate of 2.3 L ha^{-1}	1 April 2011 sprayed Dual herbicide for weed control in all non-legume treatments
	Final Harvest Date	
Plot Harvest	All plots 16 November, 2011, 27 November, 2012 and 25 September 2013; Harvested area was 45 m^2 in 2011 and 2012 season and 1 m^2 for 2013.	Switchgrass and mix grass on 4 January, 2012, 14 November, 2012 and 23 September 2013; Harvested area was 14 m^2 for 2011 and 2012 season and 1m^2 for 2013.

Table 2.2. Soil fertility characteristics (0-15 cm) at locations in 2012 and 2013 (Stillwater-12, Stillwater-13, Woodward-12, and Woodward-13). Samples were obtained within each plot before fertilization and are expressed as mean values.

Location	No.	pH	P	K	NO_3-N
				mg kg^{-1}	
Stillwater-12	45	6.1 (0.28)†	30 (5.0)	176 (28)	4 (2.4)
Stillwater-13	45	6.8 (0.37)	22 (5.8)	153 (50)	20 (19)
Woodward-12	45	6.4 (0.30)	30 (4.4)	160 (24)	6 (3.3)
Woodward-13	45	6.3 (0.45)	25 (8.0)	159 (43)	8 (5.7)

† Standard deviation in parenthesis.

Table 2.3. Narrowband NDVI (GreenSeeker) and broadband NDVI (aerial photograph) data collection for perennial grasses (PG) and high biomass sorghum (HBS) at Stillwater and Woodward locations for the 2013 growing seasons.

NDVI	Date	Days after greenup/ planting	
		Stillwater	
Narrowband		PG	HBS
1	May 16	17	
2	Jun 3	35	
3	Jun 10	42	41
4	Jun 14		45
5	Jun 21	53	52
6	Jul 2	65	64
Broadband		PG	SG
1	Jul 2	65	59
2	Aug 12	105	104
3	Sep 8	132	131
		Woodward	
Narrowband		PG	HBS†
1	Jun 23	55	45
2	Jul 24	86	76
3	Aug 26	119	109
Broadband		PG	HBS†
1	Jul 2	64	54
2	Aug 12	105	105
3	Sep 8	132	132

Perennial grasses (PG) started greening up around 30 April at both locations, high biomass sorghum (HBS) was planted 29 April and 10 May at Stillwater and Woodward respectively. †Severe lodging (>90%) in late September at Woodward did not allowed for harvest of high biomass sorghum. ‡Four band (red, green, blue and NIR) aerial image was provided by Geovantage inc for computation of the NDVI.

Table 2.4.Precipitation and temperature across 2010-2013 growing season (March – October), and 30-year average for Stillwater and Woodward, Oklahoma, USA.

		Mar	Apr	May	Jun	Jul	Aug	Sep	Oct	Total /Mean
Stillwater	30-yr average (mm)	85	89	131	114	73	74	94	82	742
	rainfall 2010 (mm)	42	92	181	139	112	64	71	44	744
	rainfall 2011 (mm)	21	50	99	43	19	3	79	15	329
	rainfall 2012 (mm)	100	156	28	55	2	67	28	15	452
	rainfall 2013 (mm)	28	135	153	100	141	65	43	40	705
	30-yr average (˚C)	10	15	20	25	28	28	23	16	21
	Average Temperature 2010 (˚C)	10	17	20	27	28	28	23	17	21
	Average Temperature 2011 (˚C)	11	18	20	29	32	31	21	16	22
	Average Temperature 2012 (˚C)	16	18	23	26	31	27	23	15	23
	Average Temperature 2013 (˚C)	9	13	20	26	26	27	24	15	20
Woodward	30-yr average (mm)	52	55	96	98	57	69	55	60	542
	rainfall 2010 (mm)	22	58	171	38	124	40	68	30	551
	rainfall 2011 (mm)	6	26	14	62	37	33	22	39	239
	rainfall 2012 (mm)	112	106	12	35	7	59	46	41	417
	rainfall 2013 (mm)	61	38	28	98	85	87	82	10	489
	30-yr average (˚C)	7	13	19	24	27	26	21	14	19
	Average Temperature 2010 (˚C)	8	16	19	27	27	28	24	17	21
	Average Temperature 2011 (˚C)	10	16	20	29	32	30	22	16	22
	Average Temperature 2012 (˚C)	15	17	22	27	31	27	23	15	22
	Average Temperature 2013 (˚C)	8	11	20	26	27	26	24	14	20

Table 2.5. Effects of nitrogen treatment and cropping system on biomass yield at Stillwater and Woodward in 2011-2013.

Treatments	Biomass Yield (Mg ha^{-1})					
	Stillwater			Woodward		
	2011	2012	2013	2011	2012	2013
			N Treatment			
0 $kgha^{-1}$	3.1 (1.0)	6.6 (2.2)	12.8 (5.8)	1.2 (0.4)	2.0 (0.6)	3.7 (2.0)
84	2.5 (1.3)	7.8 (1.5)	21.0 (9.2)	1.3 (0.3)	2.5 (0.7)	7.9 (2.4)
168	2.8 (0.6)	7.9 (2.4)	20.0 (7.1)	1.6 (0.7)	2.7 (0.7)	8.6 (1.4)
252	2.0 (1.1)	7.2 (1.3)	20.2 (9.3)	1.6 (0.5)	2.7 (0.7)	8.9 (1.8)
Legume	2.1 (1.0)	7.1 (1.8)	14.3 (4.9)	1.5 (0.4)	1.6 (0.5)	5.9 (3.3)
LSD (P<0.05)	0.8	1.4	3.6	0.5	0.6	2.1
[a] Linear	NS	NS	**	NS	NS	***
[a] Quadratic	NS	NS	*	NS	*	***
			Cropping System			
Switchgrass	2.9 (1.4)	7.3 (2.4)	12.7 (4.1)	1.5 (0.4)	2.4 (0.7)	7.2 (3.2)
Mixed grass	2.1 (0.6)	6.9 (1.2)	15.7 (5.3)	1.3 (0.5)	2.1 (0.7)	6.8 (2.7)
High Biomass Sorghum	2.5 (1.4)	7.7 (1.8)	24.4 (8.5)	NA	NA	NA
LSD (P<0.05)	2.0	3.3	5.0	0.7	2.0	5.6
Source of variation			Probability of significance			
Block	NS†	*	NS	**	*	NS
Cropping system (CS)	NS	NS	**	NS	NS	NS
Nitrogen Treatment (N Trt)	*	NS	***	NS	**	**
CS x N Trt	NS	NS	**	NS	NS	NS
CV	35	20	21	29	21	24

†NS: not significant, * significant at $p<0.05$, **significant at $p<0.01$ and *** significant at $p<0.001$. ‡ Number in parenthesis indicates standard deviation. NA - not available. HBS was not harvested due to crop failure to severe drought in 2011 and 2012 and severe lodging (> 90% of the fertilized plots) in 2013.[a] Linear and quadratic contrast was performed for 0 $kgNha^{-1}$ and applied fertilizer rates. N rates were applied in $kgha^{-1}$.

Table 2.6. Effects of nitrogen treatment and cropping system on biomass quality [TN, hemicelluloses (Hem), cellulose (Cell) and lignin (ADL)] of feedstock material from three cropping system at Stillwater and Woodward across the 2011-2013.

Treatments	Biomass Quality (%) in biomass											
	2011				2012				2013			
	TN	Hem	Cell	ADL	TN	Hem	Cell	ADL	TN	Hem	Cell	ADL
	STILLWATER											
0	0.70	27	36	7.3	1.03	25	32	6.9	0.54	27	32	6.7
84	0.83	25	33	7.3	1.12	25	31	6.7	0.89	27	33	7.0
168	1.02	25	34	7.5	1.12	25	31	6.4	0.76	27	32	7.0
252	1.09	27	34	7.0	1.10	25	31	6.7	0.97	27	32	6.8
Legume	0.82	27	36	7.0	1.04	25	31	6.6	0.61	27	32	6.8
LSD (P<0.05)	0.2	2.2	2.5	0.8	0.1	0.5	1.2	0.6	0.2	0.4	1.4	0.8
[a] Linear	**	NS	NS	NS	NS	NS	NS	NS	**	NS	NS	NS
[a] Quadratic	**	NS	NS	NS	NS	NS	NS	NS	NS	NS	NS	NS
	Cropping System											
SWG	0.54	27	38	8.5	1.07	26	34	7.6	0.50	27	34	7.7
MIXED	0.56	27	36	8.5	1.09	26	34	7.8	0.44	27	34	7.5
HBS	1.60	24	30	4.5	1.09	24	27	4.5	1.21	26	28	5.3
LSD (P<0.05)	0.4	1.2	2.0	1.4	0.3	0.7	1.7	0.7	0.3	0.4	1.8	0.9
Source of variation	Probability of significance											
Block	NS	NS	NS	**	*	NS	NS	NS	NS	NS	NS	NS
CS	**	**	***	**	NS	**	***	***	**	**	**	**
N Trt	**	NS	NS	NS	NS	NS	NS	NS	**	NS	NS	NS
CS x N Trt	NS	NS	NS	NS	NS	NS	NS	NS	*	NS	NS	NS
CV	24	9.0	7.5	11.1	9.6	2.0	4.0	9.5	31.3	1.5	4.4	11.7
	WOODWARD											
0	0.93	30	29	6.5	1.08	25	33	7.2	0.78	27	32	7.0
84	1.07	30	29	5.8	1.43	25	32	6.8	1.20	27	33	6.8
168	1.07	30	29	6.8	1.40	25	32	6.7	1.24	27	32	7.2
252	0.98	29	28	6.7	1.43	25	32	7.0	1.28	26	32	6.5
Legume	0.73	30	29	6.7	1.13	25	33	6.8	0.72	27	32	6.7
LSD (P<0.05)	0.20	1.9	2.0	1.1	0.23	0.8	1.5	0.6	0.2	0.4	1.3	0.7
[a] Linear	NS	NS	NS	NS	NS	NS	NS	NS	*	NS	NS	NS
[a] Quadratic	NS	NS	NS	NS	NS	NS	NS	NS	*	NS	NS	NS
	Cropping System											
SWG	0.93	30	29	6.3	1.25	25	33	6.9	1.25	27	32	6.7
MIXED	0.98	30	29	6.7	1.34	25	32	6.9	0.83	27	33	6.9
LSD (P<0.05)	0.5	3.0	2.2	2.3	0.2	0.9	2.0	0.8	0.5	0.6	0.3	0.5
Source of variation	Probability of significance											
Block	*	*	NS	**	NS	NS	NS	*	NS	NS	NS	NS
CS	NS	NS	NS	NS	NS	NS	NS	NS	NS	NS	**	NS
N Trt	*	NS	NS	NS	**	NS	NS	NS	***	*	NS	NS
CS x N Trt	NS	NS	NS	NS	NS	NS	NS	NS	NS	NS	NS	NS
CV	17.2	5.2	5.6	13.6	14.5	2.5	3.7	7.5	15.1	1.4	3.3	8.2

†NS: not significant, * significant at p<0.05, **significant at p<0.01 and *** significant at p<0.001. ‡ CS: cropping system, N Trt: Nitrogen treatments, SWG: switchgrass, HBS: High biomass sorghum, Mixed: Mixed grass (50% switchgrass, 25% Indian grass and 25% Big blues stem). HBS was not harvested due to crop failure to severe drought in 2011 and 2012 and severe lodging (> 90% of the fertilized plots) in 2013.[a] Linear and quadratic contrast was performed for 0 kgNha^{-1} and applied fertilizer rates. N rates were applied in kgha^{-1}.

Table 2.7. In-season prediction model parameters for final biomass yield of perennial grass (PG) at Woodward and Stillwater and high biomass sorghum (HBS) at Stillwater for the 2013 growing season using narrowband NDVI (GreenSeeker) and broadband NDVI (aerial photograph).

NDVI	Date	Prediction Models			
		Stillwater			
Narrowband		PG		HBS	
		Equation	R^2	Equation	R^2
1	May 16	Y=2.5x+12.7	0.002		
2	Jun 3	Y=54x-30	0.15		
3	Jun 10	Y=100x-67	0.31		
4	Jun 14				
5	Jun 21	Y=85x-54	0.38	Y=40x-6.2	0.14
6	Jul 2	Y=95x-60	0.43	Y=123x-69	0.52
Broadband					
1	Jul 2	Y=47x-20	0.15	Y=47.7x -2.1	0.60
2	Aug 12	Y=16.5x + 5.8	0.01	Y=109x -34	0.73
3	Sep 8	Y=129x-26.7	0.37	Y=98x -22	0.70
		Woodward			
Narrowband		PG		HBS	
1	Jun 23	Y=17.3x -4.7	0.25		
2	Jul 24	Y=25x -7.0	0.55	NA	
3	Aug 26	Y=25x-7.9	0.61		
Broadband					
1	Jul 2	Y=14.2x -0.72	0.42	NA	
2	Aug 12	Y=17x -0.4	0.40		
3	Sep 8	Y=19x -1.4	0.45		

NA- not available.

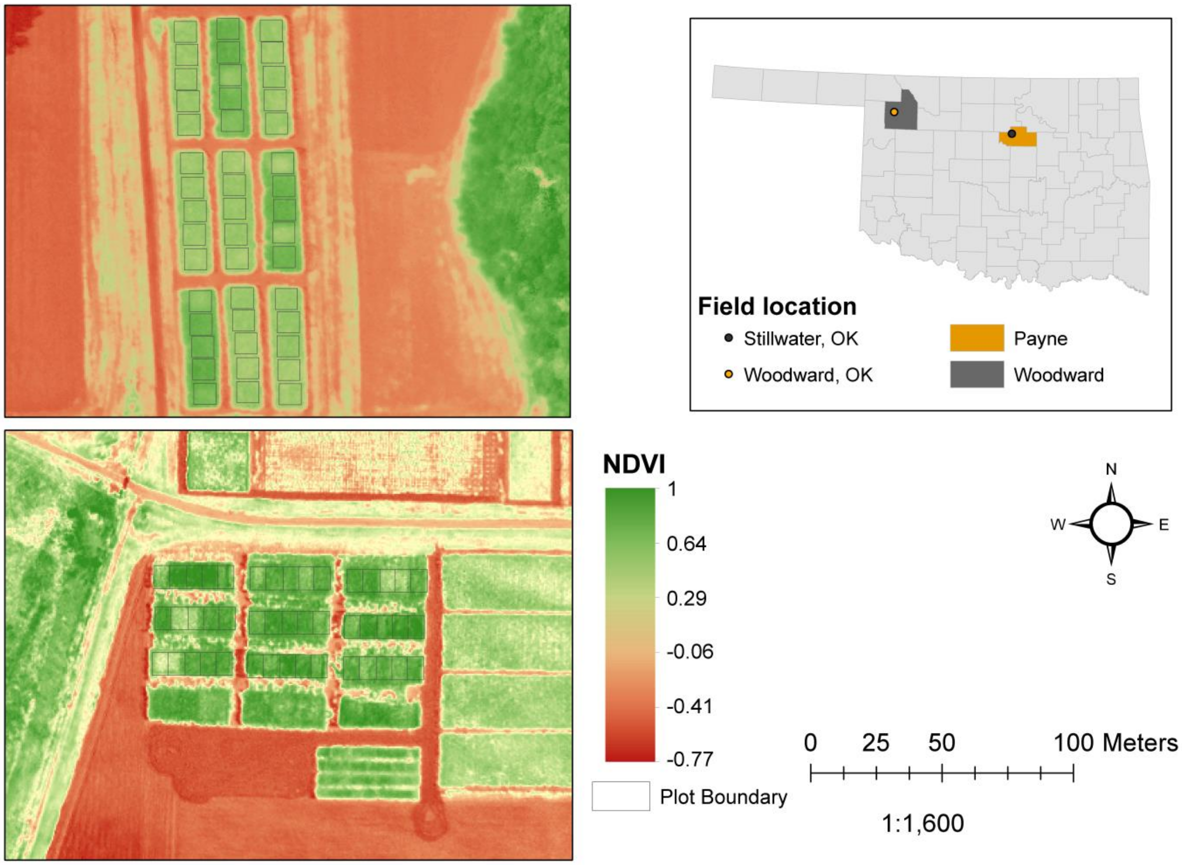

Fig. 2.1. Illustration of plot layout for Stillwater and Woodward locations and broadband NDVI values obtained from aerial photograph. Top: Stillwater and Bottom: Woodward. Aerial image was taken by Geovantage inc. (Peabody, Ma, USA).

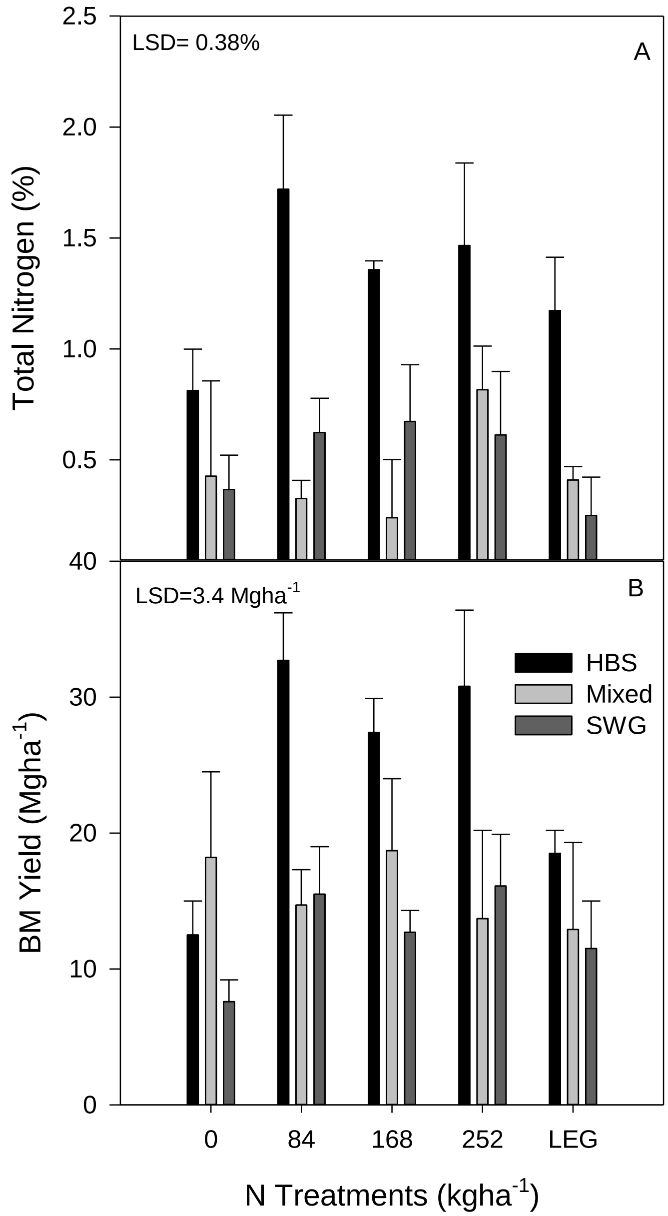

Figure 2.2. Combined effect of cropping systems (switchgrass, mixed grass and high biomass sorghum) and N treatments (0, 84, 168 and 252 kgNha^{-1}) on final biomass yield and N concentration biomass at Stillwater, Oklahoma for the 2013 growing season. A: Nitrogen concentration at harvest and B: Final biomass yield.

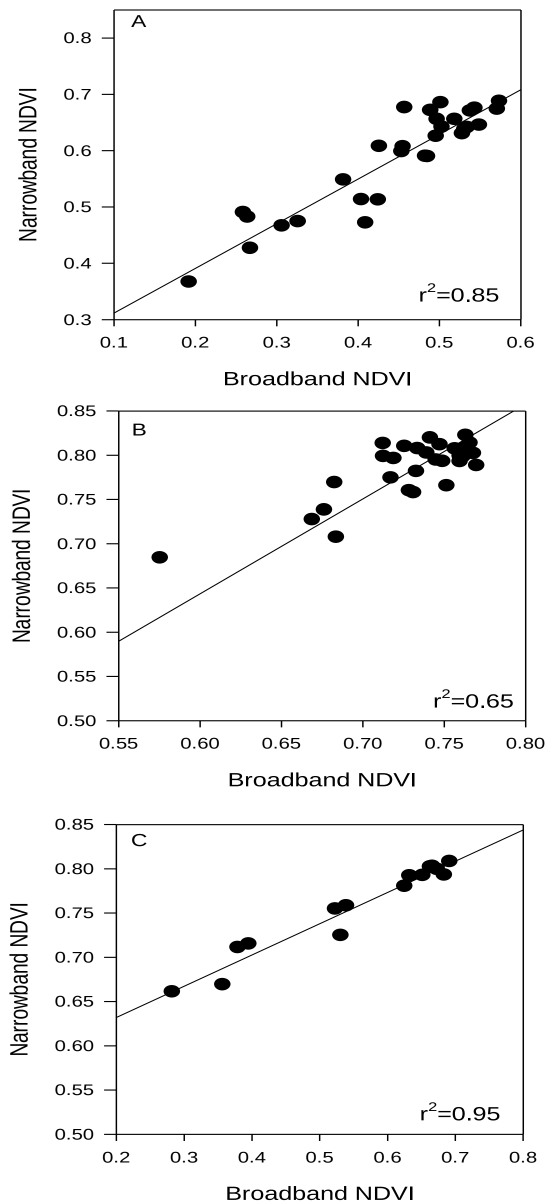

Figure 2.3. Relationship between narrowband NDVI (GreenSeeker sensor) and broadband NDVI (aerial photograph). A: Perennial grass at Woodward (26 August for GreenSeeker and 8 September for aerial photograph); B: Perennial grass at Stillwater (2 July GreenSeeker and 2 July for aerial photograph); C: High biomass sorghum at Stillwater (2 July GreenSeeker and 2 July for aerial photogra

CHAPTER III

DISCRIMINANT ANALYSIS OF NITROGEN TREATMENTS IN SWITCHGRASS AND HIGH BIOMASS SORGHUM USING LEAF AND CANOPY-SCALE SPECTROSCOPY

ABSTRACT

The recent advances in imaging spectroscopy provide a unique opportunity to obtain critical information needed for understanding nitrogen management in crop production systems. Therefore, the objectives of this study were to identify the optimal hyperspectral narrow-bands at leaf and canopy scale to discriminate N rates and to determine the ability of leaf and canopy scale hyperspectral reflectance data to discriminate N application rates. Leaf and canopy imaging spectroscopy was collected using an ASD FieldSpec FR spectroradiometer (350-2500nm) at monthly intervals in the 2011 and 2012. The crops evaluated in the study were switchgrass "Alamo" (Panicum virgatum L.) and high biomass sorghum "Blade 5200" (Sorghum bicolor) grown to evaluate N applications rates on biomass yield and quality. The optimal hyperspectral narrow-bands were determined based on principal component analysis (PCA) and the separation of the N treatments was done using stepwise discriminant analysis (SDA). Results showed similar canopy and leaf scale reflectance for high biomass sorghum but not for switchgrass. Wavebands occurring most frequently for separating the N treatments were 520-560, 650-690

nm (visible region), and 710-730 nm (red edge region).Triangular Greenness Index (TGI)was the most frequently occurring index in discriminating N application rates. The timing of separation in the N treatments indicates that N application should be done within 4-6 weeks after planting in high biomass sorghum and within 4 weeks after green-up in switchgrass. In general, indicate that hyperspectral reflectance is a viable tool that could be used to estimate biochemical and biophysical characteristics in bioenergy crop production systems.

INTRODUCTION

Soil testing and plant analysis are the most common methods used to determine N content. However, soil test and plant analysis don't always reflect the present N status. This is because N content in sample is dependent on soil moisture, growing condition at the time of sampling, time of year and depth of sample (Raun et al. 2008). Moreover, it is difficult to detect N deficiencies in actively growing crops without comparing the crop to crops with sufficient N. The easiest way to detect N deficiency in actively growing crops is to create a strip with sufficient N (N is non-limiting) and compared that strip to the other crops within the field (Raun et al. 2005). If no difference is detected, no additional N is needed as enough N had been mineralized from soil organic matter and/or deposited in the rainfall to meet all the plant needs or growth was possibility restricted by some other variables (Raun et al. 2008). Remote sensing of crop canopy and/or leaf reflectance could allow for detection of difference in N status of the reference strip and the rest of field, because our eyes are not as sensitive in picking up these differences. In season evaluation of N reference strip could assist in determining the appropriate N rates for bioenergy crop.

Imaging spectroscopy provides a unique opportunity to obtain critical information needed for understanding nitrogen management in crop production systems. Current uses of imaging spectroscopy application in agricultural cropland include detection of plant stress, measurement of chlorophyll and nitrogen content of the plant, modeling biophysical and yield characteristics, detection of moisture variation and discriminating crop type (Kokaly and Clark 1999; Huete et al. 2002; Johnson et al. 2008; Ray, Singh, and Panigrahy 2010; Foster et al. 2012; Numata 2012; Thenkabail, Lyon, and Huete 2012; Zhang 2012; Zhu, W. Wang, and Yao 2012).The leaf optical properties and canopy structure are the two main domains of remote sensing used to determine the signals originating from vegetation surfaces (Hatfield et al. 2008; Zhang 2012). Leaf optical properties are dependent on leaf structure, leaf biochemical composition, distribution of leaf biochemical components, and the complex refraction index of these components, while the canopy optical properties depend on the leaf optical properties, soil reflectance, solar illumination conditions, viewing geometry of the remote sensing instrument and the canopy structure (Baret and Guyot 1991; Haboudane et al. 2004; Gitelson et al. 2005; Zhang 2012). It is well documented, that leaf optical properties contribute directly to canopy level reflectance (Baret and Guyot 1991; Myneni and Asrar 1993; Haboudane et al. 2004; Gitelson et al. 2005; Kokaly et al. 2009; Gitelson 2012; Zhang 2012). Leaf scale sampling requires many leaves from a number of plants to obtain a representative average value and to adequately assess the spatial variability with a field. In contrast, measurement of canopy reflectance has the capability to sample a plant population or community rather than individual plants and to rapidly assess the spatial viability (Xue et al. 2004). Furthermore, the spectral signature of crop canopies in the field is more complex and often different from those of single green leaves measured under carefully illuminated conditions (Pinter et al. 2003; Kokaly et al. 2009). However, leaf level radiometric measurement is critical for accurate estimation of the canopy level biochemical properties such as chlorophyll and N content using imaging spectroscopy imaging.

Imaging spectrometer data is much more complex than multispectral data, collecting large volume of data in a short time leading to numerous complex challenges in data handling (Thenkabail et al. 2004; Thenkabail, Lyon, and Huete 2012). For example, Hyperion, the first space borne hyperspectral sensor onboard Earth observing-1(EO-1), gathers near continuous 12-bit data in 220 discrete narrow spectral bands ranging from 400-2500nm at a spatial resolution of 30m (Thenkabail et al. 2004; Thenkabail, Lyon, and Huete 2012). The continuous spectral coverage provided with many narrowbands does not necessary means more information as most of these bands especially those that are close together provide redundant information (Thenkabail et al. 2004; Thenkabail, Lyon, and Huete 2012). Thenkabail et al. (2012) suggested that a better option is to focus on the design of an optimal sensor with selected optimal bands for a given application, such as vegetation studies. The analysis of the large number of bands in an imaging spectroscopy set is complex and time consuming. Therefore, various attempts have been made to select the optimum set of narrow-bands for characterization of crop biophysical and biochemical properties (Thenkabail et al. 2004; Xue et al. 2004; Ray, Singh, and Panigrahy 2010; Gitelson 2012; Zhu, W. Wang, and Yao 2012).

There are many methods available for selection and extraction of the optimal wavebands from imaging spectroscopy such as (Bajwa and Kulkarni 2012; Numata 2012; Thenkabail et al. 2013) 1) feature selection (i.e. principal component analysis and derivative analysis); 2) λ versus λ R^2 - plots between the different wavebands; (3) partial least squares (PLS), (4) stepwise linear regressions; and (5) hyperspectral vegetation indices (HVIs). These approaches are often used for identifying optimal wavebands, eliminating redundant bands and extracting of unique information from imaging spectroscopy in agricultural cropping systems (Thenkabail et al. 2004; Kosaka, Uto, and Kosugi 2005; Ray, Singh, and Panigrahy 2010; Thenkabail et al. 2013). There are numerous other methods of imaging spectroscopy analysis for eliminating redundant wavebands and reducing the large number of wavebands to a manageable number, while retaining optimal information such as continuum removal (Clark and Roush 1984; Kokaly and Clark 1999; Jollineau and Howarth 2008), derivative vegetation indices (Thenkabail, Smith, and De Pauw 2000), neural networks (Ingram, Dawson, and Whittaker 2005; Trombetti et al. 2008; Liu, Wu, and Huang 2010), uniform design (Filippi and Jensen 2006); wavelength transformation (Bruce, Koger, and Li 2002; Hsu 2007), spectral mixture analysis (Adams et al.

1995; Roberts et al. 1999) and others (Thenkabail, Lyon, and Huete 2011). Selection of an extraction method should be dependent on the ability to identify the optimal set of features that would extract the information of interest with the highest possible accuracy and reliability in the least amount of time and computational effort and cost (Bajwa and Kulkarni 2012).

Spectral signatures of crop canopies in the field are more complex and are often different from that of single green leaves measured under carefully controlled illuminated conditions (Pinter et al. 2003). Moreover, several narrow hyperspectral wavebands and VIs are required to assess the crop status throughout the season, as no single index or wavebands are able to describe the evolution of a crop within a single season or across seasons (Strachan, Pattey, and Boisvert 2002; Hatfield and Prueger 2010). Timely information is important in agricultural crop production system for detecting nutrient deficiencies, pest infestation and other crop stress. Early detection is critical to reduce large yield loss and minimize economic loss. Therefore, approximate analyses; quickly obtained using one or more hyperspectral vegetation indices may be more useful than slow detailed retrievals based on continuum removal or similar approaches (Thenkabail et al. 2013). Recent, research has demonstrated that vegetation indices derived from imaging spectroscopy for estimation of a target variable have shown better performance than the traditional red-NIR band combinations (Thenkabail, Smith, and De Pauw 2000; Mutanga and Skidmore 2004; Cho 2007; Fava et al. 2009). Furthermore, N reference strip within a field could be separated easily and more efficiently using sensors with optimal wavebands. Thus, the objectives of this study were 1) to determine the optimal wavebands at leaf and canopy scale that discriminate N application rates, and 2) to determine if leaf and canopy scale imaging spectrometer data differed in discriminating among N application rates at different times throughout the growing season.

MATERIALS AND METHODS

Field Experimental Design

A field experiment was established the Stillwater Research Station (EFAW site, 36.13 N, 97.10 W) to evaluate the combined effect of nitrogen treatments and bioenergy crop species on biomass yield. The nitrogen treatments were: 4 applied N rates of 0, 84, 168 and 252 kgNha^{-1} and a winter legume [hairy vetch (*Vicia villosa* Roth) planted in 2011 and crimson clover (*Trifolium incarnatum* L.) planted in 2012], and two bioenergy crop species; [switchgrass (*Panicum virgatum* L*)* "Alamo" established in 2010 and high biomass sorghum (*Sorghum bicolor* L) "Blade 5200" planted in June 2011 and April 2012. Site characteristics and cultural practices are summarized in Table 3.1. The switchgrass and high biomass sorghum were seeded at rates of 5.04 and 9.5 kg ha^{-1} of pure live seeds using a no-till planter. The winter legume was planted in February each year. All plots were fertilized on 3 June 2011, while in 2012, switchgrass was fertilized on 19 April and high biomass sorghum on 4 May. The five different N treatments were applied to plots arranged in a split plot randomized design with three replications to generate plots with varying yield potential. In the split plot design, species was the main plot and fertilizer treatment was the subplot. The experimental plots (30) dimensions were 9 m x 9 m dimension.

Leaf Sampling

To separate N treatments at leaf scale to determine the need for N fertilization, the top most fully expanded green leaf was excised from 6 and 3 random switchgrass and high biomass sorghum plants, respectively, in each plot. The leaves were immediately placed in a sealed plastic bag in an ice chest and transported to the laboratory for spectral measurements. These samples were collected between 10:00 and 15:00 local time ([UTC-06:00] Central Time [US & Canada]).

Measurement of Hyperspectral Reflectance

Imaging spectrometer data were collected from switchgrass and high biomass sorghum at leaf and canopy scale throughout the 2011-2012 growing season using a spectroradiometer (FieldSpec Pro FR: Analytical Spectral Devices [ASD], Boulder, Co, USA). The ASD measures spectral reflectance in the 350-2500 nm waveband range and has a spectral sampling of 1.4 nm in the 350-1000 nm range, and 2 nm in the 1000-2500 nm range. The spectral resolution is 3 nm in the 350-1000 nm range, and 10 nm in the 1000 nm range, which were calculated as 1 nm resolution wavelength for the output data using software (RS2 for Windows; ASD). A spectralon (Labsphere, Sutton, NH, USA) white reference panel was used to optimize the ASD instrument prior to taking two canopy reflectance measurements per plot. The white reference was measured at 15-30 minutes intervals to check the stability for 100% reflectance during reflectance measurement. To reduce the amount of data for analysis, spectral data were averaged at 10-nm wavelength intervals (e.g., a band center at 400 was the averaged value between 395–405 nm) giving a total of 211 spectral bands between 400–2500 nm (Foster et al. 2012). Spectral data at start and end of spectrum due to noise (350–395 nm and 2460–2500) and in the atmospheric water absorption spectral regions (1360–1420 and 1800–1960 nm) were deleted from the data before analysis leaving 185 spectral bands for analysis.

Leaf Spectral Data

Leaf samples were collected from June to August 2011 and May to September 2012 between 10:00-14:30 hours local time ([UTC-06:00] Central Time [US & Canada]). Spectral reflectance was measured for the leaf samples using the procedure for switchgrass leaf reflectance that used by Foster et al. (2012). However, to measure the leaf reflectance of the high biomass sorghum, a single leaf rather than two leaves was used due to the larger surface area. The spectral reflectance was obtained by sandwiching a single leaf for the high biomass sorghum or two leaves for the switchgrass between a non-reflecting black body and the light probe (Kakani et al. 2004). Three replicated spectral measurements were taken on each of the leaf collected from each plot. Each measurement was the average of 25 spectral readings to enable noise reduction within the spectra (Muchovej and Newman 2004; Miphokasap et al. 2012).

Canopy Spectral Data

Canopy reflectance measurements were made on clear-sky days from June to August 2011 and May to September 2012 between 10:00-14:30 hours local time ([UTC-06:00] Central Time [US & Canada])using an ASD spectroradiometer To measure the canopy reflectance the sensor head was held approximately 60 cm above the canopy at the nadir position at each sampling interval. The radiometer was mounted on the back of pickup and raised to a height of 200 to 290 cm above the ground (Figure 1).Table 3.3.2 shows height of radiometer, canopy height and height of the sensor from ground at each sampling date. The radiometer had a 25° field of view (FOV), producing a view area of 88-128 cm diameter at ground level. Hyperspectral reflectance was collected from 30 plots of switchgrass and high biomass sorghum with varied rate of nitrogen fertilizer to create variation in biomass and quality within the plots.

Two replicated spectral measurements were taken from each plot, with each measurement being an average of 25 spectral readings to enable noise reduction within the spectra.

Vegetation Indices

Vegetation indices are designed to either detect vegetation structural parameters such as LAI, biomass, or chlorophyll/pigment concentrations (Pinter et al. 2003). The information generated from vegetation indices are dependent upon the phenological stage and plant parameter to which the index is closely related (Hatfield and Prueger 2010). Therefore, indices used in this study were selected from the most common VIs and grouped into three categories, structural indices, chlorophyll/pigment related indices and red edge indices that are related to pigments (Table 3.3).

Data Analysis

The principal component analysis (PCA) was performed using the PROC PRINCOMP procedure in SAS to identify the optimal wavebands, while stepwise discriminant analysis (SDA) was performed to find the best indices and wavebands that could distinguish the nitrogen treatments at different sampling intervals throughout the growing season. The SDA was performed using the PROC STEPWISE procedure in SAS. To determine the optimal wavebands that best described the vegetation characteristics at different time throughout the growing season a comprehensive analysis using PCA was performed. The PCA was used as a method because of its reliability and ease in determining selecting best wavebands to model biophysical and biochemical quantities. While, the SDA was carried out to identify the best vegetation indices (Table 3.3) and wavebands (from 186 bands) at each sampling intervals in the switchgrass and the high biomass sorghum for separation of the N treatments. Stepwise discrimination (SDA) was used because it provides the most rapid and straight forward results in discriminating among multiple groups (Thenkabail et al. 2004).

The PCA is a method that transformed the original data into a set of new uncorrelated variables called principal components (PC), thereby reducing the number of variables. The value of the PCA is that the importance of each wavebands in each PC can be determined by the magnitude of the eigenvectors or factor loading as the higher the eigenvector the greater the importance of the waveband in relation to the switchgrass and the high biomass sorghum N status. Therefore, the magnitude of the eigenvector in each PC was used to determine the wavebands with the greatest influence in PC1, PC2 and PC3. The PCA also provides the percent variability explained by each PC (eigenvalues). This approach allows for the selection of the best wavebands associated with the switchgrass and high biomass sorghum N status.

The SDA is a method that reduces the data set to those variables that maximize between statistical group variability while minimizing within group variability. The Wilk's lambda statistics was used to select the best indices and wavebands for differentiating the N treatments at the different sampling intervals and at the leaf and canopy scale. In addition to the Wilk's lambda, there are other SDA methods for discrimination such as Pillai's trace and canonical correlation (SAS 2009). However, the Wilk's lambda is the most commonly used and reported (Thenkabail et al. 2004; Thenkabail, Lyon, and Huete 2012; Thenkabail et al. 2013). Low Wilk's lambda value suggests a great degree of separation (Thenkabail et al. 2004; Thenkabail, Smith, and De Pauw 2002). Therefore, indices or wavebands identified at each sampling date and at leaf and canopy scale with the lowest Wilk's lambda value resulted in the greatest degree of separation among the N treatments. The difference between the PCA and SDA is that the PCA creates new set of uncorrelated variables that defines the axes of greatest variability in the data and the SDA identifies from amongst the original variables the best variable that describes differences between given groups.

RESULTS AND DISCUSSION

Growing Condition

Severe drought conditions affected the state of Oklahoma which significantly affected the productivity of crops in 2011. Stillwater received 44% and 61% of the 30 yr. average rainfall in 2011 and 2012, respectively (Table 3.1). Nitrogen fertilizer was applied in June and the plants were almost completely non-photosynthetic with little to no green material following August resulting in only three spectral samples for the 2011 season. In 2012, to take advantage of the early season moisture switchgrass was fertilized in April and high biomass sorghum planted in May. Five spectral measurements were taken in 2012 (May, June, July, August and September). The use of a mount attached to the pickup for the instrument to get above the crop canopy allowed for easier and more frequent sampling (Figure 3.1).

Visual evaluation of figure 3.2 showed greater variation in the canopy reflectance compared to the leaf reflectance across the species and the sampling dates. Variation in spectral measurements can easily be observed between species particularly at the leaf level, with greater variation in the high biomass sorghum in comparison to switchgrass. Within a species, variation was observed in switchgrass at canopy scale in comparison to at leaf level, while spectral measurement varied in leaf and canopy for high biomass sorghum with greater variation at the canopy scale in 2012. The variability in the canopy reflectance can be attributed to the changes in the proportion of soil and vegetation and architectural arrangement of plant components (Pinter et al. 2003). Moreover, the shape of the leaf spectra was very dissimilar from that of the canopy spectra of the same species. This finding was not surprising, as spectral signatures of crop canopies in the field are more complex and often quite dissimilar from those of a single green leaves measured under carefully controlled illuminated light (Pinter et al. 2003).

Figures 3.3 and 3.4 show canopy and leaf reflectance of switchgrass and high biomass sorghum at different N treatments collected at the different sampling dates in 2011 and 2012. Greater variability was observed among the five N treatments at the canopy scale in comparison to that at leaf scale that showed little to no variability. The figures at leaf scale reveal minimal separation of the N treatments in May (2012), July and August of 2011. At canopy level, significant separation could be seen in May (2012), June (2011 and 2012), July (2011), August (2011) and September (2012) with the greatest separation in July (2011) and September (2012). Greater variability was observed among the N treatments at the canopy scale in the high biomass sorghum. However, greater variability could be seen at the leaf scale in comparison to at the leaf scale of switchgrass. Visual examination of the spectral curves at leaf scale reveals significant separation in June (2011) and July (2012). At the canopy scale significant separation was seen in June (2011 and 2012), July (2011) and August (2011 and2012) with the greatest separation in June (2011 and 2012).

In general, visual examination of the spectral curves reveals that separation was greatest either early or late in the season for switchgrass and early in the season for biomass sorghum (Figures 3.3 and 3.4). Moreover, the greatest separation observed occurred in the near infrared (750-1350 nm) and mid-infrared (1400-2500 nm) regions of the spectrum, with minimal separation in the visible region (400-700 nm) (Figures 3.2-3.4). Leaf reflectance in green leaves is determined mainly by, water content, pigment and carbon content, which can be seen by the shape in the reflectance curve in the visible, NIR and mid-infrared regions of the spectrum. In the near infrared (NIR) region of the spectrum reflectance is high (40-60%) and is physically controlled by the leaf internal structures (Lusch 1999). While, in the mid infrared region (1350-2500 nm) of the spectrum reflectance decreases (5- 40%), the primary physical control is *vivo* water content and internal leaf structure plays a secondary role in controlling energy-matter interactions (Lusch 1999). It is expected that throughout the growing season water content, pigment and carbon in the individual leaf and canopy will vary (Pinter et al. 2003). Therefore, greater variability is most likely in regions of the spectrum controlled by these physical parameters. Furthermore, in a green leaf water absorption can obscure other constituents (Numata 2012), which could explain the somewhat lower variability in the visible region of the spectrum.

Principal Component Analysis

The first three principal components (PCs) explained 93-100% of the variability in switchgrass and high biomass sorghum (Tables 3.4, 3.5, 3.6 and 3.7). The amount of variability explained by the three PCs in switchgrass (Tables 4 and 5) and high biomass sorghum (Tables 3.6 and 3.7) at canopy and leaf scale for both years was greater than 90%. These results suggest that in order to explain greater than 90% of the variability, 186 wavebands can be reduced to three PC wavebands (PC1 to PC3). Tables 3.4 and 3.5 (switchgrass 2011 and 2012) and Tables 6 and 7 (high biomass sorghum2011 and 2012) provides the five wavebands with the highest factor loading for each principal components resulting in 15 bands in different regions of the spectrum. The order the bands are listed in Tables 3.4, 3.5, 3.6 and 3.7 indicates the magnitude or ranking for that band based on its factor loadings. For example, for PC waveband centered at 1770 has the highest factor loading followed by 1660, 1670, 1760 and 1650 nm (Table 3.4).

The PCA analysis of 2011 switchgrass spectral data (Table 3.4) showed that PC1 was dominated by mid-IR bands explaining 53 and 89% of the variability at leaf and canopy levels. The PC2 was dominated by NIR bands at the leaf scale accounting for 29% of the variability and mid-IR at the canopy scale explaining 7% (Table 3.4). Blue bands dominated PC3 explaining 14% of the variability at leaf scale and 2% at canopy level (Table 3.4). Overall, PC1 and PC2 dominated by mid-IR bands explained 71 and 18%, respectively, and PC3 dominated by blue bands explained 5% of the variability in switchgrass at both leaf and canopy levels (Table 3.4).

Similar to 2011, the PCA of 2012 switchgrass spectral data (Table 3.5) showed that PC1 was dominated by mid-IR bands explaining 64 and 71% of the variability at leaf and canopy levels. The PC2 was dominated by NIR bands at the leaf and canopy scale accounted for 22 and 23% of the variability (Table 3.5). Blue and red bands dominated PC3 at leaf scale explaining 9% of the variability and green bands dominated at canopy levels accounting for 4% of the variability (Table 3.5). Overall, PC1 dominated by mid-IR bands explained 68%, PC2 dominated by NIR bands explained 22% and PC3 dominated by red bands explained 7% of the variability in switchgrass at both leaf and canopy levels (Table 3.5).

The PCA of high biomass sorghum spectral data of 2011 (Table 3.6) showed that PC1 was dominated by mid-IR bands explaining 64 and 68% of the variability at leaf and canopy levels. The PC2 was dominated by NIR bands accounting for 26% of the variability at the leaf and canopy levels (Table 3.6). Green bands dominated PC3 at leaf scale explaining 7% of the variability and blue bands dominated at canopy scale accounting for 4% of the variability (Table

3.6). Overall, PC1 was dominated by mid-IR bands explained 65%, PC2 dominated by NIR bands explained 26% and PC3 dominated by blue and green bands explained 6% of the variability in high biomass sorghum at both leaf and canopy levels (Table 3.6).

Similar to 2011, the PCA of 2012 high biomass sorghum spectral data (Table 3.7) showed that PC1 was dominated by mid-IR bands explaining 66 and 68% of the variability at leaf and canopy levels. In contrast to 2011, the PC2 was dominated by red bands accounting for 23% of the variability at the leaf scale and by NIR at the canopy scale explaining 28% of the variability (Table 3.7). NIR bands dominated PC3 at leaf scale explaining 8% of the variability and green bands dominated at canopy scale accounting for 3% of the variability (Table 3.7). Overall, PC1 dominated by mid-IR bands explained 67%, PC2 dominated by NIR bands explained 26% and PC3 dominated by green bands explained 5% of the variability in high biomass sorghum at both leaf and canopy levels (Table 3.7).

In general, the PCA found mid-IR to be the dominant wavebands in PC1 explaining approximately 60% of the variation, NIR for PC2 explaining just over 20% of the variation and visible bands (red, blue and green) for PC3 explaining about 5% of the variability in switchgrass and biomass sorghum. Thenkabail et al., (2004) also found mid-IR to be the dominant waveband for PC1 accounting for a similar 62% of the variability in various weeds species and agricultural crop species. Likewise, Ray et al., (2010) studying the use of using imaging spectroscopy data in detecting crop stressed measured reflectance from 375-1075 using the PCA reported PC1 to be mostly dominated by NIR bands and PC2 and PC3 by the red region for seven nitrogen treatments in potato. The results from our study and those reported above indicate the overall importance of mid-IR and NIR wavebands in monitoring vegetation characteristics using imaging spectroscopy. Moreover, cropland biotic factors such as canopy height, basal area, biomass and LAI are often best predicted through a combination of visible and shortwave infrared (SWIR, [1100-2500 nm]) (Cho et al. 2007; White et al. 2010; Thenkabail, Lyon, and Huete 2012). The most frequent wavebands with the highest factor loading occurring more than five times among the PCs were 560 (11), 770 (10), 430 nm (7), 810 (7), 1660 (6), 500 (5) and 650 nm (5). These wavebands were similar or near-similar to waveband centers (495, 555, 495,735,885,1675-1705 and 645-665 nm)of the 22 wavebands identified by Thenkabail et al.,(2004) as the best narrow bands for discriminating among agricultural crops.

Selecting the Best Wavebands and Indices

Table 3.8 summarizes the best wavebands identified for separating the N treatments and their Wilk's lambda values. The Wilk's lambda values are indicative of discriminatory power of the wavebands, with the lesser the Wilk's lambda the greater the degree of separation between the N treatments.

Selecting Best Wavebands

The optimal Wilk's lambda for the different wavebands separating the N treatments in switchgrass was achieved in May 2012, June 2011 and 2012, July 2012, August 2011, and September 2012 at leaf level (Table 3.8). At canopy scale optimal Wilk's lambda was achieved in June 2011, August 2012 and September 2012. The lowest Wilk's lambda values obtained at leaf scale were achieved with seven wavebands (560, 410, 470, 430,650, 690 and 730 nm) in June 2011(Wilk's lambda = 0.00002) and with the single waveband (730 nm) in May 2012 (Wilk's lambda = 0.067). At the canopy scale the lowest Wilk's lambda values were achieved with the singlewaveband (400 nm) in June 2011(Wilk's lambda = 0.457) and with three wavebands (640, 1300 and 500 nm) in September 2012 (Wilk's lambda =0.018). Close to zero Wilk's lambda values were obtained at leaf level in switchgrass for the 2011 sampling, indicating a great degree of separation among the N treatments, but higher Wilk's lambda values in 2012 indicates that the narrowbands weren't has effective in separating the N treatments as in the previous year (Table 3.8).

The optimal Wilk's lambda for the different wavebands separating the N treatments in high biomass sorghum was achieved at similar sampling intervals to that observed in switchgrass at leaf scale with the exception of August 2012 (Table 3.8). Optimal Wilk's lambda at the canopy scale was also achieved in June 2011 and 2012, July 2012 and September 2012 in the high biomass sorghum (Table 3.8). The lowest Wilk's lambda at leaf scale in high biomass sorghum was achieved with five wavebands in June 2011 (720, 680,570,520, and 560 nm, Wilk's lambda = 0.0014) and 2012 (730,710,550,540, and 990 nm, Wilk's lambda = 0.002). At the canopy scale the lowest Wilk's lambda was also achieved with four wavebands (1000, 1430, 520 and 560 nm) in June of 2011 and three wavebands (710,510 and 520 nm) in 2012 with Wilk's lambda values 0.0008 and 0.023 respectively (Table 3.8). The most frequent wavebands selected for separating the N treatments across species and years were 520-560,650-690, and 710-730 nm (Table 3.8). These wavebands represent the red, green and red edge region of the spectrum. Moreover, they were also similar or near similar to the wavebands were identified using PCA by Thenkabail et al. (2004) as the best narrow bands for discriminating among agricultural crops. Lower Wilk's lambda values(closer to zero) were achieved for the high biomass sorghum at both leaf and canopy scale indicating that the narrowband data performed better in separating the high biomass sorghum compared to the switchgrass.

Selecting Best Vegetation Indices

The results of the SDA for the five N treatments showed that the optimal Wilk's lambda values were achieved with different VIs at each sampling date for the switchgrass and the high biomass sorghum at both canopy and leaf scale (Table 3.9). Table 3.9 summarizes the best indices identified for separating the N treatments at the different sampling date. Pigment related indices [TGI (7), $Cl_{red\ edge}$ (3), PRI (4), TVI (4) and TCARI (3)] were the dominant indices occurring most frequently for separating the N treatments (Table 3.9). The lowest Wilk's lambda that is indicative of the degree of separation occurred in July 2011 (0.035) with TVI, EVI, NPCI and RE740 and May 2012 (0.044) with TGI at leaf scale and in August 2011 (0.131) with $Cl_{red\ edge}$ and Cl_{green} and September 2012 (0.186) with the Red edge NDVI at canopy scale for switchgrass. In the high biomass sorghum, the lowest Wilk's lambda occurred in June 2011 at leaf scale with TGI, SR and TCARI (0.031) and at canopy scale with ZTM and Red edge (R_{740}–R_{720}) (0.031). Likewise, the lowest Wilk's lambda occurred in June 2012 at leaf scale (0.202) with TVI and at canopy scale (0.029) with TGI and MCARI. Similar to the individual wavebands (Table 3.8), lower Wilk's lambda values were observed in 2011 and at the leaf scale, except for the high biomass sorghum that showed greater separation at canopy scale in 2012 (0.029) than that of the 2012 leaf scale (0.202) and canopy scale 2011 (0.040) from the VIs (Table 3.9).

Individual Wavebands versus Vegetation Indices

Traditionally, the advantage of VIs over individual wavebands is that they take advantage of the reflectance of the wavebands in different regions of the spectrum. For example, TCARI takes advantage of reflectance in the red and red edge regions, TGI in the visible region and RNDVI in the red and NIR regions of the spectrum. Each VI has its own unique combination of wavebands that have been related to specific crop parameter (Hatfield and Prueger 2010). Therefore, it is not surprising that the lowest Wilk's lambda value or greatest separation of the N treatments occurred with different VIs (Table 3.9). Lower optimal Wilk's value was obtained with individual wavebands compared to the VIs. This indicates that the individual wavebands performed better in separating the N treatments in both the switchgrass and the high biomass sorghum. However, optimal Wilk's lambda for separation of the N treatments in the switchgrass at canopy scale were obtained in July (0.345) and August (0.150) of 2011 and May (0.237) and June (0.486) of 2012 and at leaf scale in July (0.035) 2011, whereas no optimal Wilk's lambda were obtained for individual wavebands at these sampling dates. These Wilk's lambda values were much higher than those of the individual wavebands, but they do indicate that VIs may be useful for the extraction of information from complex canopy structure where individual wavebands was not able to. Especially, if VIs could be improved by using hyperspectral narrowbands more closely related to the crop and target variable. As many VIs derived from hyperspectral narrowbands in recent studies have shown improved performance compared to the traditional red-NIR based VIs used in this study ((Hansen and Schjoerring 2003; Mutanga and Skidmore 2004; Chan and Paelinckx 2008; Thenkabail, Lyon, and Huete 2012).

Several authors have reported correlation between wavebands and N content and VIs and N content (Everitt, Richardson, and Gausman 1985; Chappelle, Kim, and Mcmurtrey 1992; Peñuelas et al. 1994; Hansen and Schjoerring 2003; Xue et al. 2004; Zhu et al. 2007; Feng et al. 2008; Fava et al. 2009; Stroppiana et al. 2009; Abdel-Rahman, Ahmed, and Van den Berg 2010; Chen et al. 2010). However, there is great disparity in the literature regarding the best wavebands and VIs for studying the N status in crops. The most frequent occurring wavebands with the lowest Wilk's lambda value for separating N treatments at leaf scale identified in this study were all in the visible and red edge regions of the spectrum (Table 3.8). This finding further substantiates that the visible and red edge wavelengths are an important spectral regions for N assessment and could be better suited than NIR wavebands which are considered to be strongly influenced by canopy parameters (Stroppiana et al. 2009). Therefore, it was not surprising that NIR wavebands were more frequent at the canopy level (Table 3.8). More so, the most frequent occurring VI was highly sensitivity to chlorophyll content and is a ratio of wavebands in the visible region of the spectrum. To accurately estimate plant N content base on reflectance data, wavebands and VIs highly related to chlorophyll content are required (Hatfield and Prueger 2010). Nitrogen primarily occur in proteins and chlorophylls in the leaf cells and of such many researchers have associated spectroscopic estimation of nitrogen to that of chlorophyll pigments (Hansen and Schjoerring 2003; Mutanga, Skidmore, and van Wieren 2003; Xue et al. 2004; Kokaly et al. 2009; Stroppiana et al. 2009; Mitchell et al. 2012; Numata 2012; Stroppiana et al. 2012; Zhu, W. Wang, and Yao 2012). Therefore, VIs capable of estimating or separating chlorophyll content in the plant was found to dominate.

The variation in the VIs are an indication of the different seasonal trends and the benefits of using multiple VIs to assess crop characteristic throughout the growing season and across growing seasons (Table 3.9). Hatfield and Prueger (2010) also concluded that multiple VIs best capture the crop characteristic throughout the growing season to quantify agricultural crop characteristics. The result of this study does suggest that imaging spectroscopy do offer the advantage for the computation of multiple indices to capture the temporal variation that could be lost using individual wavebands or a single VI for the assessment of crop characteristics. However, the greater separation from the individual wavebands suggested that performance of VIs could be improved by the use of selected optimal narrow wavebands for the computation of the indices (Thenkabail et al. 2013).

Canopy versus Leaf Spectra

The individual wavebands identified for separation of the N treatments at leaf and canopy levels were overall similar or near similar with the exception of the addition of the NIR wavebands at the canopy level. Majority of the wavebands were in the region of 400-740 nm at leaf scale and 400-1430 nm at the canopy scale (Table 3.8). Similarly, wavebands around 680 nm and those in the green reflectance region (550-580 nm) were reported to be the most important in the prediction of plant nutrient status (Mutanga et al. 2005). On the other hand, weak correlation was observed between mid-IR and plant nutrient (Mutanga, Skidmore, and Prins 2004), while biomass and LAI estimation was reported to improve with the inclusion of mid-IR wavebands (Darvishzadeh et al. 2008; Fava et al. 2009).

The VIs varied in separating the N treatments at each sampling date based on the lowest Wilk's lambda achieved at the leaf and canopy scale (Table 3.9). In switchgrass, the RENDVI, $Cl_{red\ edge}$ and Cl_{green} were the indices observed for the separation of the N treatments at the canopy scale in 2011 and 2012. These indices are computed from wavebands in the red edge (680-740 nm) and NIR (750–1350 nm) regions of the spectrum. On the other hand, at leaf scale TCARI, ZTM and TGI were the indices that separated the N treatments. The indices at the leaf scale were computed from wavebands in the visible, red and red edge regions of the spectrum. Likewise, in the high biomass sorghum red edge VIs dominated at the canopy scale, while VIs computed from visible and NIR wavebands dominated at leaf scale. The difference between the VIs at the leaf and canopy scale is the dominance of the red edge wavebands in the VIs at the canopy scale. This is not surprising as the red edge region has been well documented for use in the estimation vegetation nutritional status and productivity (Filella and Penuelas 1994; Lamb et al. 2002; Mutanga and Skidmore 2004). Wavebands and VIs identified at the canopy scale indicates that canopy scale data could provide information related to both the biochemical and biophysical characteristics.

The individual wavebands were more constant at the leaf scale for both 2011 and 2012 season in comparison to at the canopy scale. The relative constant wavebands for the leaf spectra throughout the growing season agreed with Pinter et al.(2003).They noted that leaf spectra tends to remain relatively constant throughout the season, while canopy spectra changes dynamically as the proportions of soil and vegetation change and the architectural arrangement of plants components vary. The variation in VIs and wavebands for separating the N treatments at the canopy and leaf reflectance suggest that species, growth habits and canopy structures play a critical role. In this study, the switchgrass differs from the high biomass sorghum due to growth habit. The switchgrass produces numerous amounts of tillers resulting in many leaves per individual plants and has a more erectophile leaf orientation. While the high biomass sorghum produces only a few tillers resulting in fewer leaves per individual plant and larger leaves in a more planophile leaf orientation. Kimes (1984) modeling the directional reflectance from complete homogeneous vegetation canopies with various leaf-orientation distribution found simulated reflectance distribution was unique to classical leaf-orientation (electophile, spherical, planophile, and diahelotropic). Kimes (1984) study also pointed out that erectophile canopy showed the greatest variation in reflectance as a function of view angle and planophile the least variation in reflectance. The larger leaf and planophile leaf orientation of the high biomass sorghum was considered the reason for the frequency of VIs related to biochemical properties occurring at the canopy scale and the greater separation based on Wilk's lambda value for both individual wavebands and VIs. These results confirms that leaf spectra data are less variable and may provide good estimation of the biochemical composition within the plant using chlorophyll related VIs and canopy spectra to be more variable, but could be used to estimate both biophysical such as biomass and biochemical composition of the vegetation. Greater separation in N treatment based on individual wavebands and VIs was observed at leaf scale compared to canopy scale and in the high biomass sorghum compared to the switchgrass.

Timing of Fertilization

In general, it can be expected that the time of greatest separation in N treatment is also an indication of the time of greatest N demand by the plant. Therefore, separation of N treatment could be indicative of the response to the N fertilization. The results of this study demonstrate that the time of greatest separation for the N treatments were early in the growing season within four weeks following N application. Similarly, Lofton et al. (2012) also reported strongest relationship between a NDVI response index and harvest response index occurring four weeks after N application in sugarcane. Detecting of N deficiency is very difficult in active growing crops (Raun et al. 2008; Lofton et al. 2012). Therefore, the use of the nitrogen reference strip approach proposed by Raun et al. (2008) for wheat production systems in Oklahoma for midseason N application could also be useful in bioenergy crop production systems, particularly for the high biomass sorghum. The ability to discriminate among N treatment in high biomass sorghum within 2-4wks after N fertilization suggested that the nitrogen reference strip approach could be of value in these crop production systems.

In bioenergy crop production systems, nitrogen fertilizer will most likely be applied in a single rate across the whole field at planting or within a few weeks after planting. The timing of the separation of N treatments suggests that N reference strip could be established within the high biomass sorghum at planting and switchgrass at or before green-up. Separation of the N reference strip using appropriate an optimal hyperspectral sensor could be determined as early as 4-6 weeks after planting in the high biomass sorghum and within 4-8 weeks after green-up in switchgrass. The lack of separation in switchgrass at the early stage may imply that application of N prior to or closer to green up could increase responsiveness. In fact, increase responsiveness was observed, in 2013 from N application at green-up in switchgrass. Because N response is strongly tied to the climatic condition of each growing season, it is not usually that degree of separation (Wilk's lambda value) varied greatly across seasons at both leaf and canopy scale. However, results of this study indicate that both leaf and canopy scale data could be used to separate the N treatments, but greater separation was observed at the leaf level. Leaf sampling at field scale impractical, due to the intense labor and cost factor, but canopy separation offers a more realistic approach for field scale sampling.

Optimum rate of N fertilization changes dramatically from year to year due to the dynamics of the amount of N supplied into the cropping system from residual N (previous year application), organic matter and atmospheric deposition. Soil test taken early in season does not account for the contribution of N released from organic matter. While plant testing to obtain a representative sample of an entire field would be similar to leaf sampling, labor intensive and expensive. The N reference strip approach has shown replicability across 36 on farm trials in wheat fields in Oklahoma (Roberts et al. 2011).

In addition, the results of the study also indicates that late season acquisition of crop spectra could also provide important information that could be used for forecasting the coming year nutrient status and/or current crop yield and identify portions of field affected by environmental stress. Detection of N deficiency late in the season could be used as an indication of soil N status that could be addressed in the coming growing season, as well as be used in regression models for predicting crop yield. Areas in fields affected by environmental stress could be identified and monitored for early detection in the coming season. For example, areas of weed infestation could be identified from late season spectral measurements, providing information for and early season application at a time weeds are more susceptible resulting in increased weed control.

CONCLUSIONS

Sampling dates with the greatest separation did not differ for high biomass sorghum using leaf and canopy scale reflectance data, but differed for switchgrass. The greatest separation of the N treatments in switchgrass occurred late in the season at canopy scale and early in the season at leaf scale. High biomass sorghum was best separated early in the season at leaf and canopy scale approximately four weeks after N application. Separation using individual wavebands was found to be more constant across seasons at the leaf and canopy levels in comparison to using VIs that varied greatly across season and at the leaf and canopy scale. Leaf scale spectra was found to be more easily separated by VIs and wavebands more strongly correlated with plant chlorophyll, while the canopy spectra was more easily separated by VIs and wavebands related to biomass and LAI. The benefit of hyperspectral reflectance is that it allows for the computation of multiple VIs that take advantage of wavebands in the different regions of the spectrum for monitoring changes in crop characteristics. These results indicate that hyperspectral reflectance could offer great potential for the development of models for the estimation of biomass yield and quality.

REFERENCES

Abdel-Rahman, E.M., F.B. Ahmed, and M. Van den Berg. 2010. "Estimation of sugarcane leaf nitrogen concentration using in situ spectroscopy." *International Journal of Applied Earth Observation and Geoinformation* 12:S52-S7.

Adams, John B, Donald E Sabol, Valerie Kapos, Raimundo Almeida Filho, Dar A Roberts, Milton O Smith, and Alan R Gillespie. 1995. "Classification of multispectral images based on fractions of endmembers: Application to land-cover change in the Brazilian Amazon." *Remote Sensing of Environment* 52 (2):137-54.

Bajwa, S.G. and , and S.S. Kulkarni. 2012. "Hyperspectral data mining." In *Hyperspectral Remote Sensing of Vegetation*, edited by J.G. Lyon Thenkabail P. S., and A. Huete, 93-120. Boca Raton, FL: CRC Press.

Baret, F., and G. Guyot. 1991. "Potentials and limits of vegetation indices for LAI and APAR assessment." *Remote Sensing of Environment* 35 (2–3):161-73. doi: 10.1016/0034-4257(91)90009-u.

Birth, G. S., and G. R. Mcvey. 1968. "Measuring Color of Growing Turf with a Reflectance Spectrophotometer." *Agronomy Journal* 60 (6):640-&.

Blackburn, G.A. 1998. "Quantifying chlorophylls and caroteniods at leaf and canopy scales: An evaluation of some hyperspectral approaches." *Remote Sensing of Environment* 66 (3):273-85.

Broge, N.H., and E. LeBlanc. 2000. "Comparing predictive power and stability of broad-band and hyperspectral vegetation indices for estimation of green leaf area index and canopy chlorophyll density." *Remote Sens. Environ.* 76:156-72.

Bruce, Lori Mann, Cliff H Koger, and Jiang Li. 2002. "Dimensionality reduction of hyperspectral data using discrete wavelet transform feature extraction." *Geoscience and Remote Sensing, IEEE Transactions on* 40 (10):2331-8.

Chan, Jonathan Cheung-Wai, and Desiré Paelinckx. 2008. "Evaluation of Random Forest and Adaboost tree-based ensemble classification and spectral band selection for ecotope mapping using airborne hyperspectral imagery." *Remote Sensing of Environment* 112 (6):2999-3011.

Chappelle, E. W., M. S. Kim, and J. E. Mcmurtrey. 1992. "Ratio Analysis of Reflectance Spectra (Rars) - an Algorithm for the Remote Estimation of the Concentrations of Chlorophyll-a, Chlorophyll-B, and Carotenoids in Soybean Leaves." *Remote Sensing of Environment* 39 (3):239-47.

Chen, P., D. Haboudane, N. Tremblay, J. Wang, P. Vigneault, and B. Li. 2010. "New spectral indicator assessing the efficiency of crop nitrogen treatment in corn and wheat." *Remote Sensing of Environment* 114 (9):1987-97.

Cho, MA. 2007. *Hyperspectral remote sensing of biochemical and biophysical parameters: the derivate red-edge" double-peak feature", a nuisance or an opportunity?* : PhD thesis, Wageningen University, the Netherlands.

Cho, Moses Azong, Andrew Skidmore, Fabio Corsi, Sipke E Van Wieren, and Istiak Sobhan. 2007. "Estimation of green grass/herb biomass from airborne hyperspectral imagery using spectral indices and partial least squares regression." *International Journal of Applied Earth Observation and Geoinformation* 9 (4):414-24.

Clark, Roger N, and Ted L Roush. 1984. "Reflectance spectroscopy: Quantitative analysis techniques for remote sensing applications." *Journal of Geophysical Research: Solid Earth (1978–2012)* 89 (B7):6329-40.

Darvishzadeh, R., A. Skidmore, M. Schlerf, C. Atzberger, F. Corsi, and M. Cho. 2008. "LAI and chlorophyll estimation for a heterogeneous grassland using hyperspectral measurements." *ISPRS journal of photogrammetry and remote sensing* 63 (4):409-26.

Daughtry, C. S. T., C. L. Walthall, M. S. Kim, E. B. de Colstoun, and J. E. McMurtrey. 2000. "Estimating corn leaf chlorophyll concentration from leaf and canopy reflectance." *Remote Sensing of Environment* 74 (2):229-39.

Everitt, JH, AJ Richardson, and HW Gausman. 1985. Leaf reflectance-nitrogen-chlorophyll relations in buffelgrass. Paper presented at the ASP, Annual Meeting, 51 st, Washington, DC.

Fava, F., R. Colombo, S. Bocchi, M. Meroni, M. Sitzia, N. Fois, and C. Zucca. 2009. "Identification of hyperspectral vegetation indices for Mediterranean pasture characterization." *International Journal of Applied Earth Observation and Geoinformation* 11 (4):233-43.

Feng, W., X. Yao, Y. Zhu, YC Tian, and WX Cao. 2008. "Monitoring leaf nitrogen status with hyperspectral reflectance in wheat." *European Journal of Agronomy* 28 (3):394-404.

Filella, I., and J. Penuelas. 1994. "The red edge position and shape as indicators of plant chlorophyll content, biomass and hydric status." *International Journal of Remote Sensing* 15 (7):1459-70.

Filippi, Anthony M, and John R Jensen. 2006. "Fuzzy learning vector quantization for hyperspectral coastal vegetation classification." *Remote Sensing of Environment* 100 (4):512-30.

Foster, Anserd J., Vijaya Gopal Kakani, Jianjun Ge, and Jagadeesh Mosali. 2012. "Discrimination of Switchgrass Cultivars and Nitrogen Treatments Using Pigment Profiles and Hyperspectral Leaf Reflectance Data." *Remote Sensing* 4 (9):2576-94.

Gamon, JA, J. Penuelas, and CB Field. 1992. "A narrow-waveband spectral index that tracks diurnal changes in photosynthetic efficiency." *Remote Sensing of Environment* 41 (1):35-44.

Gitelson, A. A. 2012. "Nondestructive Estimation of Foliar Pigment (Chlorophylls,, Carotenoids and Anthocyanins) contents: Evaluating a Semianalytical Three-Band Model." In *Hyperspectral Remote Sensing of Vegetation*, edited by P. S. Thenkabail, J.G. Lyon, and A. Huete, 141-66. Boca Rotan, FL: CRC Press.

Gitelson, A. A., Y. Gritz, and M. N. Merzlyak. 2003. "Relationships between leaf chlorophyll content and spectral reflectance and algorithms for non-destructive chlorophyll assessment in higher plant leaves." *Journal of Plant Physiology* 160 (3):271-82.

Gitelson, A. A., and M. N. Merzlyak. 1997. "Remote estimation of chlorophyll content in higher plant leaves." *International Journal of Remote Sensing* 18 (12):2691-7.

Gitelson, A. A., A. Vina, V. Ciganda, D. C. Rundquist, and T. J. Arkebauer. 2005. "Remote estimation of canopy chlorophyll content in crops." *Geophysical Research Letters* 32 (8). doi: Artn L08403Doi 10.1029/2005gl022688.

Goel, N.S. 1989. *Inversion of canopy reflectance models for estimation of biophysical parameters from reflectance data*: Wiley Interscience, New York.

Haboudane, D., J. R. Miller, E. Pattey, P. J. Zarco-Tejada, and I. B. Strachan. 2004. "Hyperspectral vegetation indices and novel algorithms for predicting green LAI of crop canopies: Modeling and validation in the context of precision agriculture." *Remote Sensing of Environment* 90 (3):337-52. doi: DOI 10.1016/j.rse.2003.12.013.

Haboudane, D., J. R. Miller, N. Tremblay, P. J. Zarco-Tejada, and L. Dextraze. 2002. "Integrated narrow-band vegetation indices for prediction of crop chlorophyll content for application to precision agriculture." *Remote Sensing of Environment* 81 (2-3):416-26.

Hansen, PM, and JK Schjoerring. 2003. "Reflectance measurement of canopy biomass and nitrogen status in wheat crops using normalized difference vegetation indices and partial least squares regression." *Remote Sensing of Environment* 86 (4):542-53.

Hatfield, J. L. , and J. H. Prueger. 2010. "Value of using different vegetative indices to quantify agricultural crop characteristics at different growth stages under varying management practices." *Remote Sensing* 2:562 -78.

Hatfield, JL, A.A. Gitelson, J.S. Schepers, and CL Walthall. 2008. "Application of spectral remote sensing for agronomic decisions." *Agronomy Journal* 100 (Supplement_3):S-117-S-31.

Hsu, Pai-Hui. 2007. "Feature extraction of hyperspectral images using wavelet and matching pursuit." *ISPRS journal of photogrammetry and remote sensing* 62 (2):78-92.

Huete, A., K. Didan, T. Miura, E. P. Rodriguez, X. Gao, and L. G. Ferreira. 2002. "Overview of the radiometric and biophysical performance of the MODIS vegetation indices." *Remote Sensing of Environment* 83 (1-2):195-213.

Hunt, E.R., CST Daughtry, J.U.H. Eitel, and D.S. Long. 2011. "Remote Sensing Leaf Chlorophyll Content Using a Visible Band Index." *Agronomy Journal* 103 (4):1090-9.

Hunt Jr, E. Raymond, Paul C. Doraiswamy, James E. McMurtrey, Craig S. T. Daughtry, Eileen M. Perry, and Bakhyt Akhmedov. 2013. "A visible band index for remote sensing leaf chlorophyll content at the canopy scale." *International Journal of Applied Earth Observation and Geoinformation* 21 (0):103-12. doi: 10.1016/j.jag.2012.07.020.

Ingram, J Carter, Terence P Dawson, and Robert J Whittaker. 2005. "Mapping tropical forest structure in southeastern Madagascar using remote sensing and artificial neural networks." *Remote Sensing of Environment* 94 (4):491-507.

Jacquemoud, S., and F. Baret. 1990. "PROSPECT: A model of leaf optical properties spectra." *Remote Sensing of Environment* 34 (2):75-91.

Jacquemoud, S., SL Ustin, J. Verdebout, G. Schmuck, G. Andreoli, and B. Hosgood. 1996. "Estimating leaf biochemistry using the PROSPECT leaf optical properties model." *Remote Sensing of Environment* 56 (3):194-202.

Johnson, R.M., R.P. Viator, J.C. Veremis, P.E. Richard, and P.V. Zimba. 2008. "Discrimination of sugarcane varieties with pigment profiles and high resolution, hyperspectral leaf reflectance data." *Journal Association Sugar Cane Technologists* 28:63-75.

Jollineau, MY, and PJ Howarth. 2008. "Mapping an inland wetland complex using hyperspectral imagery." *International Journal of Remote Sensing* 29 (12):3609-31.

Kakani, V. G., K. R. Reddy, D. Zhao, S. Koti, and W. Gao. 2004. "Interactive effects of ultraviolet-B radiation and temperature on cotton physiology, growth, development and hyperspectral reflectance." *Photochemistry and Photobiology* 79 (5):416-27.

Kimes, DS. 1984. "Modeling the directional reflectance from complete homogeneous vegetation canopies with various leaf-orientation distributions." *JOSA A* 1 (7):725-37.

Kokaly, Raymond F, Gregory P Asner, Scott V Ollinger, Mary E Martin, and Carol A Wessman. 2009. "Characterizing canopy biochemistry from imaging spectroscopy and its application to ecosystem studies." *Remote Sensing of Environment* 113:S78-S91.

Kokaly, Raymond F., and Roger N. Clark. 1999. "Spectroscopic Determination of Leaf Biochemistry Using Band-Depth Analysis of Absorption Features and Stepwise Multiple Linear Regression." *Remote Sensing of Environment* 67 (3):267-87. doi: http://dx.doi.org/10.1016/S0034-4257(98)00084-4.

Kosaka, Naoko, Kuniaki Uto, and Yukio Kosugi. 2005. "ICA-aided mixed-pixel analysis of hyperspectral data in agricultural land." *Geoscience and Remote Sensing Letters, IEEE* 2 (2):220-4.

Lamb, DW, M. Steyn-Ross, P. Schaare, MM Hanna, W. Silvester, and A. Steyn-Ross. 2002. "Estimating leaf nitrogen concentration in ryegrass (Lolium spp.) pasture using the chlorophyll red-edge: theoretical modelling and experimental observations." *International Journal of Remote Sensing* 23 (18):3619-48.

Liu, Zhan-Yu, Hong-Feng Wu, and Jing-Feng Huang. 2010. "Application of neural networks to discriminate fungal infection levels in rice panicles using hyperspectral reflectance and principal components analysis." *Computers and Electronics in Agriculture* 72 (2):99-106.

Lofton, J, BS Tubana, Y Kanke, J Teboh, and H Viator. 2012. "Predicting sugarcane response to nitrogen using a canopy reflectance-based response index value." *Agronomy Journal* 104 (1):106-13.

Lusch, D.P. 1999. *Introduction to environmental remote sensing*. East Lansing: Center for Remote Sensing and GIS Michigan State University

Merzlyak, M. N., A. A. Gitelson, O. B. Chivkunova, and V. Y. Rakitin. 1999. "Non-destructive optical detection of pigment changes during leaf senescence and fruit ripening." *Physiologia Plantarum* 106 (1):135-41.

Miphokasap, P., K. Honda, C. Vaiphasa, M. Souris, and M. Nagai. 2012. "Estimating Canopy Nitrogen Concentration in Sugarcane Using Field Imaging Spectroscopy." *Remote Sensing* 4 (6):1651-70.

Mitchell, Jessica J., Nancy F. Glenn, Temuulen T. Sankey, DeWayne R. Derryberry, and Matthew J. Germino. 2012. "Remote sensing of sagebrush canopy nitrogen." *Remote Sensing of Environment* 124 (0):217-23. doi: http://dx.doi.org/10.1016/j.rse.2012.05.002.

Muchovej, RM, and PR Newman. 2004. "Nitrogen fertilization of Sugarcane on sandy soil: Yield and leaf nutrient composition." *Journal American Society Sugar Cane Technologists* 24.

Mutanga, O., and A.K. Skidmore. 2004. "Hyperspectral band depth analysis for a better estimation of grass biomass (< i> Cenchrus ciliaris</i>) measured under controlled laboratory conditions." *International Journal of Applied Earth Observation and Geoinformation* 5 (2):87-96.

Mutanga, O., AK Skidmore, L. Kumar, and J. Ferwerda. 2005. "Estimating tropical pasture quality at canopy level using band depth analysis with continuum removal in the visible domain." *International Journal of Remote Sensing* 26 (6):1093-108.

Mutanga, Onisimo, Andrew K Skidmore, and Sipke van Wieren. 2003. "Discriminating tropical grass (< i> Cenchrus ciliaris</i>) canopies grown under different nitrogen treatments using spectroradiometry." *ISPRS journal of photogrammetry and remote sensing* 57 (4):263-72.

Myneni, R.B., and G. Asrar. 1993. "Radiative transfer in three-dimensional atmosphere-vegetation media." *Journal of Quantitative Spectroscopy and Radiative Transfer* 49 (6):585-98.

Numata, I. 2012. "Characterization on Pastures Using Field and Imaging Spectrometers." In *Hyperspectral Remote Sensing of Vegetation*, edited by P. S. Thenkabail, J.G. Lyon, and A. Huete, 207-26. Boca Raton, FL: CRC Press.

Penuelas, J., I. Filella, P. Lloret, F. Munoz, and M. Vilajeliu. 1995. "Reflectance Assessment of Mite Effects on Apple-Trees." *International Journal of Remote Sensing* 16 (14):2727-33.

Peñuelas, J., J. A. Gamon, A. L. Fredeen, J. Merino, and C. B. Field. 1994. "Reflectance indices associated with physiological changes in nitrogen- and water-limited sunflower leaves." *Remote Sensing of Environment* 48 (2):135-46. doi: 10.1016/0034-4257(94)90136-8.

Pinter, P.J., J.L. Hatfield, J.S. Schepers, E.M. Barnes, M.S. Moran, C.S.T. Daughtry, and D.R. Upchurch. 2003. "Remote sensing for crop management." *Photogrammetric engineering and remote sensing* 69 (6):647-64.

Raun, WR, JB Solie, ML Stone, KL Martin, KW Freeman, RW Mullen, H Zhang, JS Schepers, and GV Johnson. 2005. "Optical Sensor-Based Algorithm for Crop Nitrogen Fertilization." *Communications in soil science and plant analysis* 36 (19-20):2759-81.

Raun, WR, JB Solie, RK Taylor, DB Arnall, CJ Mack, and DE Edmonds. 2008. "Ramp calibration strip technology for determining midseason nitrogen rates in corn and wheat." *Agronomy Journal* 100 (4):1088-93.

Ray, S.S., J.P. Singh, and S. Panigrahy. 2010. "Use of hyperspectral remote sensing data for crop stress detection: Ground-based studies." In *International Archives of the Photogrammetry, Remote Sensing and Spatial Information Science* 562-7. Kyoto, Japan.

Roberts, DA, G Batista, J Pereira, E Waller, and B Nelson. 1999. "Change identification using multitemporal spectral mixture analysis: Applications in eastern Amazônia."

Roberts, David C, B Wade Brorsen, Randal K Taylor, John B Solie, and William R Raun. 2011. "Replicability of nitrogen recommendations from ramped calibration strips in winter wheat." *Precision Agriculture* 12 (5):653-65.

Roujean, J. L., and F. M. Breon. 1995. "Estimating Par Absorbed by Vegetation from Bidirectional Reflectance Measurements." *Remote Sensing of Environment* 51 (3):375-84.

Rouse, J.W., R.H. Hass, J.A. Schell, and D.W. Deering. 1973. Monitoring vegetation system in great plains with ERTS. Paper presented at the Proc. 3rd ERTS-1 Symp., GSFC, NASA,SP-351.

SAS. 2009. "Sas User's Guide." In *SAS Institute Inc.* Cary, North Carolina.

Strachan, I.B., E. Pattey, and J.B. Boisvert. 2002. "Impact of nitrogen and environmental conditions on corn as detected by hyperspectral reflectance." *Remote Sensing of Environment* 80 (2):213-24.

Stroppiana, D., M. Boschetti, P.A. Brivio, and S. Bocchi. 2009. "Plant nitrogen concentration in paddy rice from field canopy hyperspectral radiometry." *Field Crops Research* 111 (1):119-29.

Stroppiana, D., F. Fava, M. Boschetti, and P.A. Brivio. 2012. "Estimation of Nitrogen Content in Crops and Pastures Using Hyperspectral Vegetation Indices." In *Hyperspectral Remote Sensing of Vegetation*, edited by P. S. Thenkabail, J.G. Lyon, and A. Huete, 245-64. Boca Rotan, FL: CRC Press.

Thenkabail, P. S., E. A. Enclona, M. S. Ashton, and B. Van der Meer. 2004. "Accuracy assessments of hyperspectral waveband performance for vegetation analysis applications." *Remote Sensing of Environment* 91 (3-4):354-76. doi: DOI 10.1016/j.rse.2004.03.013.

Thenkabail, P. S., I. Mariotto, M. K. Gumma, E. M. Middleton, D. R. Landis, and K. F. Huemmrich. 2013. "Selection of Hyperspectral Narrowbands (HNBs) and Composition of Hyperspectral Twoband Vegetation Indices (HVIs) for Biophysical Characterization and Discrimination of Crop Types Using Field Reflectance and Hyperion/EO-1 Data." *Selected Topics in Applied Earth Observations and Remote Sensing, IEEE Journal of* 6 (2):427-39. doi: 10.1109/jstars.2013.2252601.

Thenkabail, P.S., J.G. Lyon, and A. Huete.2012. "Advances in Hyperspectral Remote Sensing of Vegetation and Agricultural Croplands." In *Hyperspectral Remote Sensing of Vegetation*, edited by P. S. Thenkabail, J.G. Lyon, and A. Huete, 3-39. Boca Raton, FL: CRC Press.

Thenkabail, P.S., R.B. Smith, and E. De Pauw. 2000. "Hyperspectral vegetation indices and their relationships with agricultural crop characteristics." *Remote Sensing of Environment* 71 (2):158-82.

Trombetti, M, D Riaño, MA Rubio, YB Cheng, and SL Ustin. 2008. "Multi-temporal vegetation canopy water content retrieval and interpretation using artificial neural networks for the continental USA." *Remote Sensing of Environment* 112 (1):203-15.

Verhoef, W. 1984. "Light scattering by leaf layers with application to canopy reflectance modeling: the SAIL model." *Remote Sensing of Environment* 16 (2):125-41.

Vogelmann, J. E., B. N. Rock, and D. M. Moss. 1993. "Red Edge Spectral Measurements from Sugar Maple Leaves." *International Journal of Remote Sensing* 14 (8):1563-75.

White, J.C., C. Gómez, M.A. Wulder, and N.C. Coops. 2010. "Characterizing temperate forest structural and spectral diversity with Hyperion EO-1 data." *Remote Sensing of Environment* 114 (7):1576-89.

Xue, L., W. Cao, W. Luo, T. Dai, and Y. Zhu. 2004. "Monitoring leaf nitrogen status in rice with canopy spectral reflectance." *Agronomy Journal* 96 (1):135-42.

Yao, X., Y. Zhu, Y.C. Tian, W. Feng, and W.X. Cao. 2010. "Exploring hyperspectral bands and estimation indices for leaf nitrogen accumulation in wheat." *International Journal of Applied Earth Observation and Geoinformation* 12 (2):89-100.

Zarco-Tejada, P. J., J. R. Miller, T. L. Noland, G. H. Mohammed, and P. H. Sampson. 2001. "Scaling-up and model inversion methods with narrowband optical indices for chlorophyll content estimation in closed forest canopies with hyperspectral data." *Ieee Transactions on Geoscience and Remote Sensing* 39 (7):1491-507.

Zhang, Y. 2012. "Forest Leaf Chlorophyll Study Using Hyperspectral Remote Sensing." In *Hyperspectral Remote Sensing of Vegetation*, edited by P. S. Thenkabail, J.G. Lyon, and A. Huete, 167-86. Boca Raton, Fl: CRC Press.

Zhu, Y., W. Wang, and X. Yao. 2012. "Estimating Leaf Nitrogen Concentration (LNC) of Cereal Crops with Hyperspectral Data." In *Hyperspectral Remote Sensing of Vegetation*, edited by P. S. Thenkabail, J.G. Lyon, and A. Huete, 187-206. Boca Raton, FL: CRC Press.

Zhu, Y., D. Zhou, X. Yao, Y. Tian, and W. Cao. 2007. "Quantitative relationships of leaf nitrogen status to canopy spectral reflectance in rice." *Crop and Pasture Science* 58 (11):1077-85.

Table 3.1.Characteristics of the experimental plot and cultural practices used for the management of crops and sampling dates

Site Characteristics	
Location	36.130 °N 97.104 °W
Soil texture	Easpur loam (Fine-loamy, mixed, superactive, thermic Fluventic Haplustolls)
Soil fertility (2012)†	pH:6.1, NO_3-N: 4 mgkg^{-1}, P:30 mgkg^{-1}, and K:176 mgkg^{-1}
Annual precipitation, mm	403 (2011) and 563 (2012)
Annual air temperature °C(Min/Max)	-28.5/43.6 (2011) and -9.8/45 (2012)
Cultural practice	
Planting	Switchgrass was planted on 5 May 2010; high biomass sorghum on 5 May 2011 and 6 April 2012; Legumes; Hairy vetch on 23 February 2011; Crimson clover on 27 February 2012
Fertilizing	Switchgrass was fertilized on 23 May 2011 and 19 April 2012 ; high biomass sorghum on 23 May 2011 and 4 May 2012
Spraying	30 July 2012 sprayed Sevin insecticide for grasshopper control at rate of 2.3 L ha^{-1} at Stillwater.
Sampling	
May	16 May 2012
June	17 June 2011; 14 June 2012
July	26 July 2011; 18 July 2012
August	27 July 2011; 20 August 2012
September	12 September 2012

*Normal annual precipitation based on 30 year average is 918 mm for Stillwater, † Soil samples were collected within each plot before fertilization and are expressed as a mean values for the Stillwater site.

Table 3.2.Sampling date (June – August 2011 and May – September 2012), canopy height, sensor height, diameter of field of view (FOV) and number of samples for canopy reflectance collected by ASD spectrophotometer on high biomass sorghum and switchgrass in Oklahoma for the 2011 and 2012 growing season

Sampling Date	Canopy height (cm)		Diameter of FOV (cm)		Sensor height aboveground (cm)	No. of Samples collected
	High Biomass Sorghum	Switchgrass	High Biomass Sorghum	Switchgrass		
			2012			
May	30-45	80-140	67-74	26-52	200	60
June	80-180	110-180	26-69	26-56	240	60
July	130-220	110-200	30-69	39-78	290	60
August	170-240	110-220	22-52	30-78	290	60
September	180-250	110-220	18-48	30-78	290	60
			2011			
June	40-80	90-120	65-82	48-60	230	60
July	40-80	90-130	65-82	47-60	230	60
August	60-140	100-150	39-73	35-56	230	60

Table 3.3. Narrowband Hyperspectal Vegetation Indices used in the study.

Index	Wavebands	References
	Structural Indices	
Simple Ratio (SR)	$SR = R_{NIR}/R_{red}$	(Birth and Mcvey 1968)
Normalized Difference Vegetation Index (NDVI)	Red $NDVI = (R_{NIR} – R_{red})/ (R_{NIR} + R_{red})$	(Rouse et al. 1973)
	Green $NDVI(R_{NIR} – R_{green})/ (R_{NIR} + R_{green})$	(Gitelson, Gritz, and Merzlyak 2003)
	Red Edge $NDVI = (R_{NIR} – R_{red\ edge}) / (R_{NIR} + R_{red\ edge})$	(Gitelson, Gritz, and Merzlyak 2003)
Renormalized Difference Vegetation Index (RDVI)	$RDVI = (R_{800} - R_{670}) / (R_{800} + R_{670})^{0.5}$	(Roujean and Breon 1995)
Enhanced Vegetation Index (EVI)	$EVI = 2.5(R_{NIR} – R_{red})/ (R_{NIR} + 6R_{red} – 7.5R_{blue} + 1)$	(Huete et al. 2002)
Plant Senescence Reflectance Index (PSRI)	$PSRI = (R_{660} – R_{510})/ R_{760}$	(Merzlyak et al. 1999; Hatfield and Prueger 2010)
Soil Adjusted Vegetation Index (SAVI)	$SAVI = (1+0.5)(R_{800} – R_{670}) / (R_{800} + R_{670} + 0.5)$	
	Chlorophyll/Pigment Related Indices	
Chlorophyll Indices (Cl)	$Cl_{green} = (R_{NIR} /R_{green}) -1$	(Gitelson, Gritz, and Merzlyak 2003; Gitelson et al. 2005)
	$Cl_{red\ edge} = (R_{NIR} /R_{red\ edge}) -1$	(Gitelson, Gritz, and Merzlyak 2003; Gitelson et al. 2005)
Normalized Pigment Chlorophyll Ratio Index (NPCI)	$NPCI = (R_{660} – R_{460}) /(R_{660} + R_{460})$	(Merzlyak et al. 1999)
Modified CARI (MCARI)	$MCARI = [(R_{700} – R_{670}) -0.2(R_{700} – R_{500}) (R_{700}/R_{670})]$	(Daughtry et al. 2000)
Transformed CARI (TCARI)	$TCARI = 3[(R_{700} – R_{670}) -0.2(R_{700} – R_{500}) (R_{700}/R_{670})]$	(Haboudane et al. 2004)
Triangular Vegetation Index (TVI)	$TVI = 0.5[120(R_{750} – R_{550}) -200(R_{670} –R_{550})$	(Broge and LeBlanc 2000)
Structural Insensitive Pigment Index (SIPI)	$SIPI = (R_{800} –R_{430}) / (R_{800} + R_{680})$	(Penuelas et al. 1995)
Triangular Greenness Index (TGI)	$TGI = -0.5[190(R_{670} – R_{550}) -120(R_{670} – R_{480})]$	(Hunt et al. 2011)
Photochemical Reflectance Index (PRI)	$PRI =(R_{550} – R_{530}) / (R_{570} + R_{531})$	(Gamon, Penuelas, and Field 1992)
	Red Edge Indices	
Red edge (750 ~700)	$R_{750} – R_{700}$	(Gitelson and Merzlyak 1997)
Red edge (740 ~720)	$R_{740} – R_{720}$	(Vogelmann, Rock, and Moss 1993)
Zarco Tejada and Miller (ZTM)	$ZTM = R_{750} / R_{710}$	(Zarco-Tejada et al. 2001)

R: spectral reflectance, NIR: Near infrared (750-1350 nm), Green (520-590 nm), Red (600-680 nm), Red edge (690-740 nm)

Table 3.4. PCA results with five wavebands, highest factor loadings (eigenvectors) and the percent variability explained by each principal for characterizing leaf and canopy spectral reflectance of five N treatments in switchgrass (2011).

	Waveband center (nm) with first 15 highest factor loadings			**Percent variability explained**			**Cumulative variability explained by first three PCs (%)**
			LEAF SPECTRA				
	PC1	PC2	PC3	PC1	PC2	PC3	
[1]17-June-11	1770;1660;1670; 1760;1650	2000;2010;1990; 1980;2020	520;510;580; 610;600	50	32	15	97
Dominating waveband	Mid-IR	Mid-IR	Green				
[1]27-Jul-11	1620;1600;1650; 1610;1630	780;790;800; 770;810	500;490;510; 480;470	54	32	10	96
Dominating waveband	Mid-IR	NIR	Blue				
[1]26-Aug-11	1730;1760;1740; 1770;1730	950;990;980; 930; 970	520;510;640; 620;630	55	23	17	95
Dominating waveband	Mid-IR	NIR	Red				
Dominating waveband for leaf spectra	Mid-IR	NIR	Blue				
Mean (%)				53	29	14	96
			CANOPY SPECTRA				
[1]17-June-11	1540;1550;1530; 1560;1510	670;680;660; 690;650	400;410;430; 420;440	90	6	2	98
Dominating waveband	Mid-IR	Red	Blue				
[1]27-Jul-11	2210;2200;2220; 2230;2140	2450;2440;2430; 2420;720	1970;2000;1980; 1990;2010	87	7	3	97
Dominating waveband	Mid-IR	Mid-IR	Mid-IR				
[1]26-Aug-11	1590;1700;1600; 1580;1630	1970;1980;1990; 2000;2010	410;500;400; 460;450	89	8	2	99
Dominating waveband	Mid-IR	Mid-IR	Blue				
Dominating waveband for canopy spectra	Mid-IR	Mid-IR	Blue				
Mean (%)				89	7	2	98
Dominating waveband for all above	Mid-IR	Mid-IR	Blue				
Overall Mean (%)				71	18	8	97

Blue (400-520 nm); Green (520-590); Red (600-690 nm); NIR: near infrared (700-1350 nm); Mid-IR: Middle infrared (1350-2500 nm). [1]Date of data collection.

Table 3.5. PCA results with five wavebands, highest factor loadings (eigenvectors) and the percent variability explained by each principal for characterizing leaf and canopy spectral reflectance of five N treatments in switchgrass (2012).

	Waveband center (nm) with first 15 highest factor loadings			**Percent variability explained**			**Cumulative variability explained by first three PCs (%)**
			LEAF SPECTRA				
	PC1	PC2	PC3	PC1	PC2	PC3	
[1]16-May-12	1330;1320;1310; 1340;1300	500;510;490; 650;660	700;710;570; 720;590	67	19	8	94
Dominating waveband	NIR	Blue	NIR				
[1]18-Jun-12	2030;2040;2020; 2060;2050	530;700;570; 580;520	410;420;400; 430;440	79	9	7	95
Dominating waveband	Mid-IR	Green	Blue				
[1]16-Jul-12	1460;1430;1440; 1450;1480	750;760;770; 740; 780	630;620;610; 700;600	63	23	7	93
Dominating waveband	Mid-IR	NIR	Red				
[1]16-Aug-12	1340;1350;1330; 1320;1660	790;770;780; 810;800	700;600;610; 620;630	57	28	9	94
Dominating waveband	Mid-IR	NIR	Red				
[1]18-Sep-12	2250;2060;2140; 2160;2050	970;960;980; 820;950	510;470;500; 490;480	53	30	12	95
Dominating waveband	Mid-IR	NIR	Blue				
Dominating waveband for leaf spectra	Mid-IR	NIR	Red/Blue				
Mean (%)				64	22	9	95
			CANOPY SPECTRA				
[1]16-May-12	1790;1780;1770; 1500;1490	2460;2450;2430;2440;2410	650;630;640;660;690	86	7	4	97
Dominating waveband	Mid-IR	Mid-IR	Red				
[1]18-Jun-12	1700;1690;1680; 1660;1670	780;790;760;770;750	710;720;560; 570;550	87	9	2	98
Dominating waveband	Mid-IR	NIR	Green				
[1]16-Jul-12	1540;1530;1550; 1520;1790	1110;1100;1010;1020;1090	550;560;720; 570;540	62	30	5	97
Dominating waveband	Mid-IR	NIR	Green				
[1]18-Aug-12	2220;1520;2080; 2110;2090	980;990;970;1120;1000	540;550;560; 530;720	66	26	5	97
Dominating waveband	Mid-IR	NIR	Green				
[1]18-Sep-12	1690;1680;1660; 1670;1630	750;780;760; 770;790	650;640;630; 700;690	55	41	3	99
Dominating waveband	Mid-IR	NIR	Red				
Dominating waveband for canopy spectra	Mid-IR	NIR	Green				
Mean (%)				71	23	4	98
[2]Dominating waveband for all above	Mid-IR	NIR	Red				
Overall Mean (%)				68	22	7	97

Blue (400-520 nm); Green (520-590); Red (600-690 nm); NIR: near infrared (700-1350 nm); Mid-IR: Middle infrared (1350-2500 nm). [1]Date of data collection

Table 3.6. PCA results with five wavebands, highest factor loadings (eigenvectors) and the percent variability explained by each principal for characterizing leaf and canopy spectral reflectance of five N treatments in high biomass sorghum (2011).

	Waveband center (nm) with first 15 highest factor loadings			Percent variability explained			Cumulative variability explained by first three PCs (%)
LEAF SPECTRA							
	PC1	PC2	PC3	PC1	PC2	PC3	
[1]17-June-11	2200;2190;2210; 2220;2170	410;420;430; 1970;1980	550;570;560; 540;530	68	23	6	97
Dominating waveband	Mid-IR	Blue	Green				
[1]27-Jul-11	750;740;760; 770;790	1630;1610;1640; 1620;1650	690;600;560; 580;610	52	36	8	96
Dominating waveband	NIR	NIR	Red				
[1]26-Aug-11	1530;1520;1540; 1660;1510	920;910;900; 890; 930	560;550;710; 570;720	73	20	6	99
Dominating waveband	Mid-IR	NIR	Green				
Dominating waveband for leaf spectra	Mid-IR	NIR	Green				
Mean (%)				64	26	7	97
CANOPY SPECTRA							
[1]17-June-11	1530;1590;1610; 1570;1540	820;830;840; 850;810	550;530;540; 560;570	60	31	6	97
Dominating waveband	Mid-IR	NIR	Green				
[1]27-Jul-11	1590;1580;1600; 1570;2190	830;820;840; 850;810	400;410;420; 430;440	69	25	4	98
Dominating waveband	Mid-IR	NIR	Blue				
[1]26-Aug-11	1590;1580;1600; 1570;1610	770;760;780; 790;800	440;430;420; 410;400	76	23	1	100
Dominating waveband	Mid-IR	NIR	Blue				
Dominating waveband for canopy spectra	Mid-IR	NIR	Blue				
Mean (%)				68	26	4	98
Dominating waveband for all above	Mid-IR	NIR	Blue/Green				
Overall Mean (%)				65	26	6	97

Blue (400-520 nm); Green (520-590); Red (600-690 nm); NIR: near infrared (700-1350 nm); Mid-IR: Middle infrared (1350-2500 nm). [1]Date of data collection.

Table 3.7. PCA results with five wavebands, highest factor loadings (eigen vectors) and the percent variability explained by each principal for characterizing leaf and canopy spectral reflectance of five N treatments in high biomass sorghum (2012).

	Waveband center (nm) with first 15 highest factor loadings			**Percent variability explained**			**Cumulative variability explained by first three PCs (%)**
			LEAF SPECTRA				
	PC1	PC2	PC3	PC1	PC2	PC3	
[1]16-May-12	2050;2030;2040; 2060;2070	510;690;650; 520;630	800;770;840; 780;790	70	21	5	96
Dominating waveband	Mid-IR	Red	NIR				
[1]18-Jun-12	2360;2340;2350; 2330;2370	710;580;590; 600;570	1060;1070;1080; 1090;1050	76	11	9	96
Dominating waveband	Mid-IR	Green	NIR				
[1]16-Jul-12	2440;2450;2460; 2430;2420	700;600;610; 620;630	1010;1020;1140; 1130;1030	75	21	3	99
Dominating waveband	Mid-IR	Red	NIR				
[1]16-Aug-12	1720;1700;1730; 1710;1690	510;520;680; 500;740	420;430;410; 440;450	55	32	9	96
Dominating waveband	Mid-IR	Blue	BLUE				
[1]18-Sep-12	2340;2250;2260; 2330;2280	790;810;780; 770;820	710;720;560; 550;580	53	32	12	97
Dominating waveband	Mid-IR	NIR	Green				
Dominating waveband for leaf spectra	Mid-IR	Red	NIR				
Mean (%)				66	23	8	97
			CANOPY SPECTRA				
[1]16-May-12	1510;2170;2180; 2190;2160	1250;1180;1260; 1230;1240	450;520;430; 440;490	58	37	4	99
Dominating waveband	Mid-IR	NIR	Blue				
[1]18-Jun-12	1560;1550;1570; 1780;1770	1970;1980;1990; 2000;2450	550;560;540; 530;570	70	24	4	98
Dominating waveband	Mid-IR	Mid-IR	Green				
[1]16-Jul-12	1570;1560;1580; 1550;1760	790;780;800; 810;770	440;420;430; 410;400	74	23	2	99
Dominating waveband	Mid-IR	NIR	Blue				
[1]18-Aug-12	1670;1690;1680; 1700;1660	780;790;800; 770;810	720;550;710560;570	76	22	2	100
Dominating waveband	Mid-IR	NIR	Green				
[1]18-Sep-12	2170;2190;2220; 2180;2230	1140;1150;1160; 1130;980	720;550;560; 540;710	61	35	3	99
Dominating waveband	Mid-IR	NIR	Green				
Dominating waveband for canopy spectra	Mid-IR	NIR	Green				
Mean (%)				68	28	3	99
Dominating waveband for all above	Mid-IR	NIR	Green				
Overall Mean (%)				67	26	5	98

Blue (400-520 nm); Green (520-590); Red (600-690 nm); NIR: near infrared (700-1300 nm); Mid-IR: Middle infrared (1350-2500 nm). [1]Date of data collection.

Table 3.8. Stepwise discriminant analysis of N treatments by individual wavebands for switchgrass and high biomass sorghum at leaf and canopy levels at the different sampling dates.

	2011		2012	
Sampling Date	Waveband (nm)	Wilk's lambda	Waveband (nm)	Wilk's lambda
		Switchgrass Leaf		
May			730	0.067 (0.93)*
June	560, 410, 470, 430, 650, 690, 730	0.00002 (0.97)	720	0.520 (0.48)
July			410	0.325 (0.68)
August	710, 690, 680,	0.00035 (0.97)		
September			730, 710	0.166 (0.55)
		Switchgrass Canopy		
May				
June	400	0.457 (0.54)		
July				
August			420, 700,1300	0.033 (0.58)
September			640, 1300, 500	0.018 (0.79)
		High Biomass Sorghum Leaf		
May			1480	0.382 (0.62)
June	720,680,570,520, 560	0.0014 (0.73)	730,710,550,540, 990	0.002 (0.73)
July			1060, 1070	0.103 (0.74)
August			1540,680,630,620	0.011 (0.60)
September			530, 570	0.149 (0.51)
		High Biomass Sorghum Canopy		
May				
June	1000, 1430, 520, 560	0.0008 (0.94)	710,510,520	0.023 (0.54)
July			520, 1500	0.139 (0.72)
August				
September			520	0.500 (0.50)

*Values in parenthesis indicate coefficient of determination.

Table 3.9. Stepwise discriminant analysis of N treatments by Vegetation Indices for switchgrass and high biomass sorghum at leaf and canopy levels at the different sampling dates.

	2011		**2012**	
Sampling date	Vegetation index	Wilk's lambda	Vegetation index	Wilk's lambda
		Switchgrass Leaf		
May			TGI	0.069 (0.93)*
June	TGI	0.367 (0.63)	$Cl_{red\ edge}$	0.365 (0.64)
July	TVI, EVI, NPCI , RE740	0.035 (0.65)	TGI	0.486 (0.54)
August	TCARI, ZTM	0.150 (0.51)		
September			TCARI	0.372 (0.63)
		Switchgrass Canopy		
May			NPCI, PRI	0.237 (0.50)
June			PRI	0.486 (0.51)
July	NPCI	0.509 (0.49)		
August	$Cl_{red\ edge}$, Cl_{green}	0.131 (0.68)		
September			RENDVI	0.186 (0.81)
		High Biomass Sorghum Leaf		
May				
June	TGI, SR, TCARI,	0.031 (0.62)	TVI	0.202 (0.80)
July	TGI	0.345 (0.65)		
August	PRI, EVI	0.172 (0.65)	RNDVI	0.380 (0.62)
September			PSRI	0.265 (0.74)
		High Biomass Sorghum Canopy		
May				
June	ZTM, RE740	0.040 (0.63)	TGI, MCARI	0.029 (0.62)
July			$Cl_{red\ edge}$, ZTM	0.124 (0.59)
August			PRI, TGI	0.065 (0.75)
September				

*Values in parenthesis indicate coefficient of determination.

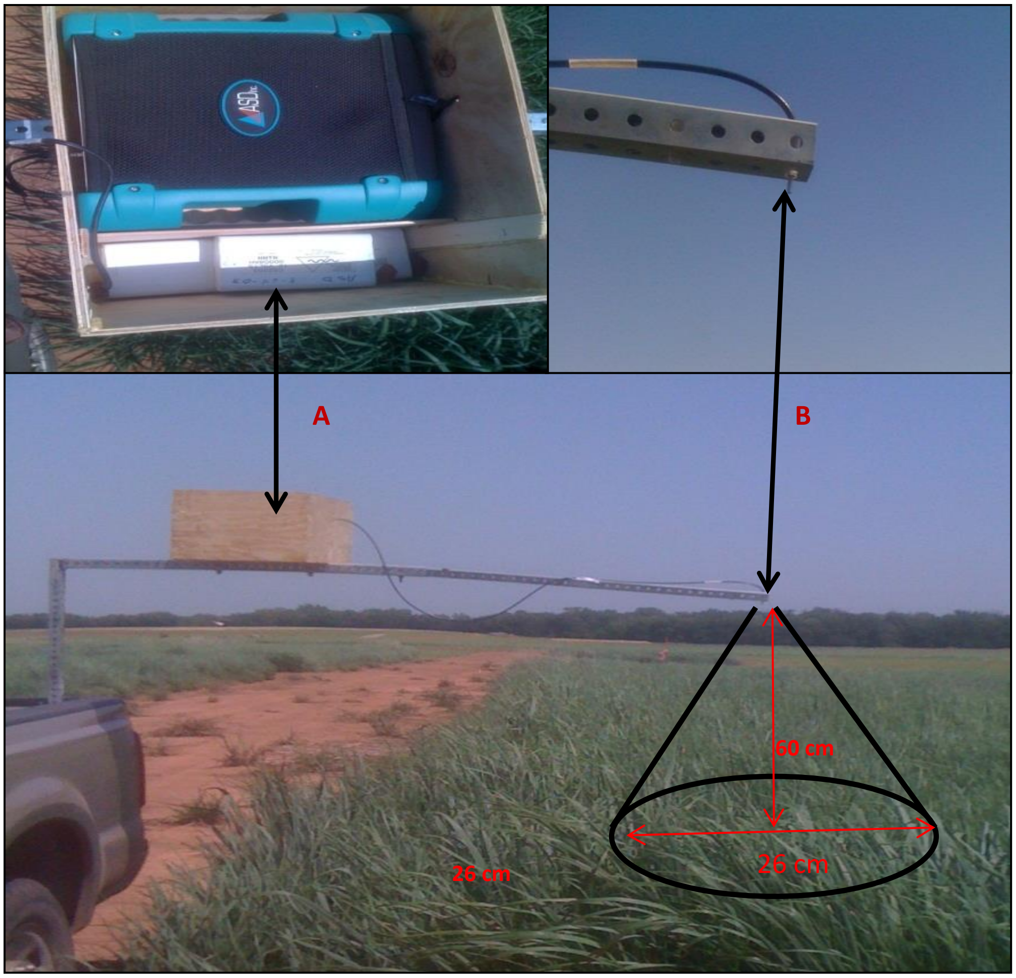

Figure 3.1. Illustration of canopy reflectance measurement with an ASD spectrophotometer mounted to the back of a pickup truck. A – Analytic spectral Device (ASD) Spectrophotometer in holding case and B – fiber optic sensor at viewing angle above canopy. The instrument was raised to > 60 cm above the canopy during sampling (sampling area of 24 cm diameter and 60 cm above canopy).

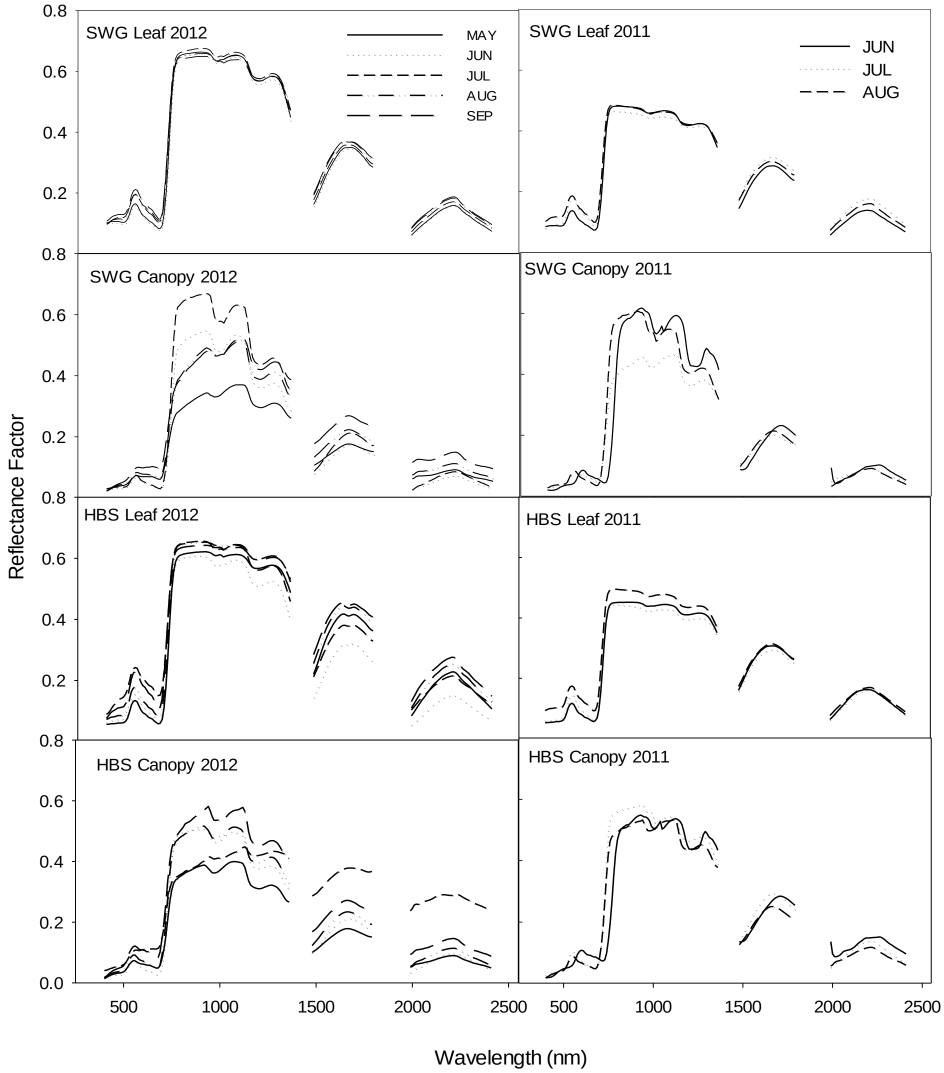

Figure 3.2.Mean canopy and leaf spectra for switchgrass and high biomass sorghum collected at different times during the growing seasons of 2011 and 2012. Spectral measurements were collected in June to August in 2011 and May to September in 2012. Measurements were collected across five nitrogen treatments (0, 82, 168, 252 $kgha^{-1}$ and a legume treatment seeded with hairy vetch in 2011 and crimson clover 2012).

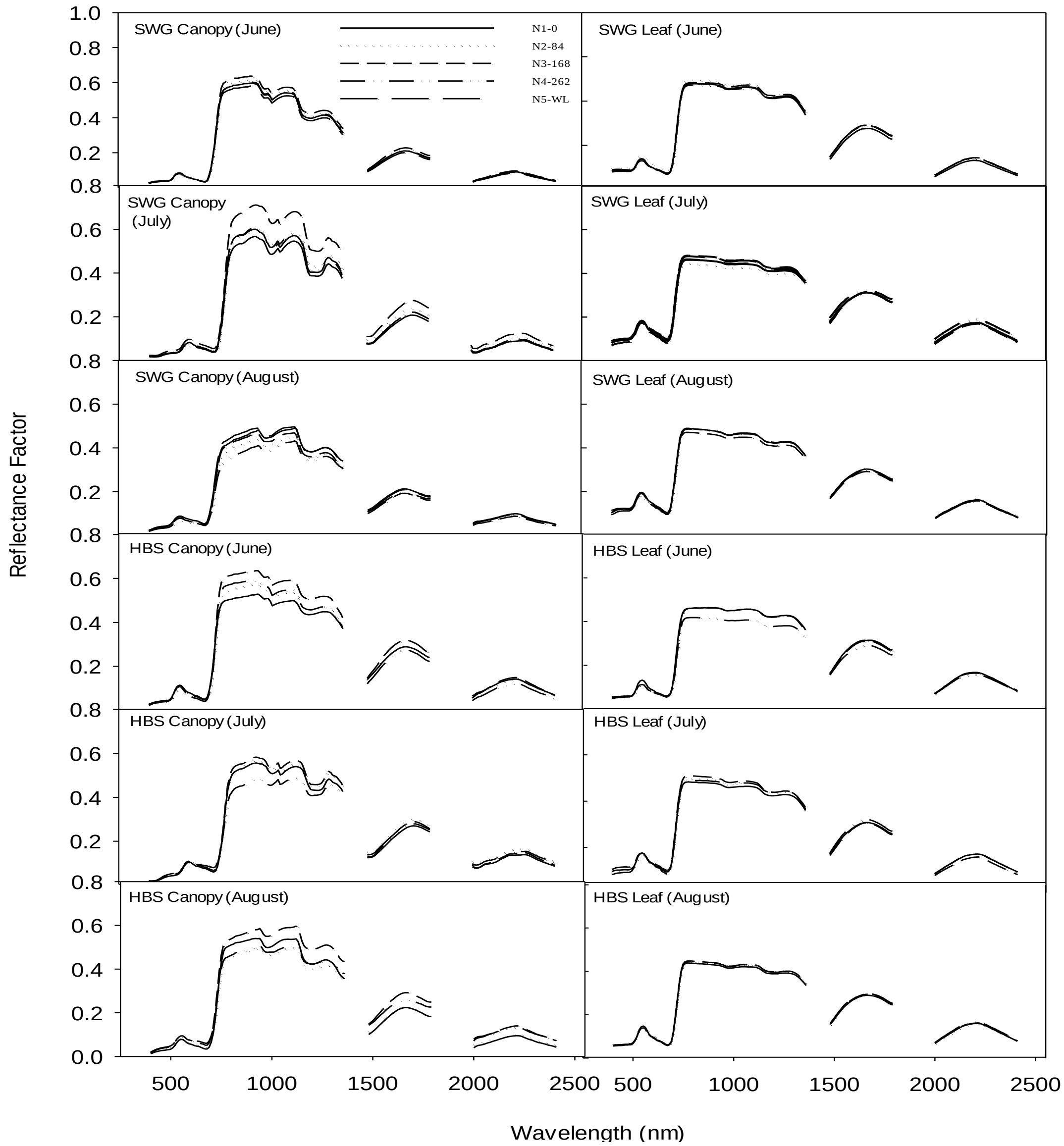

Figure 3.3. Mean canopy and leaf spectra for switchgrass and high biomass sorghum collected across five N treatments [N1-0: 0 $kgNha^{-1}$, N2-84: 84$kgNha^{-1}$, N3-168: 168 $kgNha^{-1}$, N4-252: 252 $kgNha^{-1}$, and N5-WL: Winter legume (hairy vetch)] collected in June, July and August of 2011. Six spectral measurements were taken at each monthly sampling interval.

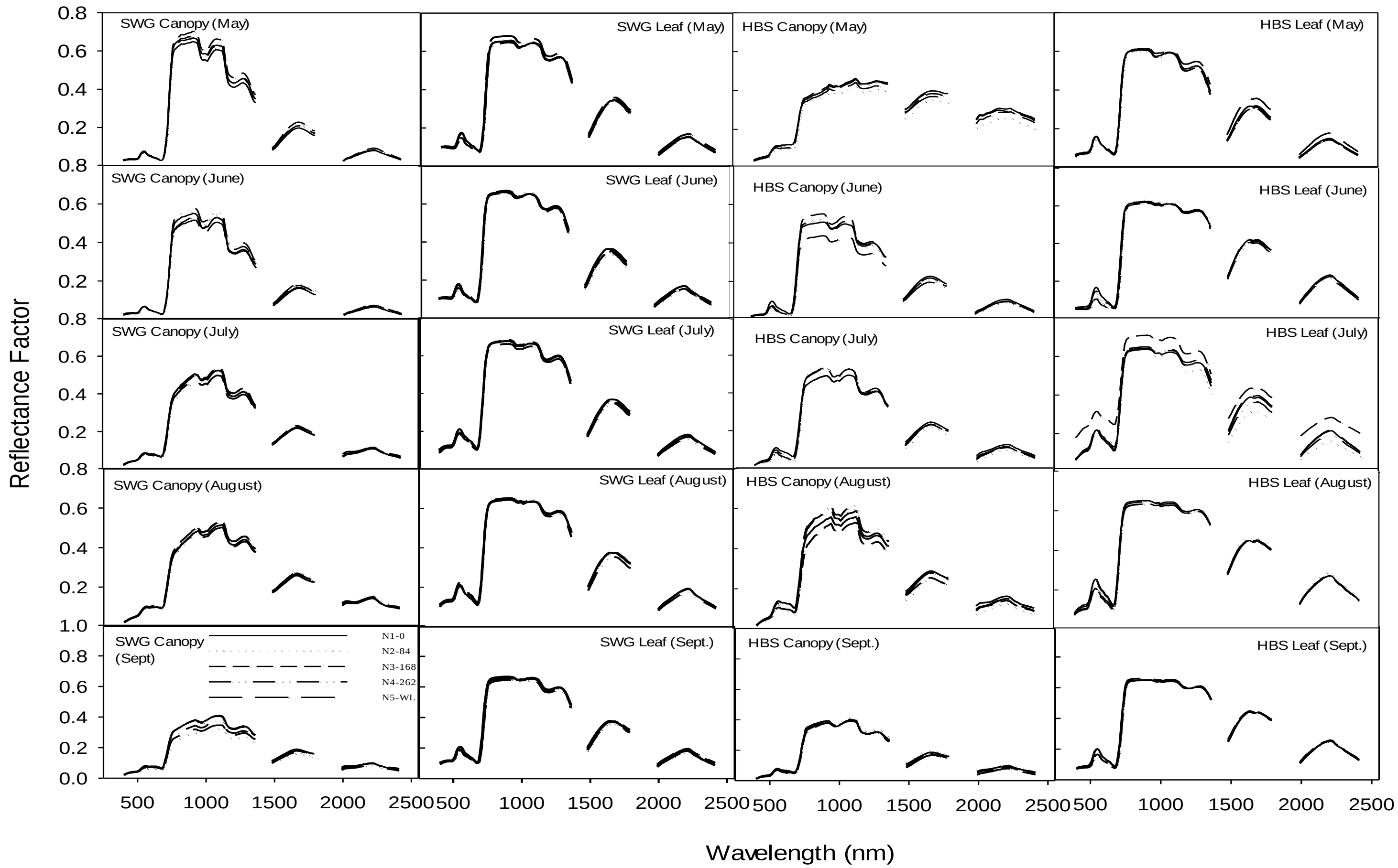

Figure 3.4.Mean canopy and leaf spectra for switchgrass and high biomass sorghum collected across five N treatments [N1-0: 0 kgNha^{-1}, N2-84: 84kgNha^{-1}, N3-168: 168 kgNha^{-1}, N4-252: 252 kgNha^{-1}, and N5-WL: Winter legume (crimson clover)] from May to September during the 2012 growing season. Six spectral measurements were taken per N treatment at each sampling interval.

CHAPTER IV

ESTIMATION OF BIOENERGY CROP YIELD AND N STATUS BY HYPERSPECTRAL CANOPY REFLECTANCE AND PARTIAL LEAST SQUARE REGRESSION

ABSTRACT

The objective of this study was to compare performance of PLSR (Partial Least Square Regression) and best narrowband NNVI (normalize nitrogen vegetation index) linear regression models for predicting N concentration and best narrowband NDVI (normalize different vegetation index) for end of season biomass yield in bioenergy crop production systems. Canopy hyperspectral data was collected using an ASD FieldSpec FR spectroradiometer (350-2500nm) at monthly intervals in 2012 and 2013. The cropping systems evaluated in the study were perennial grass [mixed grass (50% switchgrass (*Panicum virgatum* L.), 25% Indian grass "Cheyenne" (*Sorghastrum nutans* (L.) Nash) and 25% big bluestem "Kaw" (*Andropogon gerardii* Vitman)) and switchgrass "Alamo"] and high biomass sorghum "Blade 5200" (*Sorghum bicolor* (L.) Moench) grown under variable N applications rates to estimate biomass yield and quality. The predictive performance of the best narrowband NNVI and NDVI and PLSR models were determined and compared. The best narrowband NNVI was computed with the wavebands pair of 400 and 510 nm for the high biomass sorghum and 1500 and 2260 nm for the perennial grass that were strongly correlated to N concentration for both years. Wavebands used in computing best narrowband NDVI were highly variable,

but the wavebands from the red edge region (710-740 nm) were the most dominant. Narrowband NDVI was weakly correlated with final biomass yield of perennial grass (r^2=0.30 and RMSE =1.6 $Mgha^{-1}$ in 2012 and r^2=0.37 and RMSE =4.0 $Mgha^{-1}$, but was strongly correlated for the high biomass sorghum in 2013 (r^2=0.77 and RMSE = 4.2 $Mgha^{-1}$. The PLSR model improved model performance for estimation of the N concentration and final biomass yield. Compared to the best narrowband VI, the RMSE of the PLSR model was 19-41% lower for estimating N concentration and 5-471% lower for final biomass. These results indicates that PLSR was best for predicting the final biomass yield using spectral sample obtained in June to July and narrowband NNVI was more robust and useful in predicting N concentration in the biomass.

INTRODUCTION

Traditional measurement of crop biochemical characteristics normally relies on plant sampling from the field followed by laboratory analysis. This approach is relatively reliable, but is a laborious, time consuming process and unable to provide real-time diagnostics of crop (Hansen and Schjoerring, 2003; Nguyen and Lee, 2006; Zhu et al., 2012). Likewise, measurement of harvestable biomass in perennial grass production systems has always been a challenge to producers. The most accurate method of measuring harvestable biomass in a grassland system requires clipping of samples, which is laborious and time consuming (Sanderson et al., 1996; Schmer et al., 2010; Starks and Brown, 2010; Ward et al., 2011). It is our perspective that the intense labor and time requirements of these methods are a major limitation for producers using these methods. Remote sensing techniques have been recognized as a reliable method that can provide real-time estimation of biophysical, physiological or biochemical characteristics with sufficient accuracy in several crops (Hansen and Schjoerring, 2003; Nguyen and Lee, 2006; Cho et al., 2007). Thus, the seasonal variation that is often missed by destructive sampling because of the limitations imposed by the time and human resources required for intensive sampling can now be achieved through remote sensing that is fast, non-destructive, relatively cheap, with potential for expansion to regional level (Bouman, 1995; Hatfield and Prueger, 2010).

Monitoring of crop biophysical and biochemical characteristics at the canopy scale using canopy spectral reflectance measurements can be challenging, because canopy spectral reflectance provides a comprehensive information of the plant population, including leaf properties, canopy structure, soil background and atmospheric noise (Pinter et al., 2003; Zhu et al., 2012). Therefore, to extract only the green plant reflectance, vegetation indices were developed to minimize solar irradiance, canopy architecture and soil background effects to some extent (Pinter et al., 2003; Zhao et al., 2007; Hatfield et al., 2008). Vegetation indices are computed as ratios, indices, and by forming linear combinations of spectral bands of two or more wavelengths (Jackson and Huete, 1991; Pinter et al., 2003). Vegetation indices to estimate crop yield and N status are either broadband or narrowband indices. For example, the normalize difference vegetation index (NDVI), where red reflectance (R_{red}) and near-infrared reflectance (R_{nir}) is used (NDVI = $R_{nir} – R_{red}/ R_{nir} + R_{red}$) a classic index that is widely used for modeling and estimation of crop biomass and N status, can be computed either using broad wavebands (50-100 nm scale) from the Landsat Thematic mapper satellite using the TM-spectrometer ™, or narrow wavebands (<10 nm scale) from field-based sensors such as Greenseeker or crop scan and spectroradiometers such as ASD. In principle, vegetation index computed from average spectral information over broad waveband widths results in loss of critical information available in specific narrow wavebands (Blackburn, 1998; Thenkabail et al., 2000). The selection of specific narrow wavebands for the construction of an index requires the use of spectrometers capable of acquiring images in many (<10 nm) wavebands. Hyperspectral remote sensing acquires images in narrow (< 10 nm) continuous spectral bands that provide a continuous spectrum for each pixel. Therefore, hyperspectral imaging allows for the selection of narrow wavebands and for the construction of narrowband indices, which are sensitive to specific crop variables. In general, most studies select the most sensitive wavebands for the construction of a single spectral index by pooling spectral reflectance data collected across several experiments during the entire growing period. However, the environmental conditions are not homogeneous across experiments/sites and the canopy backgrounds as well as spectral reflectance are changing with growth stages (Pinter et al., 2003; Hatfield and Prueger, 2010). Moreover, vegetation indices and wavebands are reported to be strongly correlated with the plant biophysical and biochemical characteristics which are a function of growth stage or time of sample collection (Hatfield and Prueger, 2010; Foster et al., 2012). Therefore, the selection of the most sensitive wavebands for construction of a single index for establishing a relationship with crop characteristics is expected to affect the growth stage of the crop or the time during the growing season the spectra was measured. As a consequence different measurement conditions often results in some degree of disagreement in the selection of wavebands as well as inconsistency in the relationships between vegetation index and crop status during different growing stage and across locations (Zhu et al., 2012). Thus, it is necessary to explore time sensitive crop monitoring models with high accuracy that can be associated with crop phenology and management practices.

The partial least square regression (PLSR) method was developed to construct predictive models when the explanatory variables are many and highly collinear such as hyperspectral reflectance data (Yeniay and Goktas, 2002). It is a multivariate statistical technique that is widely used by chemometricians (Cho et al., 2007). The PLSR is closely related to principal component regression (PCR). A PCR is a linear regression which first decomposes the spectra into a set of principal components (PCs) that provides the maximum variation of the spectra with the aim of optimizing the predictive ability of the model and then regresses the PCs against the response variable (Yeniay and Goktas, 2002; Cho et al., 2007). The difference between PLSR and PCR is that while PCR uses only the variation of the spectra to construct the new factors (PCs), the PLSR uses both the variation of the spectra and the response variable to construct new factors (PCs) that will play the role of explanatory variables (Yeniay and Goktas, 2002; Cho et al., 2007). Partial least square regression is a widely accepted laboratory calibration method used with great success with NIR spectra for predicting forage quality parameters such as crude protein (CP), acid detergent fiber, acid detergent lignin and neutral detergent fiber (Starks et al., 2004; Kawamura et al., 2008; Labbé et al., 2008; Foster et al., 2013).

The PLSR models use reflectance data from all the wavebands in developing the calibration equations and depend on cross-validation to prevent over fitting. Using the full spectra eliminates the inconsistency that often occurs with selected wavebands and VIs due to change in spectral reflectance from changing canopy characteristics and crop type. Therefore, PLSR models may have potential for the development of more robust multiple crop models for predicting crop biomass and N concentration. However, few studies have explored the use of PLSR for predicting plant biomass (grasses and wheat), LAI (wheat), N(wheat and rice) and chlorophyll (wheat) concentration using canopy reflectance measurements (Hansen and Schjoerring, 2003; Nguyen and Lee, 2006; Cho et al., 2007). Cho et al. (2007) reported that PLSR produced lower prediction error (SEP =149 to 256 g m^2) in comparison to NDVI (SEP =264 to 331 g m^2) and red-edge position (REP) (SEP =261 to 295 g m^2). Similarly, Hansen and Schjoerring (2003) found PLRS to improve the prediction of green biomass (GBM) and N concentration by lowering the RMSE by 22% and 24%, respectively, compared to the best narrowband indices. In general, all these studies reported that PLSR improved the accuracy in creating reliable models for predicting crop biophysical and biochemical characteristics in comparison to the best narrowband indices. Therefore, the objective of this study was to compare the performance of PLSR and NDVI linear regression models based on canopy hyperspectral reflectance data for predicting N concentration and end of season biomass yield in bioenergy crop production systems.

MATERIALS AND METHODS

Study Area

The study site is located at the Stillwater Research Station (EFAW site, 36˚.13´ N, 91˚.10´ W) at Oklahoma State University, Stillwater, Oklahoma USA. The soil type is an Easpur loam with pH: 6.8; P: 49.3 kg ha^{-1}; K: 342.7 kg ha^{-1}; OM: 21.7 g kg^{-1}; total N: 1.3 g kg^{-1} sampled 17 March 2013. Perennials grasses were established at site in June 2010. In 2012, perennial grasses (switchgrass and mixed grass cropping) season started growing from early-March (greened up) and annual grass (high biomass sorghum) was planted in mid-April 2012. In 2013, perennial grasses started in April and high biomass sorghum was planted in late-April 2013. The study site received annual precipitation of 562 mm (2012) and 623 mm (2013) with a mean annual air temperature of 23 ˚C (2012) and 21 ˚C (2013). Table 4.1 summarizes the annual precipitation and temperature for the site.

Field Experiment Design and Management

The experiment was a split plot design with three replications and two factors: cropping system (main plot factor) and nitrogen (N) treatment (subplot factor). The N treatments and energy crop cropping systems were randomly assigned into main and subplots, respectively. The subplot size was 81 m^2. The experiment included three cropping systems; two perennial grass systems 1) 'Alamo' switchgrass (*Panicum virgatum* L.) and 2) perennial grass mixture (50% 'Alamo' switchgrass, 25% 'Cheyenne' indiangrass (*Sorghastrum nutans* (L.) Nash) and 25% 'Kaw' big bluestem (*Andropogon gerardii* Vitman)); and 3) an annual grass system of 'ES5200' high biomass sorghum (*Sorghum bicolor* (L.) Moench). The N treatments were cover crop [hairy vetch (*Vicia villosa*)] as a source of N and four N fertilization rates (0, 84, 168, 252 kg N ha^{-1}). The winter legume was planted in February each year and the high biomass sorghum on 16 April

2012 and 29 April 2013. In 2012, perennial grass was fertilized on 19 April, high biomass sorghum on 4 May, and all plots sprayed with Sevin (Carbaryl [1-naphthyl N-methylcarbamate]) insecticide (Bayer Environmental Science, Research Ttriangle Park, NC, USA) for grasshopper control at rate of 2.3 L ha^{-1} on 31 July. In 2013, perennial grass was fertilized on 30 April, high biomass sorghum on 15 May, and all plots sprayed with Sevin insecticide for grasshopper control at rate of 2.3 L ha^{-1} on 24 July.

Measurements of Hyperspectral Reflectance

Canopy spectral reflectance measurements were made under cloudless days on a monthly basis between 10:00-14:30 hrs local ([UTC -06:00] Central Time [US & Canada]) using a spectroradiometer (FieldSpec Pro FR, Analytical Spectral Devices [ASD], Boulder, Co, USA). Measurement of canopy reflectance started in the month of May for all cropping systems in 2012, while it was May for perennial grass and June for high biomass sorghum in 2013, and ended in August in 2012 and July in 2013 for all cropping systems (Table 4.2). The measurement range was from 350-2500 nm with spectral resolution of 3 nm in the 350-1000 nm range, and 10 nm in the 1000 -2500 nm range, which were calculated as 1 nm resolution waveband for the output data using software (RS2 for Windows; ASD) and has a spectral sampling of 1.4 nm in the 350-1000 nm range, and 2 nm in the 1000-2500 nm range. A spectralon (Labsphere, Sutton, NH, USA) white reference panel was used to optimize the ASD instrument prior to taking canopy reflectance measurements. The white reference was measured at 15-30 minutes intervals to check the stability for 100 % reflectance during canopy reflectance measurement. To reduce the amount of data for analysis, spectral data were averaged at 10-nm waveband intervals (e.g., a band center at 400 was the averaged value between 395–405 nm) giving a total of 211 spectral bands between 400–2,500 nm (Foster et al., 2012). Spectral regions between (350–395 nm and

2460-2,500) and (1,360–1,420 and 1,800–1,960 nm) which are associated with noise and atmospheric water absorption respectively were excluded from the analysis.

Field Data Collection

To measure the canopy reflectance the sensor head was held approximately 60 cm above the canopy at the nadir position at each sampling interval. The radiometer was mounted on the back of vehicle (pickup truck) and raised to a height of 200 to 290 cm above the ground (Figure 4.1). Table 4.2 shows height of radiometer, canopy height and height of the sensor from ground at each sampling date. The radiometer had a 25° field of view (FOV), producing a view area of 88-128 cm diameter at ground level. Hyperspectral reflectance was collected from all 45 plots of switchgrass (15), mixed grass (15) and high biomass sorghum (15). Two replicated spectral measurements were taken from each plot, with each measurement being an average of 25 spectral readings which enables noise reduction within the spectra. Following the measurement of the canopy spectra, a biomass subsample from 0.5 m within a row from each plot was collected. Samples were oven dried at 70°C for 72 h, then ground in a shear mill (Cyclone Sample Mill, Udy Corp., Fort Collins, CO) to pass a 1 mm screen. Total N concentration was determined based on near-infrared spectroscopy calibration with wet chemistry from a simple NIR ratio equation [TN =38 x (2080 nm/2190 nm) -35] developed by Foster et al. (2013). Calibration equation was validated with laboratory analyzed samples for 2012 (r^2= 0.83 and RMSE =3.0 gkg^{-1}) and 2013 (r^2=0.95 and RMSE = 2.0 gkg^{-1}). Nitrogen concentration was determined from monthly samples of a 0.5 m row from each plot. Biomass yield was obtained from a plot area of 44.59 m^2 cut to stubble height of 10-15cm following the first frost on 27 November 2012 with a farm size swather (Deere and Company, Moline, IL, USA) and baled with a John Deere 568 round baler (Deere and Company, Moline, IL, USA) which were individually weighed. In 2013 biomass yield was obtained from a plot area of 1 m^2 cut to stubble height of 10-15 cm on 25 September. In both years, subsamples were collected from each plot weighed and dried for dry matter.

Data Pre-treatment

A database was established consisting of all observations from the 2012-2013 growing seasons. Dataset comprising of normalize different vegetation index (NDVI) and normalized nitrogen vegetation index (NNVI) computed from wavebands averaged across 10 nm (narrowband) were created. The narrowband NDVI was computed from two-waveband combinations using equation1.

$$\text{NDVI and NNVI} = \frac{(\lambda_2 - \lambda_1)}{(\lambda_2 + \lambda_1)} \qquad (1)$$

where λ_1 =540-740 nm and λ_2 =750-1350 nm for biomass, and λ_1 = 400-2500 nm, and λ_2 = 400-2500 nm for N concentration. The short-wave infrared wavebands were included in the prediction of N concentration, because estimation accuracy has been reported to improve by using sharp absorption features in the short-wave infrared wavebands (Inoue et al., 1998; Mutanga and Skidmore, 2004). Figure 4.2 shows representative correlation contour plots for the two-waveband combinations used in computing the narrowband NNVI for estimating the N concentration and NDVI for final biomass yield. From all the possible two-waveband combinations the best narrowband NNVI that strongly correlate with N concentration and NDVI with end of season biomass yield of the high biomass sorghum and perennial grasses were selected. Separate narrowband NNVI that best correlated with N concentration for each season and cropping system was selected. Likewise, the narrowband NDVI that across all sampling dates that best correlated with the final biomass yield was selected for each season and cropping system. The index with the highest r^2 was determined to be the best index.

Data Analysis

Models were developed using simple linear regression and partial least square regression (PLSR). Simple linear regression prediction models were computed using the best selected NDVI for predicting final biomass and NNVI for N concentration for the annual and perennial cropping systems (Switchgrass and Mixed grass combined). Partial least square regression prediction models were computed using the entire spectra (400-2500 nm) excluding the wavebands associated with noise (350-395 nm and 2460-2500 nm), water and atmospheric absorption (1360-1420 and 1800-1960 nm). Likewise, PLSR was carried out per sampling period to determine the best sampling time for predicting final biomass yield and using N concentration collected throughout each growing season to predict N concentration. This was done to make the relationship between crop variables and reflectance measurements more realistic and universal as possible.

The simple linear regression analysis was performed using PROC REG procedure in SAS 9.3 (SAS, 2009). Partial least square regression (PLSR) was performed using the Partial Least Square procedure using one at a time cross-validation to select the number of factors. This cross-validation technique involves using all the observations except one for calibrated model which then was used to predict the left out observation. This process was repeated for every observation. The calibration equations developed from the 2012 season was also applied to the 2013 season to evaluate the predictive accuracy of the models across seasons.

Performances of the prediction models were summarized and reported in terms of the coefficient of determination (r^2), root mean square error (RMSE) and predicted residual sum of squares (PRESS) for the PLSR models. Partial least square regression model that is associated with the best sampling time for estimating biomass yield determined based on the regression model with the lowest PRESS. The RMSE was determined by the equation 3 of Yeniay and Goktas, 2002:

$$\text{RMSE} = \sqrt{\frac{\sum_{i=1}^{n}(y_i - \hat{y}_i)^2}{n}} \qquad (3)$$

where the $\hat{y}_i$ are the estimated samples from validation test data, y_i are the measured samples in validation dataset and n is the number of observations.

The optimal model for predicting in-season N concentration and end of season biomass yield was selected based on low RMSE and high r^2.

RESULTS AND DISCUSSION

Growing Condition

The 2012 and 2013 growing seasons differed significantly in terms of the weather conditions. In 2012, perennials greening up started as early as March and reached reproductive stage by late June to early July. Conversely, in 2013 perennials started greening up in early April, but was affected by a late spells of freeze in April that setback early season growth to mid-May. The availability of moisture from the above normal precipitation and cooler temperatures in 2013 for the months of June and July was contrast to the 2012 season that was dry and hot during the same period (Table 4.1). Wetter condition in 2013 in combination with lodging of the perennial grasses significantly affected the frequency of spectra data collection.

Variation in N Concentration and Final Biomass Yield

The wide range of N concentration and high standard deviation reported in Table 4.3 are a representation of samples collected throughout the growing season from May to August in 2012 and May to July in 2013. Higher N concentration was found in high biomass sorghum compared to the perennial grasses (Table 4.3). Nitrogen concentration in biomass was 6.6 and 5.1 g kg^{-1} higher in 2013 (24.0 and 19.6 g kg^{-1}) compared to the 2012 (17.4 and 14.5 g kg^{-1}) for high biomass sorghum and perennial grass, respectively. Final biomass yield for 2012 and 2013 was also high with dry matter yield for high biomass sorghum ranging from 5.5 – 12.8 Mg ha^{-1} in 2012 and 9.5 – 36.7 Mg ha^{-1}, respectively and for perennial grass 2.3-10.5 Mg ha^{-1} and 5.7 – 24.6 Mg ha^{-1}, respectively (Table 4.3). On average, the high biomass sorghum produced more biomass compared to the perennial grass.

Canopy spectra collected throughout the growing season were highly variable due to changes in architecture and arrangement of plant components and changes in the proportion of soil and vegetation. Figure 4.3 shows the variations, magnitude and position of absorption between the cropping systems and sampling dates. In general, the spectra for the high biomass sorghum and the perennial grass were consistent across the growing seasons for samples collected around the same period. The mean spectrum of the high biomass sorghum discriminated from the perennial grasses in the Mid-IR (SWIR) region of the spectrum.

Estimating N Concentration in Biomass

The wavebands for estimating N concentration with both the NNVI were mainly in the visible (blue) and Mid-IR (SWIR) region of the spectrum. Waveband ratio λ_1= 400 nm and λ_2 = 510 nm in high biomass sorghum and λ_2 =1500 nm and λ_2 =2260 nm in perennial grass constitute the sensitive wavebands for determining the nitrogen status (Table 4.4). The waveband pairs were the same for estimating N concentration for both seasons in the high biomass sorghum and the perennial grass. The two-waveband combinations derived from the hyperspectral data for estimation of N concentration did not include wavebands of the classical NDVI (red and NIR combination). The NNVI with 400 nm and 510 nm reported strong correlation with N concentration in both 2012 and 2013 for the high biomass sorghum. Likewise, NNVI with 1500 and 2260 nm was moderate and strongly correlated with N concentration in the perennial grass in 2012 and 2013 respectively. Hansen and Schjoerring (2003) also found wavebands in the visible spectral range, mainly in the blue (440-501 nm) region paired with a green (573-586 nm) or a red (692 nm) wavebands to be strongly correlated with N concentration. Similarly, Stroppiana et al. (2009) also found that the combination of two visible wavebands ($\lambda 1 = 483$ and $\lambda 2 = 503$nm) produced the highest correlation with field measurements of nitrogen concentration. In general, a strong relationship between the visible absorption wavebands and nitrogen concentration is not uncommon in the literature. However, the best waveband combinations for computing NNVI for the perennial grass system occurred with wavebands from the SWIR. It is reported, that presence of water can often mask the biochemical absorption features, particularly in the SWIR region that could often lead to a weak correlation between nutrients and hyperspectral data in this region (Kokaly and Clark, 1999; Mutanga et al., 2004). Mutanga and Skidmore (2004) included the SWIR in estimating nitrogen concentration in African savanna rangeland reported a calibration equation with r^2=0.92 and RMSE =0.02, while the predictive ability with a test dataset reported r^2=0.60 and RMSE=0.13. Similarly, when the 2012 dataset was used for calibration and the 2013 for validation, the SWIR wavebands remain strongly correlated with N concentration in the perennial grass system. Measurement of canopy NDVI using red and NIR wavebands is reported to saturate at LAI exceeding 2.5 (Mutanga and Skidmore, 2004). In this study, LAI ranges from 2.0 – 6.5 for the perennial grasses and 1.4 – 4.5 for the high biomass sorghum during the sampling period. According to Hansen and Schjoerring (2003) plant N concentration is supposed to be related to the color of the canopy, therefore the amount of biomass is of less importance at least when LAI exceeded 2.5. Therefore, saturation due to LAI exceeding 2.5 is expected to have more of an effect on biomass rather than on N estimation. Moreover, a denser canopy should result in a stronger linear relationship. These results indicates that visible wavebands used to compute NNVI were more strongly correlated with N concentration in high biomass sorghum, while SWIR were more strongly correlated with N concentration the perennial grass system.

The most important aspect of PLSR is selecting the number for factors. Selecting models with too many factors can result in over fitting, reducing the potential of the model for prediction on a validation dataset. The number of factors was determined using one at a time cross-validation and the model with lowest PRESS was selected as the best prediction model. An eleven factor model was selected as the best model for estimating the N concentration in the high biomass sorghum in 2012 and a six factor in 2013 (Table 4.5). Prediction models of seven and eight factors were best for estimating the N concentration in the perennial grass for 2012 and 2013 respectively. Overall, the PLSR models performed very well in estimating the N concentration for years, 2012 and 2013. In fact, the PLSR models reported decrease in RMSEP of 19-41% compared to the best narrowband NNVI linear fit (Table 4.6). Similarly, Hansen and Schjoerring (2003) showed PLSR models to improve prediction of N concentration in wheat lowering RMSE by 24% compared to the best narrow-band indices.

Estimating Final Biomass Yield

The best narrow-band NDVI was most strongly correlated with the final biomass yield occurred in July of both years for the high biomass sorghum and the perennial grasses (Table 4.4). Likewise, the best PLSR models for estimating final biomass yield were observed in July and June of both 2012 and 2013 for the high biomass sorghum and perennial grasses respectively (Table 4.6). Overall, the optimum sampling time observed with the PLSR was similar to that obtained with the best narrow-band index, except for perennial grass in 2012. The optimal time for estimating above ground net primary productivity (ANPP) in central Great Plain grassland at the Rannells Flint Hills Prairie Preserve (RFHPP) (39◦ 08_ N, 96◦ 32_ W), and the Washington Marlatt Memorial Park (WMMP) (39◦ 13_ N, 96◦ 37_ W), all near Manhattan, Kansas, USA, using AVHRR NDVI composite was late July (An et al., 2013). This period was determined from derived relationship between NDVI computed from images obtained from the AVHRR satellite and ANPP from the period of 1989-2005. Based on the site locations, the June to mid-July period are most appropriate for estimating the final biomass yield in the high biomass sorghum and the perennial grass.

Wavebands in the red edge (680-750 nm) were represented in 50% of all selected wavebands in 2012 and 100% in 2013 (Table 4.4). The waveband combinations for the NDVI most strongly correlated with the final yield were in the green (580 nm), red edge (730-750 nm) and NIR (1080-1240 nm). The best NDVI in 2012 was weakly correlated with the final yield r^2= 0.46 and RMSE=1.4 Mg ha^{-1} and 0.30 and RMSE=1.6 Mg ha^{-1} for high biomass sorghum and the perennial grass in respectively. However, in 2013 the best NDVI was strongly related with final yield for the high biomass sorghum r^2= 0.77 and RMSE= 4.2 Mg ha^{-1}, but was again weakly correlated for the perennial grass r^2= 0.35 and RMSE= 4.0 Mg ha^{-1}. Improved performance of modified NDVI not including the classical red and NIR waveband combinations have also been observed by Mutanga and Skidmore (2004). They demonstrated that modified NDVI (r^2 =0.78) with 746 and 755 nm to be more strongly correlated with biomass of tall grass compared to the standard NDVI (r^2=0.25). In general, the final biomass yield of the perennial grasses was not strongly correlated with the best narrow-band indices in both years of the study. Unlike the high biomass sorghum that showed strong correlation in 2013. Lower LAI (< 4) at the time of sampling due to the later planting date in 2013 and the benefit of the red edge wavebands was considered reasons for the improvement in the prediction using narrow-band indices. The inclusion of red edge band in computing NDVI has been reported to be more strongly related to LAI and biomass and more robust to the saturation problems at LAI values < 3.0 often suffered by the classical NDVI (Danson and Plummer, 1995; Gitelson et al., 1996; Hansen and Schjoerring, 2003). The improvement with the modified NDVI using the red edge waveband in estimating biomass reported by Mutanga and Skidmore (2004) was a result of the ability of the red edge to overcome saturation in the dense tall grass. Likewise, Cho et al. (2007) also reported improved predictive performance of NDVI involving red edge bands compared to the classic NDVI.

Predictability of final biomass yield improved significantly with the PLSR model for the high biomass sorghum and the perennial grass in both years (Table 4.5). The PLSR models produced higher r^2 and lower RMSE compared to narrow-band NDVI regression models. The greatest improvement with the PLSR was observed for the perennial grasses with 100 and 471 % reduction in RMSE for 2012 and 2013, respectively, compared to the best narrow-band NDVI linear fit (Table 4.6). Reduction in RMSE for the high biomass sorghum of 5 and 75% in 2012 and 2013, respectively, was also observed with the PLSR. Similarly, Improvement with PLSR model by lowering the RMSE over narrow-band NDVI was also observed by Cho et al. (2007) in estimating grass/herb biomass compared to NDVI and red-edge position and by Hansen and Schjoerring (2004) in estimating wheat biomass compared to the best narrow-band NDVI. According to Geladi et al. (199) the improvement in predictability using the PLSR compared to the narrow-band NDVI, could be a result of a non-linear relationship between the narrow-band NDVI and final biomass yield.

Model Predictability

To test the predictability of the model developed for estimating the final biomass in 2012. The 2012 model was used as a calibration equation for estimating the final biomass yield in 2013. In all occasions, validation of the 2012 model on the 2013 dataset was weak. The inability to predict the 2013 yield using the 2012 data indicates that multiple years of data is required to develop models for accurately predicting the final biomass yield. Growing environment are dynamic and require large amount of data that includes seasons or multiple locations of high (i.e. 2013), average and low yield variation. Conversely, application of 2012 calibration equation (Table 4.7) for the high biomass sorghum and perennial grass in estimating the N concentration in 2013 reported a validation r^2=0.80 and RMSEP = 2.0 g kg^{-1} for high biomass sorghum and r^2 =0.71 and RMSEP = 3.6 g kg^{-1} for the perennial grasses. However, application of the 2012 calibration equation for predicting the N concentration in 2013 for both high biomass sorghum and the perennial grasses were unsuccessful with the PLSR models. The models reported r^2=0.25 and RMSEP =6.0 g kg^{-1} for high biomass sorghum and r^2=0.35 and RMSEP = 4.1 g kg^{-1} for the perennial grasses. These results confirm earlier findings by Foster et al. (2013) that a simple ratio of two NIR wavebands was more stable in estimating N concentration in feedstock material across different growing seasons. Having continuous spectral coverage with many narrow-bands does not necessary mean more information as most of these bands, especially the ones that are close to one another provide redundant information (Thenkabail et al., 2012). Prediction using PLSR is based on a high number of factors. A high number of factors might result in over fitting and poor predictability of the PLSR model.

CONCLUSIONS

The results of this study show that use of PLSR models improved model performance for estimation of the N concentration and final biomass yield. In fact, RMSE of the PLSR model was 19-41% lower for estimating N concentration and 5-471% lower for final biomass compared to the best narrowband VIs. However, despite the large reduction in the RMSE obtained with the PLSR model, the best narrowband NNVI was more robust and stable in predicting N concentration across seasons. Biomass yield seems to be more a function of the environment affected by factors such as the combination of rainfall and temperature for each growing season. Therefore, PLSR might offer great potential for model development for predicting biomass yield, while narrowband NNVI might be more useful for predicting N concentration. Finally, in predicting the final biomass yield, spectral measurements collected during June and July were the best for predicting the final biomass yield in the bioenergy cropping systems.

REFERENCES

An N., Price K.P., Blair J.M. 2013. Estimating above-ground net primary productivity of the tallgrass prairie ecosystem of the Central Great Plains using AVHRR NDVI. International Journal of Remote Sensing 34:3717-3735.

Blackburn G.A. 1998. Quantifying chlorophylls and caroteniods at leaf and canopy scales: An evaluation of some hyperspectral approaches. Remote Sensing of Environment 66:273-285.

Bouman B. 1995. Crop modelling and remote sensing for yield prediction. NJAS wageningen journal of life sciences 43:143-161.

Cho M.A., Skidmore A., Corsi F., Van Wieren S.E., Sobhan I. 2007. Estimation of green grass/herb biomass from airborne hyperspectral imagery using spectral indices and partial least squares regression. International Journal of Applied Earth Observation and Geoinformation 9:414-424.

Danson F., Plummer S. 1995. Red-edge response to forest leaf area index. Remote Sensing 16:183-188.

Foster A., Kakani V., Ge J., Mosali J. 2013. Rapid Assessment of Bioenergy Feedstock Quality by Near Infrared Reflectance Spectroscopy. Agronomy Journal 105:1-11.

Foster A.J., Kakani V.G., Ge J., Mosali J. 2012. Discrimination of Switchgrass Cultivars and Nitrogen Treatments Using Pigment Profiles and Hyperspectral Leaf Reflectance Data. Remote Sensing 4:2576-2594.

Gitelson A.A., Merzlyak M.N., Lichtenthaler H.K. 1996. Detection of red edge position and chlorophyll content by reflectance measurements near 700 nm. Journal of Plant Physiology 148:501-508.

Hansen P., Schjoerring J. 2003. Reflectance measurement of canopy biomass and nitrogen status in wheat crops using normalized difference vegetation indices and partial least squares regression. Remote Sensing of Environment 86:542-553.

Hatfield J., Gitelson A.A., Schepers J.S., Walthall C. 2008. Application of spectral remote sensing for agronomic decisions. Agronomy Journal 100:S-117-S-131.

Hatfield J.L., Prueger J.H. 2010. Value of using different vegetative indices to quantify agricultural crop characteristics at different growth stages under varying management practices. Remote Sensing 2:562 -578.

Inoue Y., Moran M.S., Horie T. 1998. Analysis of spectral measurements in paddy field for predicting rice growth and yield based on a simple crop simulation model. Plant Production Science-Tokyo- 1:269-279.

Jackson R.D., Huete A.R. 1991. Interpreting vegetation indices. Preventive Veterinary Medicine 11:185-200.

Kawamura K., Watanabe N., Sakanoue S., Inoue Y. 2008. Estimating forage biomass and quality in a mixed sown pasture based on partial least squares regression with waveband selection. Grassland Science 54:131-145.

Kokaly R.F., Clark R.N. 1999. Spectroscopic determination of leaf biochemistry using band-depth analysis of absorption features and stepwise multiple linear regression. Remote Sensing of Environment 67:267-287.

Labbé N., X.P. Ye, J. A. Franklin, A. R. Womac, D. D. Tyler, Rials T.G. 2008. Analysis of switchgrass characteristics using near infrared spectroscopy. BioRes. 3:1329-1348.

Mutanga O., Skidmore A.K. 2004. Hyperspectral band depth analysis for a better estimation of grass biomass (< i> Cenchrus ciliaris</i>) measured under controlled laboratory conditions. International Journal of Applied Earth Observation and Geoinformation 5:87-96.

Mutanga O., Skidmore A.K., Prins H. 2004. Predicting in situ pasture quality in the Kruger National Park, South Africa, using continuum-removed absorption features. Remote Sensing of Environment 89:393-408.

Nguyen H.T., Lee B.-W. 2006. Assessment of rice leaf growth and nitrogen status by hyperspectral canopy reflectance and partial least square regression. European Journal of Agronomy 24:349-356.

Pinter P.J., Hatfield J.L., Schepers J.S., Barnes E.M., Moran M.S., Daughtry C.S.T., Upchurch D.R. 2003. Remote sensing for crop management. Photogrammetric engineering and remote sensing 69:647-664.

Sanderson M.A., Agblevor F., Collins M., Johnson D.K. 1996. Compositional analysis of biomass feedstocks by near infrared reflectance spectroscopy. Biomass & Bioenergy 11:365-370.

SAS. 2009. Sas User's Guide, SAS Institute Inc., Cary, North Carolina.

Schmer M.R., Schacht W.H., Marx D.B., Mitchell R.B., Vogel K.P. 2010. Efficient Methods of Estimating Switchgrass Biomass Supplies BioEnergy research 3:243-250.

Starks P.J., Brown M.A. 2010. Prediction Of Forage Quality From Remotely Sensed Data: Comparison Of Cultivar-specific And Cultivar-independent Equations Using Three Methods Of Calibration. Crop Sci. 50:2159-2170.

Starks P.J., Coleman S.W., Phillips W.A. 2004. Determination of Forage Chemical Composition Using Remote Sensing. Journal of Range Management 57:635-640.

Thenkabail P.S., Smith R.B., De Pauw E. 2000. Hyperspectral vegetation indices and their relationships with agricultural crop characteristics. Remote Sensing of Environment 71:158-182.

Thenkabail P.S., Lyon J.G., Huete A. 2012. Advances in Hyperspectral Remote Sensing of Vegetation and Agricultural Croplands, in: P. S. Thenkabail, J.G. Lyon, and A. Huete (Ed.), Hyperspectral Remote Sensing of Vegetation, CRC Press, Boca Raton, FL. pp. 3-39.

Ward A., Nielsen A.L., Møller H. 2011. Rapid Assessment of Mineral Concentration in Meadow Grasses by Near Infrared Reflectance Spectroscopy. Sensors 11:4830-4839.

Yeniay O., Goktas A. 2002. A comparison of Partial Least Squares Regression with Other Prediction Methods. Hacettepe Journal of Mathematics and Statistics 31:99-111.

Zhao D., Starks P.J., Brown M.A., Phillips W.A., Coleman S.W. 2007. Assessment of forage biomass and quality parameters of bermudagrass using proximal sensing of pasture canopy reflectance. Grassland Science 53:39-49.

Zhu Y., W. Wang, Yao X. 2012. Estimating Leaf Nitrogen Concentration (LNC) of Cereal Crops with Hyperspectral Data, in: P. S. Thenkabail, J.G. Lyon, and A. Huete (Ed.), Hyperspectral Remote Sensing of Vegetation, CRC Press, Boca Raton, FL. pp. 187-206.

Table 4.1. Monthly precipitation (mm) and average temperature (°C) at Stillwater, Oklahoma, during 2012 and 2013 growing seasons.

Months	Rainfall (mm)		Temperature (°C)	
	2012	2013	2012	2013
Mar	100	28	16	9
Apr	156	135	18	13
May	28	153	23	20
Jun	35	100	26	26
Jul	2	141	31	26
Aug	67	65	27	27
Sep	28	43	23	24
Oct	15	40	15	15
Total/ Mean	452	705	23	20

Table 4.2. Sampling date (May – August 2012 and May – July 2013), canopy height, sensor height, diameter of field of view (FOV) and number of samples for canopy reflectance collected by ASD spectrophotometer on high biomass sorghum and perennial grass in Oklahoma for the 2012 and 2013 growing seasons.

Sampling Date	Canopy height (cm)		Diameter of FOV (cm)		Sensor height aboveground (cm)	No. of Samples collected
	High Biomass Sorghum	Perennial Grass	High Biomass Sorghum	Perennial Grass		
			2013			
22 May	-	40-70	-	44-57	170	60
7 June	10-50	60-120	53-70	22-48	170	90
21 June	25-80	75-130	57-81	35-59	210	90
12 July	35-130	90-190	48-90	22-66	240	90
			2012			
16 May	30-45	80-140	67-74	26-52	200	90
14 June	80-180	110-180	26-69	26-56	240	90
18 July	130-220	110-200	30-69	39-78	290	90
20 August	170-240	110-220	22-52	30-78	290	90

Table 4.3. Descriptive statistics of the end of season biomass yield and biomass average nitrogen concentration throughout the growing season (May to August in 2012 and May to July in 2013) measured with NIR in high biomass sorghum, mixed grasses and switchgrass. Nitrogen concentration was measured monthly and final biomass yield following first frost in November 2012 and before first frost in September 2013.

Year	# of Samples	Mean	STD†	Min	Max
		Biomass yield (Mg ha^{-1})			
		High biomass sorghum			
2012	15	7.7	1.7	5.5	12.8
2013	15	24.4	8.5	9.5	36.7
		Perennial grasses			
2012	30	7.0	1.9	2.3	10.5
2013	30	14.1	4.9	5.7	24.6
		N (g kg^{-1})			
		High biomass sorghum			
2012	60	17.4	7.2	5.0	33.0
2013	45	24.0	6.9	8.2	34.5
		Perennial grasses			
2012	117	14.5	4.3	7.0	34.0
2013	120	19.6	5.1	7.6	30.0

†Standard deviation

Table 4.4. Performance of selected narrow-band normalized nitrogen vegetation index (NNVI) calculated from spectral reflectance for estimating nitrogen concentration and normalized difference index (NDVI) for final biomass yield in perennial grasses (switchgrass and mixed grass) and high biomass sorghum in 2012 and 2013 growing seasons.

		R_1/R_2 (nm)	**Model Performance**	
			R^2	RMSE
		Nitrogen Concentration in Biomass (gkg^{-1})		
2012	High Biomass Sorghum	400/510	0.74	3.8
	Perennial grass	1500/2260	0.50	3.1
2013	High Biomass Sorghum	400/510	0.79	3.2
	Perennial grass	1500/2260	0.71	2.7
2012				
		Dry matter yield for high biomass sorghum ($Mgha^{-1}$)		
	16 May	710/1170	0.30	1.6
	14 June	580/1170	0.36	1.5
	18 July	740/1080	0.46	1.4
	20 August	730/1060	0.34	1.5
		Dry matter yield for perennial grass ($Mgha^{-1}$)		
	16 May	670/950	0.15	1.8
	14 June	660/1070	0.12	1.8
	18 July	580/750	0.30	1.6
	20 August	740/1100	0.32	1.6
2013				
		Dry matter yield for high biomass sorghum ($Mgha^{-1}$)		
	7 June	730/880	0.46	8.2
	21 June	730/1280	0.66	5.2
	12 July	730/1240	0.77	4.2
		Dry matter yield for perennial grass ($Mgha^{-1}$)		
	22 May	730/1140	0.15	4.6
	7 June	740/820	0.37	4.0
	21 June	740/780	0.31	4.1
	12 July	730/1080	0.35	4.0

Table 4.5. Performance of partial least square regression models (PLSR) in estimating the nitrogen concentration nitrogen concentration and final biomass yield in perennial grasses (switchgrass and mixed grass) and high biomass sorghum in 2012 and 2013 growing seasons.

		No. Factors	Model Performance		
			PRESS	R^2	RMSE
		Nitrogen Concentration in Biomass (gkg^{-1})			
2012	High Biomass Sorghum	11	0.59	0.86	2.7
	Perennial grass	7	0.62	0.67	2.5
2013	High Biomass Sorghum	6	0.62	0.85	2.7
	Perennial grass	8	0.44	0.84	2.1
2012					
		Dry matter yield for high biomass sorghum ($Mgha^{-1}$)			
	16 May	6	1.52	0.67	1.1
	14 June	4	1.62	0.56	1.2
	18 July	6	1.37	0.83	0.80
	20 August	6	1.48	0.65	1.1
		Dry matter yield for perennial grass ($Mgha^{-1}$)			
	16 May	7	1.42	0.73	1.0
	14 June	8	1.01	0.83	0.80
	18 July	6	1.13	0.55	1.3
	20 August	7	1.07	0.70	1.0
2013					
		Dry matter yield for high biomass sorghum ($Mgha^{-1}$)			
	7 June	3	0.79	0.62	5.4
	21 June	3	0.66	0.76	4.3
	12 July	3	0.73	0.79	4.0
		Dry matter yield for perennial grass ($Mgha^{-1}$)			
	22 May	6	0.91	0.68	2.8
	7 June	10	0.86	0.98	0.70
	21 June	5	1.12	0.46	3.7
	12 July	4	0.95	0.44	3.7

Table 4.6. Results comparison of Partial least squares regression (PLSR) and the best narrow-band NNVI linear models for estimating N concentration and NDVI for final biomass yield in high biomass sorghum and perennial grass [switchgrass and mixed grass (Switchgrass, Indian grass and big bluestem)] systems for the 2012 and 2013 growing seasons.

		PLSR			The best narrowband VI linear fit	
		No. Factors	R^2	RMSE	RMSE	% difference to PLSR
				Nitrogen concentration Biomass (g kg^{-1})		
2012	High biomass sorghum	11	0.86	2.7	3.8	41
	Perennial grass	7	0.67	2.5	3.1	24
				Final Biomass yield (Mg ha^{-1})		
	High biomass sorghum	6	0.83	0.8	1.4	75
	Perennial grass	8	0.83	0.8	1.6	100
				Nitrogen concentration Biomass (g kg^{-1})		
2013	High biomass sorghum	6	0.85	2.7	3.2	19
	Perennial grass	8	0.84	2.1	2.7	29
				Final Biomass yield (Mg ha^{-1})		
	High biomass sorghum	3	0.79	4.0	4.2	5
	Perennial grass	10	0.98	0.7	4.0	471

Table 4.7. Linear regression equation for the best NNVI for estimating the N concentration and NDVI for final biomass yield high biomass sorghum and perennial grass in 2012 and 2013.

		Regression Equation	R^2	P value
		Nitrogen Concentration in Biomass (g kg^{-1})		
2012	High Biomass Sorghum	TN = 3.3-4.1* NDVI	0.74	< 0.0001
	Perennial grass	TN=3.8 +13.8* NDVI	0.50	< 0.0001
2013	High Biomass Sorghum	TN = 4.5-6.8*NDVI	0.79	< 0.0001
	Perennial grass	TN =3.0 + 9.1 *NDVI	0.71	< 0.0001
		Dry matter yield (M gha^{-1})		
2012	High Biomass Sorghum (18 July)	FY = -2.0 + 131*NDVI	0.46	0.005
	Perennial grass (18 July)	FY= -13.0 +145*NDVI	0.30	0.004
2013	High Biomass Sorghum (18 July)	FY= -2.0 + 131*NDVI	0.77	< 0.0001
	Perennial grass (7June)	FY = -13.0 + 145*NDVI	0.37	< 0.0001

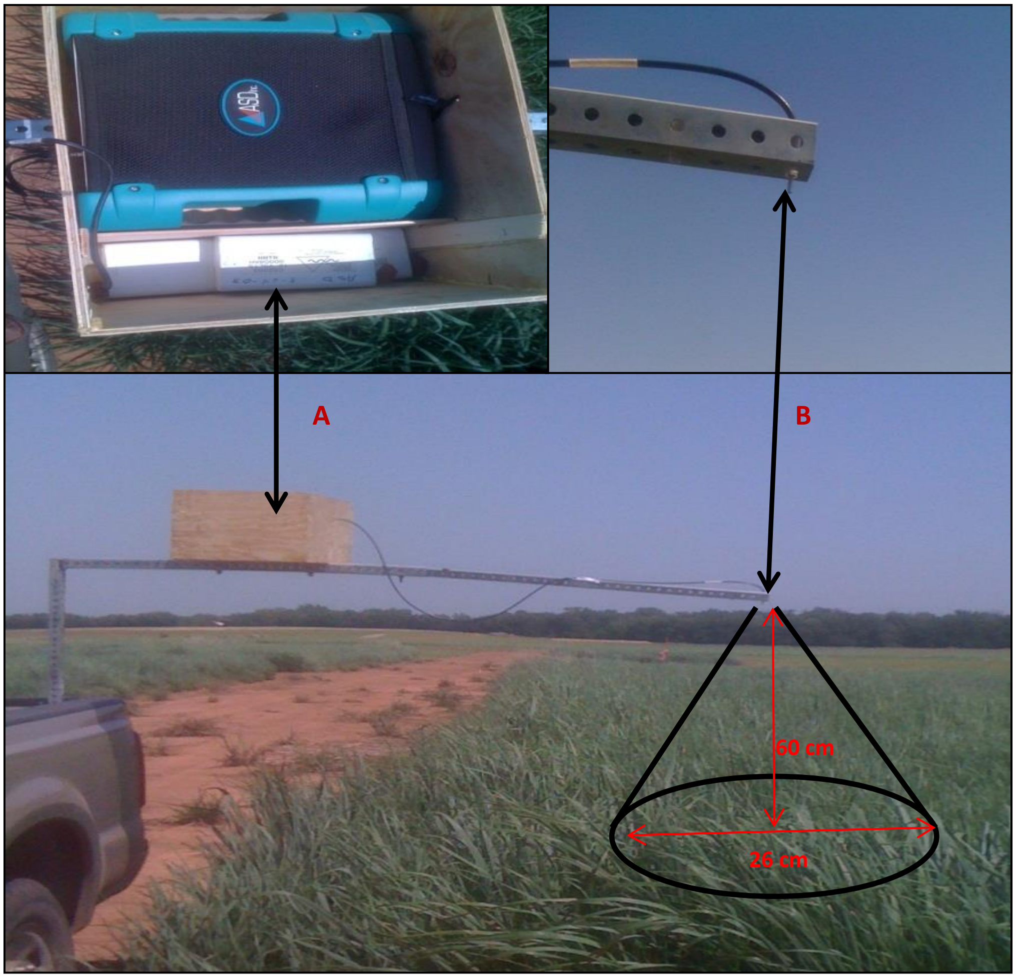

Figure 4.1. Illustration of canopy reflectance measurement with an ASD spectrophotometer mounted to the back of a vehicle (pickup truck). A – Analytic spectral Device (ASD) Spectrophotometer in holding case and B – fiber optic sensor at viewing angle above canopy. The instrument was raised to > 60 cm above the canopy during sampling (sampling area of 24 cm diameter and 60 cm above canopy).

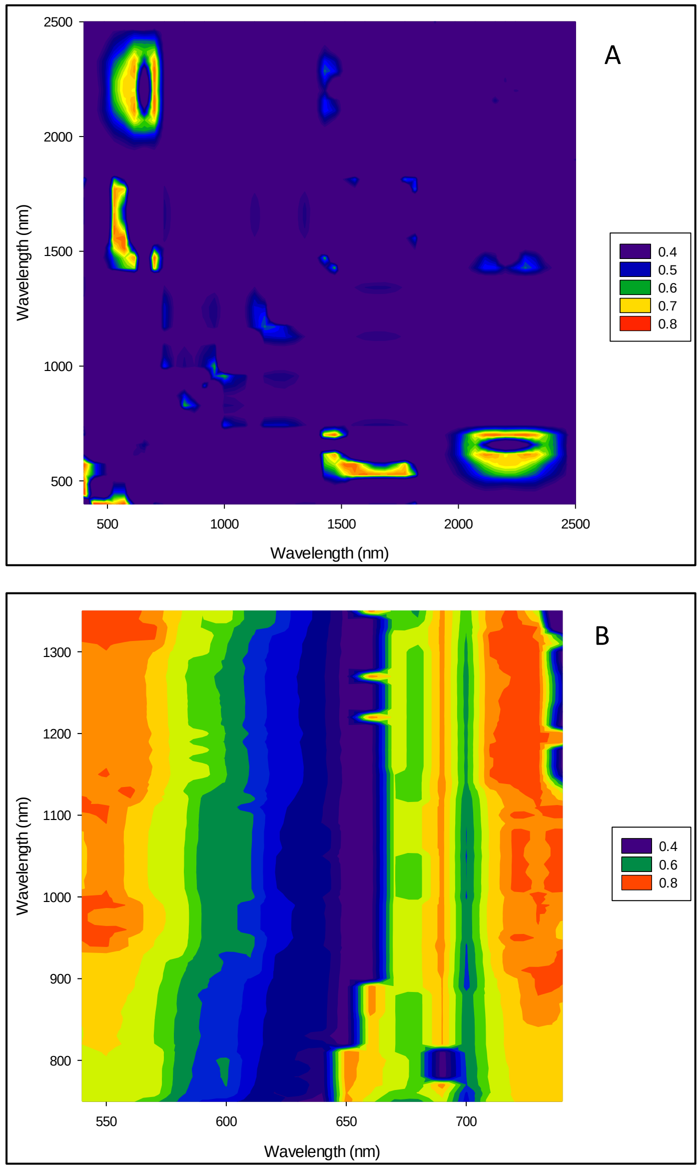

Figure 4.2. Representation of contour plots for determining the two -wavelength combinations of the normalized difference vegetation index $(\lambda_2 - \lambda_1)/ (\lambda_2 + \lambda_1)$; λ_2-Y-axis wavelength and λ_1-x-axis wavelength. The two-wavelength combination was selected from the region with high coefficient of determination (r^2) between NDVI and nitrogen concentration and between NDVI and final biomass yield. (A) Represents contour plot of nitrogen concentration in the 2013 high biomass sorghum and (B) the final biomass yield in the 2013 high biomass sorghum.

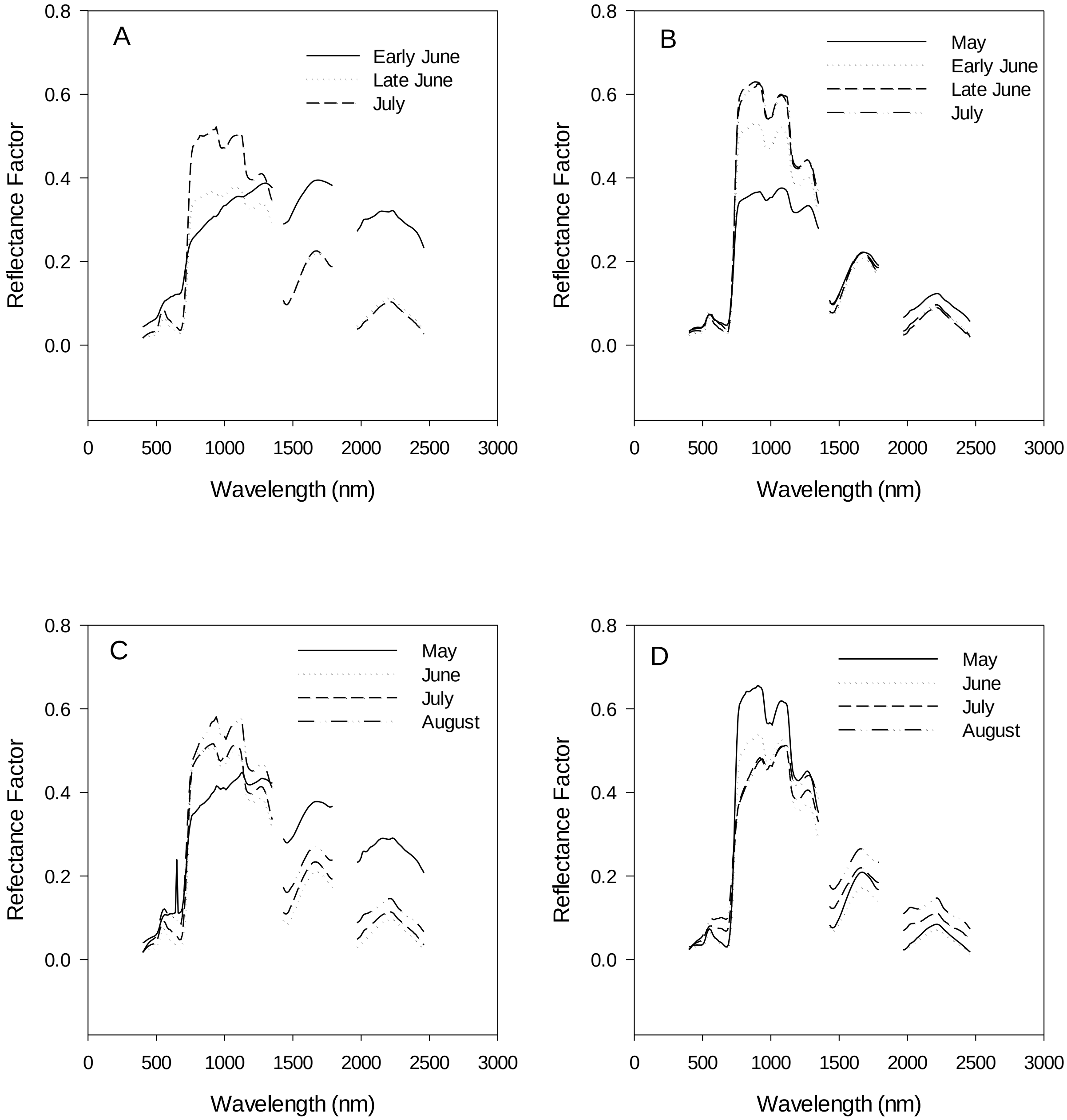

Figure 4.3. Mean canopy reflectance spectra of high biomass sorghum (N= 15 for each sampling period) and perennial grass (switchgrass and mixed grass) systems (N= 30 for each sampling period) collected at different period during the 2012 and 2013 growing seasons. (A) High biomass sorghum spectra collected in 2013; (B) Perennial grass spectra collected in 2013; (C) High biomass sorghum spectra collected in 2012; (D) Perennial grass spectra collected in 2012.

CHAPTER V

RAPID ASSESSMENT OF BIOENERGY FEEDSTOCK QUALITY BY NEAR INFRARED REFLECTANCE SPECTROSCOPY

ABSTRACT

The portability, quick turnaround time, and low long-term maintenance costs of Near Infrared Reflectance Spectroscopy (NIRS) offers rapid determination of feedstock quality. The objective of this study was to estimate biomass composition [total nitrogen (TN), acid detergent fiber (ADF), neutral detergent fiber (NDF) and acid detergent fiber (ADL)] with NIRS. Linear regression of simple ratios (SR), and partial least square (PLS) regression models with all wavebands (WB) and selected waveband (SB) approach were used. Laboratory analysis was conducted for TN, ADF, NDF and ADL. Samples from thirteen switchgrass (*Panicum virgatum* L.) cultivars, and 'ES5200' high biomass sorghum (*Sorghum bicolor* (L.) Moench) cultivar, and mixed grasses composed of 'Alamo' switchgrass, 'Cheyenne' Indian grass (*Sorghastrum nutans* (L.) Nash) and 'Kaw' big bluestem (*Andropogon gerardii* Vitman) fertilized at different rates of nitrogen (N) ranging from 0 to 252 kg N ha^{-1} yr^{-1} were collected from two locations in Oklahoma. Spectral reflectance between 1000 nm and 2500 nm was collected with an ASD FieldspecPro spectrometer from all samples. Results showed that TN can be estimated using SR of R_{2080}/R_{2190} (r^2=0.84), while an SR of R_{2190}/R_{2230} (r^2=0.65) was able to estimate ADF (r^2=0.70), NDF (r^2=0.65) and ADL (r^2=0.67). In comparison with SR, SB PLS model gave better

prediction accuracy with 9 wavebands for TN (r^2=0.93) and 7 wavebands for ADF (r^2=0.78), NDF (r^2=0.78), and ADL (r^2=0.65). In conclusion, the success of both SR and SB PLS for estimating bioenergy feedstock composition indicates opportunities for instrument development for practical purposes.

INTRODUCTION

The growing interest in use of biomass for liquid fuels and other energy related products has increased the need for cost effective, efficient, and accurate analytical methods for determining nitrogen, cellulose, hemicellulose and lignin in biomass. The ability to predict the biomass composition of a feedstock could be used for assessing N concentration for fertilizer management and biomass quality for ethanol conversion (Labbé et al., 2008). The cost of nitrogen fertilization, which is one of the most unsettling concerns for farmers, is guaranteed to play a major role in the decision to include bio-energy crops into their conventional system (Di Virgilio et al., 2007). Likewise, the composition of available feedstock will also play a critical role in the process used in conversion of biomass to fuel (Labbé et al., 2008). Direct methods for determining composition of feedstock are labor intensive, expensive and time consuming (Sanderson et al., 1996; Labbé et al., 2008; Ward et al., 2011). Biomass composition can be determined using the near infrared (NIR) portion of the spectrum (Sanderson et al., 1996; Labbé et al., 2008; Ward et al., 2011).

Lignocellulosic biomass can be converted into liquid fuels and other energy related products using biochemical processes or thermochemical processes (Sanderson et al., 1996; Labbé et al., 2008). Both ethanol and methane are the products from the biochemical processes, while methanol, synthesis gas, and pyrolysis oils are the products of the thermochemical processes. The quality of the lignocellulosic biomass for energy conversion depends on the conversion method. Elevated N, cellulose, sugar and starch concentration are desired for ethanol conversion using biochemical processes, while greater lignin and cellulose concentration are more suitable for the thermochemical conversion processes (Sanderson et al., 1996; Labbé et al., 2008). Greater N concentration in feedstock material reduces hydrocarbon yields during thermochemical conversion and increase nitric oxide (NOx) emissions. On the other hand, greater N is favorable for biochemical processes (Sanderson et al., 1996), as N is essential for microbial metabolism and growth. Similarly, greater lignin concentration is favorable for the thermochemical processes but can interfere with biochemical conversion by reducing the availability of cellulose and non-structural carbohydrate (Sanderson et al., 1996; Labbé et al., 2008).

Furthermore, near infrared reflectance spectroscopy is a proven analytical method in forage research to estimate neutral detergent fiber (NDF), acid detergent fiber (ADF), acid detergent lignin (ADL), and crude protein(CP) in forage crops (Sanderson et al., 1996; García-Ciudad et al., 1999; Gislum et al., 2004; Starks et al., 2004; Zhao et al., 2007; Kawamura et al., 2008; Labbé et al., 2008). Recently, Labbé et al., (2008) evaluated a dispersive NIR (D-NIR) using an Analytical Spectral Device (ASD) with scan range of 350-2500 nm and a Fourier Transform (FT-NIR) using a Varian Excalibur instrument with scan range 1000 – 2500 nm developed PLS models for estimating starch, sugar, total non-structural carbohydrate and N concentration in different switchgrass cultivars. They concluded that NIR can be used as a tool for rapid analysis of switchgrass composition and that the spectra collected by the D-NIR resulted in more accurate models than the FT-NIR. The use of NIR spectrum is not limited to developing prediction models for a single feedstock, but is capable of developing robust models that can predict the N concentration of a broad-range of feedstocks (Sanderson et al., 1996). Currently, the PLS regression method is the most common method of NIRS calibration and has been used by various studies in the development of models for the prediction of forage quality parameters such as CP, ADL, ADF, and NDF (Sanderson et al., 1996; Starks et al., 2004; Zhao et al., 2007; Kawamura et al., 2008; Labbé et al., 2008) and forage mineral composition (Ward et al., 2011). The PLS method is a full spectral calibration method that uses reflectance data from all wavebands in developing the calibration equations and depends on cross-validation to prevent over-fitting. However, (Kawamura et al., 2008) noted that waveband selection can refine the performance of the PLS analysis. The PLS models combine the most useful information from hundreds of wavebands into the first several factors, whereas less important factors might likely be included as background effects with little to no contribution to the model (Bolster et al., 1996). The PLS procedure in SAS (SAS, 2009) offers the regression coefficient profile and variable importance plots that give a direct indication of which predictors are most useful for the dependent variable. This approach can improve waveband selection and prediction capability of the PLS model. Partial least square models using the waveband selection were reported by Kawamura et al. (2008) to improve model coefficient of determination (r^2) for ADF from 0.30 to 0.65 and for CP from 0.38 to 0.62. The coefficient of determination (r^2), which indicates the proportion of variability explained by the model, is the most common tool for determining the performance. Davies and Fearn (2006) reported that r^2 is not a good evaluator of the performance of a model as it is dependent on the range of the dataset. In contrast, the RMSEP which measures the variability in the difference between the predicted and measured values for a set of validation samples is a much better evaluator of model performance (Davies and Fearn, 2006). Likewise, the RPD is a good evaluator that relates the RMSEP to the range of the measured data (Malley et al., 2005; Ward et al., 2011).

From a practical standpoint, simple linear models offer more usefulness with greater potential for wider adaptation. Furthermore, simple instruments similar to the greenseeker handheld and pocket sensors can easily be developed with ratios of two or more wavebands that could be utilized by farmers in the field to estimate the composition of feedstock material

(Lukina et al., 2001; Raun et al., 2002; Crain et al., 2012). The computation of ratios provides a very simple method for extracting the nutrient quantity signal from the sample spectra (Kakani and Reddy, 2010). Ratios are often calculated by using a ratio, differencing, ratio differences and sums, and by forming linear combinations of spectral band data (Jackson and Huete, 1991; Pinter et al., 2003). For example, vegetation indices such as normalized difference vegetative index (NDVI) are ratios that take advantage of reflectance relationship in different portion of the spectrum.

Development of prediction model to estimate the composition of plant standing in the field is often very challenging. Pinter et al. (2003) noted that spectral signatures of crop canopies in the field are more complex and often dissimilar from those of single green leaves measured under controlled conditions. Measurements of optical properties of plants canopies are strongly affected by illumination and viewing angles, row orientation, topography, climatic condition and other factors that are not directly related to agronomic or biophysical plant properties (Pinter et al., 2003). The use of dried ground samples to developed models for predicting feedstock composition provides a more stable source which optical properties are mostly by the material. In addition, the fewer external interfering factors allows for greater repeatability from NIR models developed for estimating nutrient concentration in the dried ground samples. Few studies have used the waveband selection approach in developing PLS models and simple ratios for N content prediction from NIRS in bioenergy feedstock materials. The objective of this study is to estimate bioenergy feedstock composition (TN, ADF, NDF and ADL) using linear regression of simple wavebands ratio and PLS regression models with both all and selected wavebands.

MATERIALS AND METHODS

Plant Materials

Biomass samples were collected from different experimental plots across two locations in Oklahoma during the 2011 and 2012 growing season. The plots, from which majority of the samples were collected from was a switchgrass variety trial located in Stillwater, Oklahoma (36.12ºN, 97.09ºW). The variety trial consisted of thirteen cultivars of switchgrass and was harvested on a biweekly basis. The remaining samples were obtained from a nitrogen rate x species experiment with sites located near Woodward (36.43 °N, 99.41°W) and Stillwater, Oklahoma (36.13ºN, 97.10ºW). The treatments were a cover crop (hairy vetch in 2011 and crimson clover in 2012) as a source of N and four N fertilization rates (0, 84, 168, 252 kgNha^{-1}), whereas the cropping systems treatments were 'Alamo' switchgrass (*Panicum virgatum* L.), 'ES5200' high biomass sorghum (*Sorghum bicolor* (L.) Moench), and a perennial grass mixture of 'Alamo' switchgrass, 'Cheyenne' indiangrass (*Sorghastrum nutans* (L.) Nash) and 'Kaw' big bluestem (*Andropogon gerardii* Vitman). The Stillwater site was harvested at approximately 14 day intervals during each growing season. Final harvests were taken following the first frost in November 2011 and 2012. The final harvest for 2011 growing season at the Woodward site was done in January 2012.

Subsamples were collected from 0.5 m within a row from each plot biweekly from April to September. Samples were oven dried at 70°C for 72 h, then ground in a shear mill (Cyclone Sample Mill, Udy Corp., Fort Collins, CO) to pass a 1 mm screen. A total of 404 samples collected in 2011 were analyzed for TN using dry combustion analysis (LECO TruSpec CHN, St. Joseph, MI, USA) and 143 samples also collected in 2011 were analyzed for ADF, NDF and ADL using acid detergent and neutral detergent extractions (Van Soest, 1963; Goering and Van

Soest, 1970). Twenty six (26) samples collected during the 2012 growing season from the three experiments used in 2011 were also analyzed for TN, ADF, NDF, and ADL. The samples represent sampling dates from April to the final harvest in November 2012. The ADF was considered to be the sum of the lignin and cellulose components, NDF the sum of hemicellulose, cellulose and lignin and ADL the lignin component of biomass. Therefore, the cellulose component of biomass can be computed from the difference between ADF and ADL and the hemicellulose from the difference between NDF and ADF. The TN samples comprised of the biweekly and the final harvest samples, while the ADF, NDF, and ADL samples were from final harvest and a few random biweekly samples.

Spectral Data

Near infrared spectra were collected on the ground plant samples using an ASD Field Spec Pro spectrometer (Analytical Spectral Devices Inc., Boulder, CO, USA) that consisted of a spectral range of 350-2500 nm and a 25° field of view. The spectrometer is equipped with three sensors (visible and near infrared-VNIR, shortwave infrared- SWIR1 and SWIR2) with spectral sampling of 3, 10 and 10 nm, respectively. The instrument was periodically calibrated to white spectral reflectance using a standard white reference panel (Labsphere Inc., North Sutton, NH, USA). The white reference was measured at 15 min intervals to check the instrument stability for 100% reflectance. To measure the sample reflectance, the samples (1 mm) were sandwiched between a petri dish painted black to create a non-reflecting black body and the light probe. This ensured that no extraneous light entered the sensor during these measurements. Thirty scans were collected and averaged into a single average spectrum. Two average spectra were obtained for each sample. Built-in spectral resolution output of the data from the ASD spectrometer is 1 nm along the whole spectrum. To reduce the amount of data for analysis, spectral data were averaged at 10-nm wavelength intervals (e.g. a band center at 1000 was the averaged value between 995-1005 nm) giving a total of 151 spectral bands between 1000 – 2500 for the NIR spectra.

Calibration Procedure

Feedstock Composition

Model calibration and validation were performed using procedure used by Ward et al. (2011) and Sanderson et al. (1996). The TN models were constructed using 293 samples collected throughout the growing season as the calibration dataset. Likewise, the ADF, NDF, and ADL models were constructed with 95 samples, mostly from the final harvest and a few random samples throughout the growing season. Samples used in the model calibration dataset were obtained from both the switchgrass variety trial and nitrogen x species experiments. The accuracy and precision of the predictive equations were validated using an actual test set of laboratory values of 111 selected samples for TN and 48 samples for ADF, NDF, and ADL as well as from both switchgrass variety trial and nitrogen x species experiment not included in the calibration of the model. To further validate the models a second validation dataset of 26 samples collected in 2012 from April to September from both switchgrass variety trial and nitrogen x species experiment were evaluated.

Linear Model

A total of 22650 simple ratios were computed using all the 1000-2500 nm wavebands as the numerator and 1000-2500 nm as the denominator in all the possible combinations in SAS. Coefficients of determination (r^2) were calculated and used to evaluate the linear relationships of TN, ADF, NDF, and ADL concentration with the computed reflectance value obtained from each ratio.

Partial Least Square (PLS) Models

The spectra were also used to create PLS regression calibration models for N concentrations. Partial least square regression is a full spectrum bilinear regression method that is widely used in laboratory calibrations of pasture nutritive value. This method uses reflectance data from all wavebands in developing calibration equations and relies on cross-validation to prevent over-fitting (Shenk and Westerhaus, 1991; Sanderson et al., 1996). All prediction models were developed using a single constituent determination and validation dataset. The regression equation used to describe a PLS model is defined as:

$$Y = \beta_o + \beta X + \varepsilon \qquad (1)$$

where Y is a (n x 1) vector with the measured variables of interest, X is a (n x p) matrix with reflectance values per spectral band, β_o is an unknown constant, β is a (p x 1) vector of regression coefficients and ε is a (n x 1) vector of errors identically and independently distributed with mean zero and variance σ^2 vector. In principle, the regression equation is similar to multivariate linear regression (MLR) except the values of the weighted coefficients (β_w) are calculated using PLS. Whereby, the β_w is calculated directly from the PLS loading corresponding to the model with the optimum number of latent factors, according to the following equation (Kawamura et al., 2008):

$$\beta_w = W \times (P^T \times W)^{-1} \times Q^T \qquad (2)$$

where W is the X-weight loading matrix, P is the X loading matrix and Q is the Y loading matrix. The latent factors are computed as certain linear combinations of the spectral amplitudes, and the responses are predicted linearly based on these extracted factors (SAS, 2009). The minimum value of root mean square error from the validation with test dataset was used as the criterion to select the appropriate number of latent factors and the coefficient of determination for the validation (r^2) to access the performance of the model.

Waveband Selection for PLS Model

There is increasing evidence indicating that PLS models include some redundant wavelengths and that waveband selection might improve the predictive accuracy of the model (Kawamura et al., 2008). Kawamura et al. (2008) pointed out that large absolute coefficients β_w indicates an important X variable. This implies that wavebands with large absolute coefficient explain more variability, thus identifying the more informative wavebands. The wavebands with the largest absolute β_w were selected from the PLS models with all the wavebands. After which, stepwise removal of wavebands was done based on the β_w value. The updated predicted residual sums of squares (PRESS) and coefficient of determination (r^2) were recorded at each step. PRESS is the sum of squares prediction error that SAS calculated for the number of factor included in the model (Yeniay and Goktas, 2002). The best PLS model was determined by choosing the one with the smallest PRESS and largest r^2. The result obtained for the PLS model with all the spectra was compared to the PLS model with selected wavebands.

Model Evaluation

The root mean square error of prediction (RMSEP) estimates the likely difference between prediction and measured values when the model is used with another dataset (Yeniay and Goktas, 2002). Thus, RMSEP is considered a good criterion to assess the performance of models (Davies and Fearn, 2006). The RMSEP was determined by the equation of (Yeniay and Goktas, 2002):

$$\text{RMSEP} = \sqrt{\frac{\sum_{i=1}^{n}(y_i - \hat{y}_i)^2}{n}} \qquad 3$$

where the $\hat{y}_i$ are the values of the predicted variables obtained from the validation dataset, y_i are the measured values from the validation dataset and n is the number of observations. Calibration models were also evaluated using the coefficient of determination (r^2), which indicates the proportion of variability explained by the model and the residual prediction deviation (RPD). This is actually the standard deviation of the reference data divided by the RMSEP, thus relating the RMSEP to the range of the reference measurements.

These parameters were used to classify the success of the predictions using the criteria described by Malley et al. (2005); excellent- r^2 is greater than 0.95 and RPD greater than 4; successful - r^2 0.9–0.95 and RPD 3–4; moderately successful - r^2 0.8–0.9 and RPD 2.25–3; and moderately useful - r^2 0.7–0.8 and RPD 1.75–2.25.In addition to these criteria, some calibrations with r^2< 0.70 were considered to be useful for screening purposes (Malley et al., 2005).

RESULTS AND DISCUSSION

Representative spectral samples show small variation at the baseline in the range of 1000 – 1400 nm for the thirteen (13) switchgrass cultivars (Fig. 5.1) and N treatments in high biomass sorghum and switchgrass (Fig. 5.2). Greater variation was observed among the species (Fig. 5.2) and N treatments in the mixed grass (Fig. 5.2) across the NIR spectra. Near infrared region of the spectrum is a unique representation of a substance or a mixture that consist of signals from bonds such C-O, C=O, O-H, C-H and N-H (Sanderson et al., 1996; Labbé et al., 2008; Kawamura et al., 2008). Therefore, the determination of TN, ADL, ADF, and NDF by NIRS in the dry ground sample can be explained by the absorption of infrared radiation by the N-H, C-H and O-H bonds present in the plant dry material. The N-H bond is primarily associated with TN, while the C-H and O-H with cellulose, hemicellulose, and lignin (Curran, 1989; Elvidge, 1990; Kawamura et al., 2008).

In general, the mean spectral reflectance across N treatments was greater in high biomass sorghum than for switchgrass and mixed grass (Fig. 5.2). Similar difference was also observed by Sanderson et al. (1996) in switchgrass, black locust, bagasse, sericea lespedeza, corn stover, and hybrid poplar in the 1100 – 1400 nm range. They attributed the difference to particular size of the materials as larger particles tend to absorb more infrared radiation than smaller (Windham et al., 1991). In this study, all samples were treated similarly and all the necessary steps were taken to achieve homogeneity as best as possible. All samples were ground to pass through 1 mm sieve. Windham et al. (1991) reported that high ash concentrations (7- 33wt %) as a result of soil contamination of forages may also cause similar baseline differences in reflectance. Ash concentration was not determined in this study, but the variations observed among the species indicate some variability in feedstock composition. As the variation is often greater in the 1000-1400 nm range, Sanderson et al. (1996) developed calibrations with and without this region and reported little to no effect on models performance and predictive ability.

Calibration Models

Summary data for calibration and validation data are presented in Table 5.1. Calibration equations were developed for ADF, NDF, ADL, and TN using PLS regressions of the entire spectrum (WB) 1000-2500nm and with selected wavebands (SB) based on the regression coefficient of each waveband obtained in the whole band PLS model and linear regression of simple ratios computed from all the reflectance wavebands (R_γ/R_γ). In general, the best calibrated model has the greatest coefficient of determination (r^2) and least root mean square error of calibration (RMSEC). Similar r^2 and RMSEC were obtained for all three model approaches.

For simple ratio (SR) model, the linear regression with the greatest coefficient of r^2 was selected and the calibration equation developed by regressing the SR with TN, ADF, NDF, and ADL in the calibration dataset (Fig. 3). The SR (R_{2080}/R_{2190}) selected for the TN range was from 0.90 -1.02 (Fig. 5.4). The range of SR is an indication of the variation of N concentration in biomass material due to cultivars, species and N treatments differences. A single SR (R_{2190}/R_{2230})

was found to be highly correlated with ADF, NDF, and ADL concentration in the biomass (Fig. 5.4). The SR values ranged for ADF, NDF, and ADL ranges from 0.99-1.03 (Fig. 5.4). The narrow range of SR values is an indication of the small variability in lignin, cellulose and hemicellulose in the feedstock materials. The calibration equation reported r^2 and RMSEC for TN of 0.92 and 2.0 g kg^{-1}, respectively, 0.78 and 27.0 g kg^{-1}, respectively, for ADF, 0.82 and 27.0 g kg^{-1}, respectively, for NDF, and 0.78 and 8.0 g kg^{-1}, respectively for ADL (Table 5.2).

Among the PLS models, WB PLS model results indicate that r^2 and RMSEC for the calibration of the TN was 0.96 and 1.2 g kg^{-1} respectively, 0.82 and 25.0 g kg^{-1}, respectively, for the ADF, 0.82 and 27.0 g kg^{-1}, respectively, for the NDF, and 0.77 and 8.0 g kg^{-1} respectively, for the ADL (Table 5.2). The SB PLS model reduced the number of wavebands in PLS model and resulted in nine selected wavebands (1450, 1580, 1630, 1830, 2030, 2100, 2180, 2250, and 2490 nm for TN and six (1610, 1730, 2160, 2230, 2310, 2420, and 2500 nm) for ADF, NDF, and ADL (Fig. 5.6). The number of wavebands selected represents 3 to 4% of the total wavebands. Calibration equations reported r^2 and RMSEC of 0.94 and 1.6 g kg^{-1} respectively, for TN, 0.85 and 23.0 g kg^{-1}, respectively, for ADF, 0.81 and 28.0 g kg^{-1}, respectively, for NDF, and 0.80 and 8.0 g kg^{-1}, respectively, for ADL (Table 5.2).

Prediction Models

Predictive ability of models was determined using several different criteria in the literature. Sanderson et al. (1996) used r^2, SEP and bias, Labbé et al. (2008) used r^2 and root mean square error of cross-validation (RMSECV), while Kawamura et al. (2008) used r^2 and RMSEP. The predictive ability of the models (SR, WB PLS and SB PLS) developed in this study were evaluated based on RMSEP, the r^2, and RPD criteria described by Malley et al. (2005).

Calibration of our SR model based on Malley et al. (2005) criteria using the 2011 and 2012 validation datasets indicates that the model was moderately successful and moderately useful for TN, respectively, moderately useful and unsuccessful, respectively for ADF, and unsuccessful with both datasets for NDF and ADL (Table 5.2).

Application of the WB-PLS model calibration equation to the 2011 and 2012 validation datasets were excellent and moderately useful, respectively, for the prediction of TN, and moderately successful and unsuccessful, respectively, for predicting ADF, NDF and ADL (Table 2). Similarly, the application of SB PLS calibration equations to the 2011 and 2012 validation datasets indicates that models were successful and moderately useful, respectively for TN, moderately useful and unsuccessful, respectively for ADF and NDF, and unsuccessful with both datasets for ADL (Table 5.2). In general, the reduction of wavebands was found to improve model predictive ability for ADF, NDF, and ADL. The best SB PLS model comprised of 9 wavebands for TN and 7 wavebands for ADL, ADF, and NDF (Table 5.2). Similarly, Kawamura et al. (2008) reported improvement using waveband reduction model with 6 wavebands for ADF and 47 for NDF out of a total 277 wavebands.

Models Comparison

The application of the calibration equations to two different validation datasets yielded varied results. As evaluation of the predictive ability of the models using the r^2, RMSEP and RPD suggest similar predictive ability for the WB and SB PLS and the SR models for ADF, NDF, ADL, but not TN (Table 5.2). Higher RMSEP and lower $r^2$and RPD values were observed with the 2012 validation dataset in comparison to the 2011 dataset for all the parameters (TN, ADL, ADF, and NDF) and all three models (Table 5.2). All three models performed poorly ranging from moderately useful to unsuccessful for the prediction of ADF, NDF and ADL. The poor model performance for the 2012 dataset can be attributed to the narrow range and minimal variability of ADL, ADF and NDF concentrations within the biomass materials. This can be attributed to the fact that majority of the calibration dataset used in the ADL, ADF and NDF models were obtained at the final harvest in 2011, while the 2012 validation dataset was obtained from random samples collected throughout the growing season. The cell wall components are reported to vary less within a species, while the variation is greater among species, plant parts and maturity (Jung and Vogel, 1992). Our study only had amalgamated samples of switchgrass, mixed grass (Indian grass, switchgrass, and big bluestem) and high biomass sorghum feedstock sources.

All three models (SR, WB and SB PLS) were somewhat successful for predicting TN in the feedstock materials. All models reported lowest RMSEP and highest RPD and r^2 values with the 2011 dataset. However, WB PLS model reported lowest RMSEP and highest RPD and r^2 with both validation datasets. Figure 6 shows the regression plot of predicted versus measured values for each biomass component for the 2011 validation dataset. The spread of the points around the regression line for ADF, ADL and NDF indicates the large variation in the estimation of the measured values. However, in the TN plots the points are clustered around the regression line (Fig. 5.6). In general, the models predict TN, ADF, NDF, and ADL with greater precision for the 2011 validation dataset than the 2012 validation dataset. For example, prediction of the TN was most precise with the WB PLS model (RMSEP = 1.2 g kg^{-1} and RPD =5) for the 2011 validation dataset, but did not differ (RMSEP =3.0 g kg^{-1} and RPD 1.80-1.97 for WB, SB and SR models) among the models for the 2012 validation dataset. The greatest variation was found among the PLS models, while variation within SR model for the 2011 (RMSEP = 3.0 g kg^{-1} and RPD = 2.20) and 2012 (RMSEP = 3.0 g kg^{-1} and RPD =1.87) dataset was small. These results indicate that the performance of the SR model was most reliable across multiple datasets. The variation of the calibration equation when applied to the two datasets can be attributed to the year-to-year variation that exists within the samples as well as possible variation in the selected waveband identified using 2011 samples. It is suggested that the best way to overcome year-to-year variation and selected wavebands would be to include samples from multiple years in the calibration dataset and develop a new calibration equation (Shetty et al., 2011). But our study demonstrates the stability of the SR model suggests the robustness and applicability of the SR model across years.

The main purpose of a PLS model is to extract the minimum number of factors that can explain as much sample variation as possible. The more extracted factors improve the model fit to the observed data, but can also result in tailoring the model to the current data, thus affecting the usefulness of the model in making future predictions (SAS, 2009). In SAS PLS procedure, the number of factors to be included in the model is determined by the cross-validation. Therefore, while both PLS models have somewhat similar RSMEP and r^2 values for each component, they differed in the number of extracted factors. Four factors were able to explain more than 75% of the predictor sample variation in the models with SB PLS model for estimating ADL, ADF, and NDF and five factors were required to explain more than 75% variation with the WB PLS models. Likewise, four factors explained 94% in the SB PLS model for TN and seven factors were required to explain 96% with the WB PLS model. These results agrees with Kawamura et al. (2008) that waveband reduction actually improved the predictive ability of the PLS models.

The wavebands identified in the TN prediction models presented in this study were similar to those previously published for biomass feedstock. Previous studies of several plant species suggest that tissue concentration of TN, ADL, ADF, and NDF in dry ground materials are most highly correlated with reflectance wavebands in the range of 1200-2400 nm (Garcia-Ciudad et al., 1999; Labbe et al., 2008; Kawamura et al., 2008). Moreover, wavebands 1510, 1700, 1690, 2150, 2180, 2300, and 2350 nm were reported to be associated with TN in plant materials (Curren, 1989; Elvidge, 1990). Wavebands 1200, 1580, 1685, 1690, 2100, 2270, 2276, 2280, 2336, 2340 and 2350 nm are reported to associate with lignin and cellulose concentration in dried plant material (Curran, 1989; Elvidge, 1990). The wavebands identified in this study were found to be similar or almost similar to those reported for each of the measured feedstock components.

The predictive ability of the models is also consistent with earlier published work estimating TN concentration in plant material (Sanderson et al., 1996; Gislum et al., 2004; Ward et al., 2011) and ADF and NDF in dried plant materials using NIR reflectance (Kawamura et al., 2008), but not for ADL (Sanderson et al., 1996). However, few studies reported using two validation datasets across years. Sanderson et al. (1996) reported $r^2$of prediction and RPD values of 0.90 and 3.33 for N and 0.99 and 6.83 for lignin across numerous bioenergy feedstock materials (switchgrass, sugarcane bagasse, corn, lespedeza and various woody species). More recently, Ward et al. (2012) reported an r^2 of prediction value of 0.76, RMSEP value of 3.2g kg^{-1}, and RPD of 2.33 for N in meadow fescue; Labbé et al. (2008) reported $r^2$of prediction value of 0.97 and RMSEP value of 27 kg N ha^{-1} within the switchgrass biomass. The samples used in this study were not as diverse as those used in Sanderson et al. (1996), but were more diverse than that of Labbé et al. (2008). Kawamura et al. (2008) reported $r^2$and RMSEP values of 0.35 and 29.4 g kg^{-1} for ADF and 0.24 and 45 g kg^{-1} for NDF with whole band and 0.53 and 2.49 % for ADF and 0.31 and 4.28% for NDF with selected PLS models from canopy reflectance of perennial pasture (ryegrass, orchardgrass, and white clover). Clearly, a global model that includes more diverse feedstock materials cannot be expected to have the same predictive ability as one or two species model (Gislum et al., 2004). However, our results demonstrate excellent potential for prediction of TN by NIR in botanically diverse biomass feedstock materials using WB PLS regression models. The predictive accuracy of the TN model using remote sensing is not expected to be better than laboratory methods because both plant materials and measurements configurations are much better controlled (Kawamura et al., 2008). However, these approaches can provide rapid assessment of biomass quality, particularly TN on a near real time basis.

To the best of our knowledge this is the first report of simple ratio NIR models for predicting the quality of bioenergy feedstocks. Therefore, predictability of the SR model was determined in relation to the WB PLS model. In general, both WB PLS and SR models were successful in predicting feedstock quality, particularly N. The success of the SR model, particularly for predicting N concentration suggests possible application for use by farmers and bio-refineries. Feedstock with high N concentration is more desirable as a feedstock source for the biochemical process and is less desirable for the thermochemical process. However, since it is unlikely that bio-refineries would employ the use of both conversion processes, or even if the refineries utilize both processes, rapid quality assessment of feedstock will be essential to maximize the efficiency of the conversion process. In addition, feedstock materials have several uses such as hay for animal feed and paper pulp production. The robust SR model identified in this study has potential for the development of simple inexpensive instrumentations that could be used by farmers to rapidly assess the feedstock quality. The potential for farmers to rapidly determine feedstock quality in a labor and cost efficient manner could improve management decisions for feedstock use.

The use of dried ground samples can be seen as a disadvantage due to the amount of labor required to prepare the sample for analysis. However, this process can be mechanized at factory gate to sample and grind for analysis. Moreover, ground samples do not require immediate analysis and thus can be stored and used at a later date, are more homogeneous, reduce the effect of tissue moisture on spectral reflectance and have been used in many previous studies (Sanderson et al., 1996; García-Ciudad et al., 1999; Gislum et al., 2004; Labbé et al., 2008; Ward et al., 2011).

CONCLUSIONS

Based on r^2, RMSEP and RPD calibration models for ADL, ADF and NDF performed better with selected wavebands suggesting that these parameters can be predicted with only a few selected wavebands and the TN WB PLS performed excellently using 2011 dataset and was moderately useful with 2012 dataset. Significant year-to-year variation was observed when calibration equations were applied across year for all models and quality parameters, except for the SR model. The SR model was found to be moderately useful for estimating TN across years. This result suggests that a SR linear equation could be used to estimate TN concentration for many feedstocks. The simplicity of the SR linear model could provide opportunities for development of simple and inexpensive instrumentation with practical application at the farm and field scale.

REFERENCES

Bolster K.L., Martin M.E., Aber J.D. 1996. Determination of carbon fraction and nitrogen concentration in tree foliage by near infrared reflectances: a comparison of statistical methods. Canadian Journal of Forest Research 26:590-600. DOI: 10.1139/x26-068.

Crain J., Ortiz-Monasterio I., Raun B. 2012. Evaluation of a reduced cost active NDVI sensor for crop nutrient management. Journal of Sensors, vol. 2012, Article ID 582028, 10 pages, 2012. doi:10.1155/2012/582028.

Curran P.J. 1989. Remote sensing of foliar chemistry. Remote Sensing of Environment 30:271-278. http://dx.doi.org/10.1016/0034-4257(89)90069-2.

Davies A., Fearn T. 2006. Back to basics: calibration statistics. Spectroscopy Europe 18:31-32.

Di Virgilio N., Monti A., Venturi G. 2007. Spatial variability of switchgrass (Panicum virgatum L.) yield as related to soil parameters in a small field. Field Crops Research 101:232-239. DOI: DOI 10.1016/j.fcr.2006.11.009.

Elvidge C.D. 1990. Visible and near infrared reflectance characteristics of dry plant materials. Remote Sensing 11:1775-1795. http://dx.doi.org/10.1080/01431169008955129.

García-Ciudad A., Ruano A., Becerro F., Zabalgogeazcoa I., Vázquez de Aldana B.R., García-Criado B. 1999. Assessment of the potential of NIR spectroscopy for the estimation of nitrogen content in grasses from semiarid grasslands. Animal Feed Science and Technology 77: 91-98. DOI: 10.1016/s0377-8401(98)00237-5.

Gislum R., Micklander E., Nielsen J.P. 2004. Quantification of nitrogen concentration in perennial ryegrass and red fescue using near-infrared reflectance spectroscopy (NIRS) and chemometrics. Field Crops Research 88:269-277. DOI: 10.1016/j.fcr.2004.01.021.

Goering H., Van Soest P.J. 1970. Forage fiber analyses (apparatus, reagents, procedures, and some applications) Handbook No. 379, US Agricultural Research Service, Washington.

Jackson R.D., Huete A.R. 1991. Interpreting vegetation indices. Preventive Veterinary Medicine 11:185-200. http://dx.doi.org/10.1016/S0167-5877(05)80004-2.

Jung H.-J.G., Vogel K.P. 1992. Lignification of switchgrass (*Panicum virgatum*) and big bluestem (*Andropogon gerardii*) plant parts during maturation and its effect on fibre degradability. Journal of the Science of Food and Agriculture 59:169-176. DOI: 10.1002/jsfa.2740590206.

Kakani, V. G., & Reddy, K. R. (2010). Reflectance properties, leaf photosynthesis and growth of nitrogen deficient big bluestem (*Andropogon gerardii*). Journal of Agronomy and Crop Science, 196: 379-390. doi:10.1111/j.1439-037X.2010.00425.x.

Kawamura K., Watanabe N., Sakanoue S., Inoue Y. 2008. Estimating forage biomass and quality in a mixed sown pasture based on partial least squares regression with waveband selection. Grassland Science 54:131-145. DOI: 10.1111/j.1744-697X.2008.00116.x.

Labbé N., X.P. Ye, J. A. Franklin, A. R. Womac, D. D. Tyler, Rials T.G. 2008. Analysis of switchgrass characteristics using near infrared spectroscopy. Bioenergy Resources. 3:1329-1348.

Lukina E., Freeman K., Wynn K., Thomason W., Mullen R., Stone M., Solie J., Klatt A., Johnson G., Elliott R. 2001. Nitrogen fertilization optimization algorithm based on in-season estimates of yield and plant nitrogen uptake. Journal of plant nutrition 24:885-898. http://dx.doi.org/10.1081/PLN-100103780.

Malley D., McClure C., Martin P., Buckley K., McCaughey W. 2005. Compositional analysis of cattle manure during composting using a field-portable near-infrared spectrometer.

Communications in Soil Science and Plant Analysis 36:455-475. http://dx.doi.org/10.1081/CSS-200043187.

Pinter P.J., Hatfield J.L., Schepers J.S., Barnes E.M., Moran M.S., Daughtry C.S.T., Upchurch D.R. 2003. Remote sensing for crop management. Photogrammetric Engineering and Remote Sensing 69:647-664.

Raun W.R., Solie J.B., Johnson G.V., Stone M.L., Mullen R.W., Freeman K.W., Thomason W.E., Lukina E.V. 2002. Improving nitrogen use efficiency in cereal grain production with optical sensing and variable rate application. Agronomy Journal 94:815-820. http://dx.doi.org/10.2134/agronj2002.0815.

Sanderson M.A., Agblevor F., Collins M., Johnson D.K. 1996. Compositional analysis of biomass feedstocks by near infrared reflectance spectroscopy. Biomass & Bioenergy 11:365-370. http://dx.doi.org/10.1016/S0961-9534(96)00039-6.

SAS. 2009. Sas User's Guide, SAS Institute Inc., Cary, North Carolina.

Shenk J.S., Westerhaus M.O. 1991. Population Definition, Sample Selection, and Calibration Procedures for Near Infrared Reflectance Spectroscopy. Crop Sci. 31:469-474. DOI: 10.2135/cropsci1991.0011183X003100020049x.

Shetty N., Gislum R., Jensen A.M.D., Boelt B. 2011. Development of NIR calibration models to assess year-to-year variation in total non-structural carbohydrates in grasses using PLSR. Chemometrics and Intelligent Laboratory Systems. 111:34–38. http://dx.doi.org/10.1016/j.chemolab.2011.11.004.

Starks P.J., Coleman S.W., Phillips W.A. 2004. Determination of Forage Chemical Composition Using Remote Sensing. Journal of Range Management 57:635-640. http://dx.doi.org/10.2307/4004021.

Van Soest P.J. 1963. Use of detergents in analysis of fibrous feeds: a rapid method for the determination of fiber and lignin. Association of Official Analytical Chemists 46:829-835.

Ward A., Nielsen A.L., Møller H. 2011. Rapid assessment of mineral concentration in meadow grasses by near infrared reflectance spectroscopy. Sensors 11:4830-4839. http://dx.doi.org/10.3390/s110504830.

Windham W.R., Hill N.S., Stuedemann J.A. 1991. Ash in Forage, Esophageal, and Fecal Samples Analyzed Using Near-Infrared Reflectance Spectroscopy. Crop Sci. 31:1345-1349. DOI: 10.2135/cropsci1991.0011183X003100050053x.

Yeniay O., Goktas A. 2002. A comparison of Partial Least Squares Regression with Other Prediction Methods. Hacettepe Journal of Mathematics and Statistics 31:99-111.

Zhao D., Starks P.J., Brown M.A., Phillips W.A., Coleman S.W. 2007. Assessment of forage biomass and quality parameters of bermudagrass using proximal sensing of pasture canopy reflectance. Grassland Science 53:39-49. DOI: 10.1111/j.1744-697X.2007.00072.x.

Table 5.1. Descriptive statistics of samples total nitrogen (N) content (%) acid detergent fiber (ADF), neutral detergent fiber (NDF) and acid detergent lignin (ADL) measured in laboratory.

Data	Parameter	TN	ADF	NDF	ADL
		———g kg^{-1}———			
Calibration	N	293	95	95	95
	Min	2.5	280	490	40
	Max	41.1	520	820	110
	Mean	11.6	410	677	73.5
	Range	38.6	240	330	70
	SD†	7.1	63.4	70	19.4
Validation1	N	111	48	48	48
	Min	4.0	290	510	40
	Max	41.4	540	770	90
	Mean	11.3	390	660	60
	Range	37.4	250	260	50
	SD†	6.3	58.8	53.7	16.2
Validation2	N	26	26	26	26
	Min	5.0	300	530	40
	Max	25.0	460	700	90
	Mean	12.5	370	610	65
	Range	19.6	160	170	50
	SD†	6.3	58.8	53.7	16.2

†Standard deviation (SD) and n is the number of samples. Validation 1 and validation 2 datasets were collected in 2011 and 2012 from the switchgrass variety trial and species x nitrogen treatment experiments.

Table 5.2. Optimum number of factors, coefficient of determination from PLS models, root mean square error for the calibration and validation datasets, and residual prediction deviation for PLS models with all wavebands (1000-2500nm), selected wavebands (SB) and simple ratio (SR).

Method		TN (g kg^{-1})	ADF (g kg^{-1})	NDF (g kg^{-1})	ADL (g kg^{-1})
WB-PLS	$R^2_{calibration}$	0.96	0.82	0.82	0.77
	$RMSEC_{calibration}$	1.2	25.0	27.0	8.0
	R^2_{val1}	0.96	0.70	0.76	0.60
	$RMSEP_{val1}$	1.2	30.0	28.0	10.0
	R^2_{val2}	0.77	0.01	0.22	0.01
	$RMSEP_{val2}$	3.0	36.0	38.0	11.0
	No. F.	7	5	5	5
	RPD_{val1}	5.00	1.80	1.93	1.60
	RPD_{val2}	1.97	1.00	1.11	1.00
SB- PLS	$R^2_{calibration}$	0.94	0.85	0.81	0.80
	$RMSEC_{calibration}$	1.6	23.0	2.80	8.0
	R^2_{val1}	0.93	0.78	0.78	0.65
	$RMSEP_{val1}$	2.0	25.0	2.50	9.0
	R^2_{val2}	0.63	0.22	0.23	0.28
	$RMSEP_{val2}$	3.4	38.5	4.70	11.0
	No. F.	5	4	4	4
	No. WB	9	7	7	7
	RPD_{val1}	3.10	2.08	2.21	1.70
	RPD_{val2}	1.80	1.11	1.12	1.16
SR	$R^2_{calibration}$	0.92	0.78	0.82	0.78
	$RMSEC_{calibration}$	2.0	27.0	2.70	8.0
	R^2_{val1}	0.84	0.70	0.65	0.67
	$RMSEP_{val1}$	3.0	23.0	3.30	9.0
	R^2_{val2}	0.70	0.12	0.10	0.23
	$RMSEP_{val2}$	3.0	35.0	40.0	10.0
	RPD_{val1}	2.20	2.10	1.70	1.70
	RPD_{val2}	1.87	1.03	1.04	1.12
	Ratio	R_{2080}/R_{2190}	R_{2190}/R_{2230}	R_{2190}/R_{2230}	R_{2190}/R_{2230}

No.F- number of factors used in PLS model; *No.WB* – number of wavebands used in model; *RMSEC* – root mean square error of calibration; $RMSEP_{val1}$ – root mean square error of prediction using validation dataset from samples collected in 2011; $RMSEP_{val2}$ -root mean square error of prediction using validation dataset from samples collected in 2012; *RPD*- residual prediction deviation using validation datasets for 2011 and 2012.

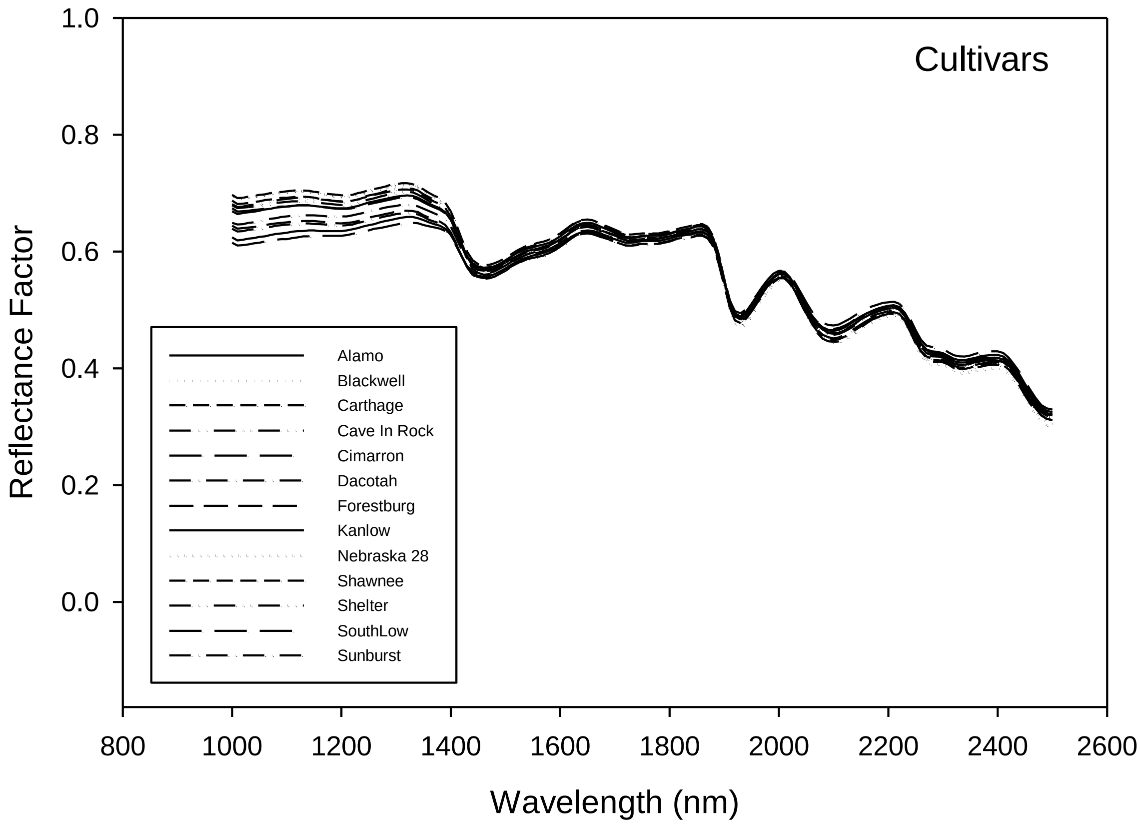

Fig.5.1. Representative NIR (1000-2500 nm) spectra for thirteen (13) switchgrass cultivars used in the study.

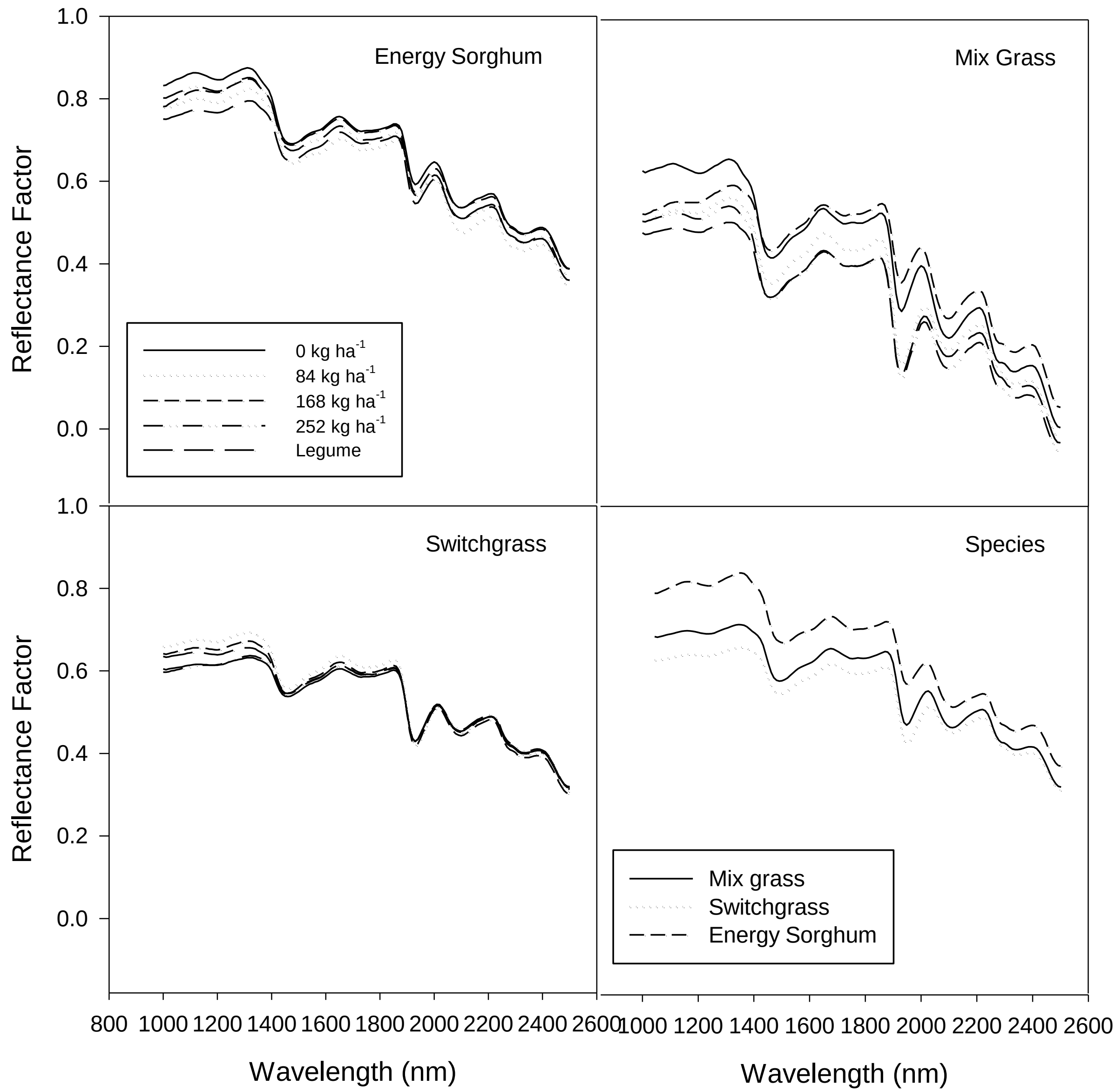

Fig.5.2. Representative near infrared (NIR) spectra, the effects of N treatments on the NIR spectra, and the meas spectra across N treatments of three biomass feedstocks: high biomass sorghum, switchgrass, mixed grass.

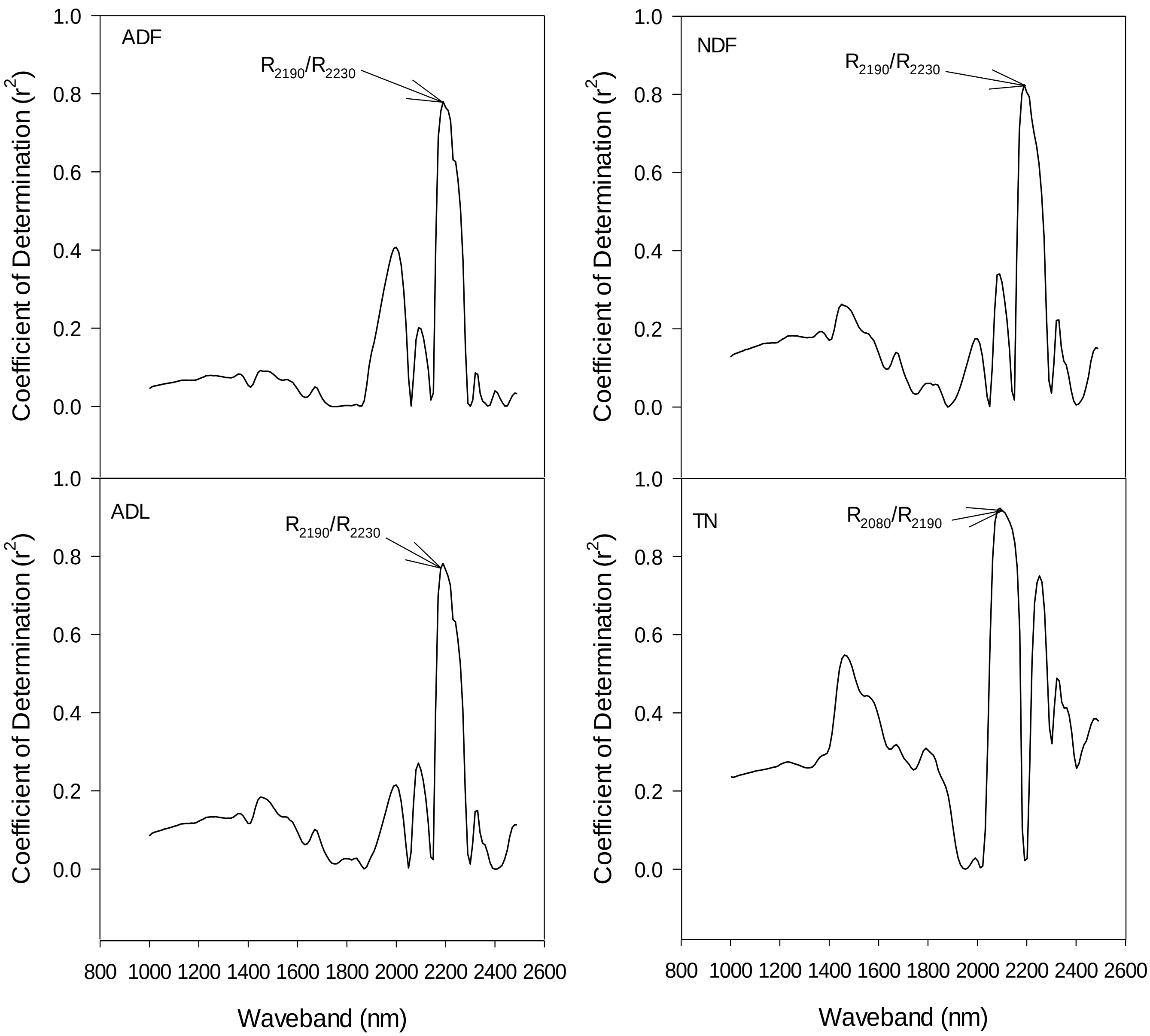

Fig.5.3. Coefficients of determinations (r^2) for reflectance ratios of R_λ/R_λ to highlight the selected ratio with highest r^2 value. The r^2 values were based on a linear model using the calibration dataset.

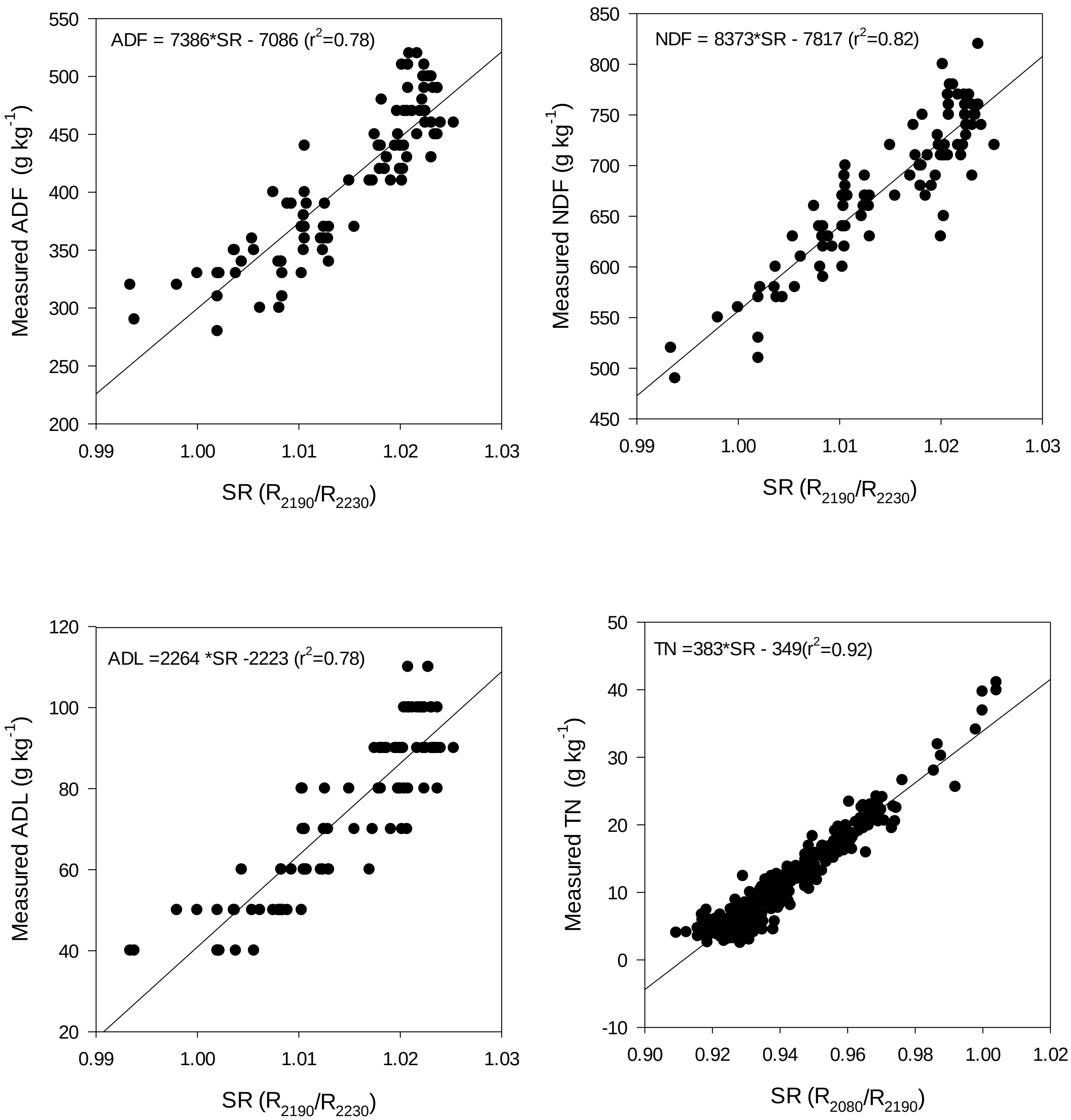

Fig.5.4. Calibration equation development for SR for predicting ADF, NDF, ADL, and TN concentration in feedstock material obtained from switchgrass variety trial and species x nitrogen treatment experiments in 2011.

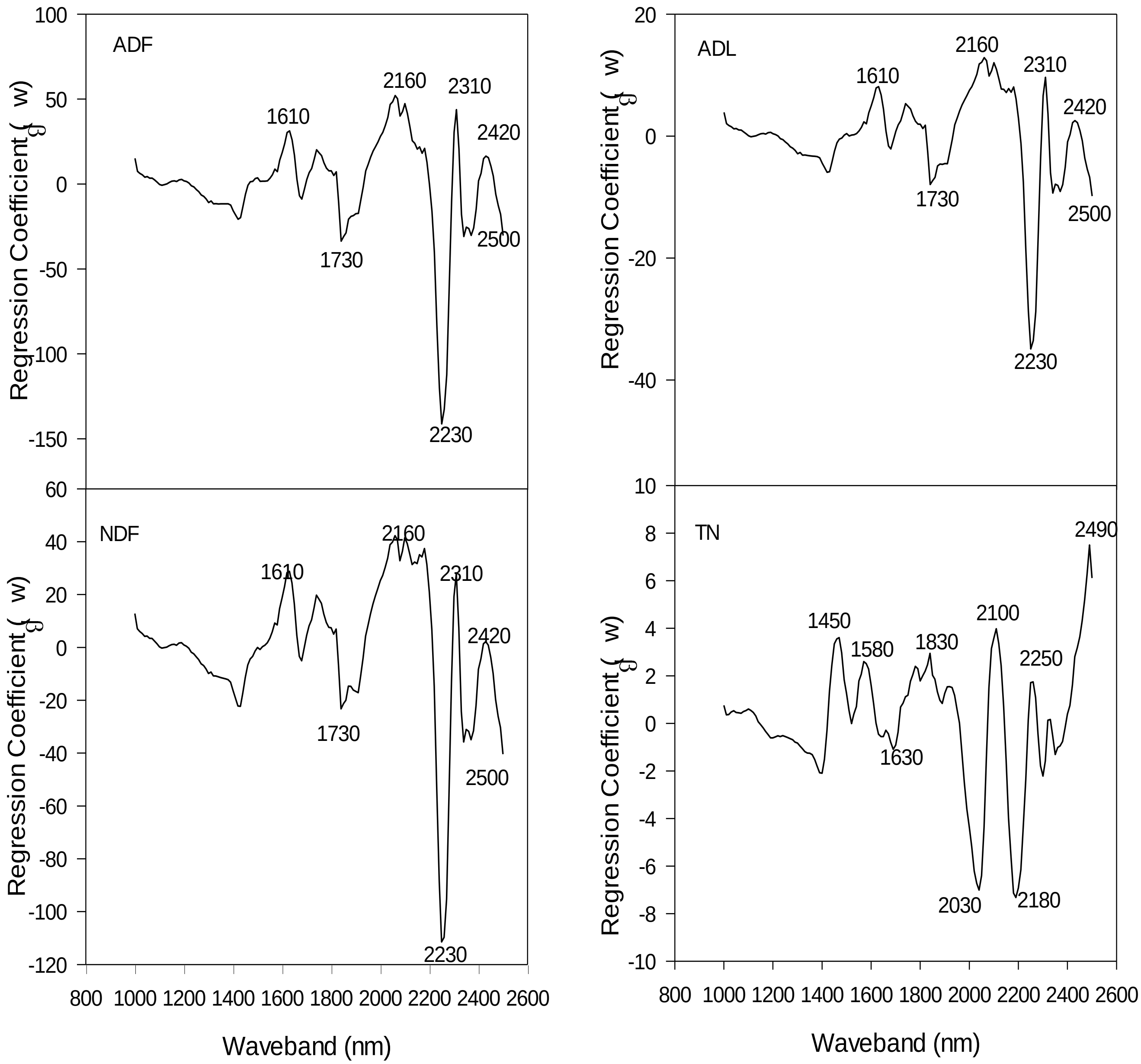

Fig.5.5. Selection of the optimum number of wavebands based on their large regression coefficient (βw) calculated by the whole band PLS model for each waveband.

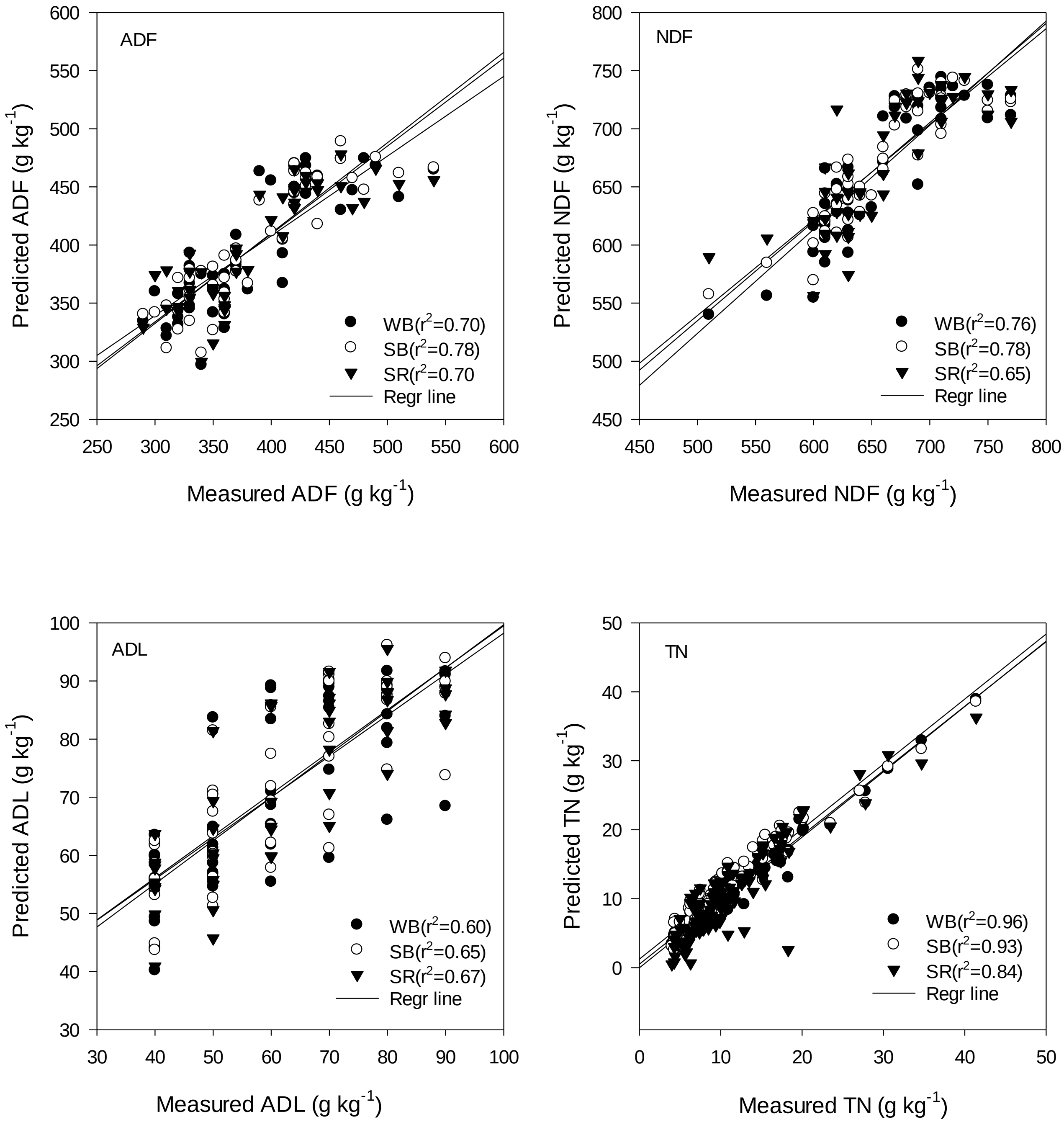

Fig.5.6. Regression of NIRS predicted values for biomass extractives ADF, NDF, ADL, and TN on measured laboratory values obtained from PLS model using the whole band (1000-2500nm), selected waveband and simple ratio of NIR waveband using validation dataset for samples collected in 2011.

CHAPTER VI

SPATIAL VARIABILITY WITHIN A SWITCHGRASS FIELD AT FINE AND COARSE SCALE SAMPLING IN OKLAHOMA

ABSTRACT

The objective of this study was to describe the spatial patterns of selected soil properties and biomass yield at fine and coarse scale in a switchgrass field to determine the appropriate sampling approach to enable the calculation of means with minimum variance. Spatial variability of biomass yield and soil properties at fine (2.5m sampling interval) and coarse (10m sampling interval) scales was assessed through semivariogram analysis. The site was located in Chickasha, Oklahoma, consisted of two soil types a Dale silt loam (Fine-silty, mixed, superactive, thermic Pachic Haplustolls) and McLain silty clay loam (Fine, mixed, superactive, thermic Pachic Argiustolls). Eighty soil samples were collected along two 100m transects at 2.5 and 10 m intervals established across each soil type in 2012 and 2013. The semivariograms revealed coarse scale OC to be strongly correlated with range values from 56 – 78 m for both soils. A strong correlation with a range of 5 m was observed for switchgrass yield at the fine scale McLain silty clay for both years. The fine scale Dale silt loam switchgrass yield showed a weak spatial dependence over a range of 36 m in 2012 and 5 m in 2013. NDVI was consistently moderately correlation with a distance less than 30m at the fine scale for both years. Conversely, a reliable spatial dependence could not be identified for TN. These results indicates that spatial

correlation of coarse scale OC might have been imposed by the cropping system, while spatial correlation of switchgrass yield was influenced by the soil texture, particularly clay content . The use of the NDVI measurement was useful to describe the spatial distribution of switchgrass yield with good precision at the fine scale. Based on the results presented the appropriate sampling approach to obtain the best estimate of OC could be achieved by systematic sampling, while random sampling maybe the most practical way for estimating switchgrass yield.

INTRODUCTION

The challenge for agronomy researchers is to characterize crop yield variation in space and time to provide farmers with useful information to make good management decision (Larscheid and Blackmore 1996). Several studies have identified a number of reasons for the difficulties in charactering crop yield variation in space and time. Growing season precipitation, annual temperature, N fertilizer and ecotype are some of the reasons for variation in switchgrass yield (Wullschleger et al. 2010). In the Ozzano Dell'Emilia valley area in Spain, Di Virgilio et al. (2007) conducted a study using GIS and geostatistic methods to produce thematic maps of soil parameters and switchgrass yield to quantify the relationship between biomass yield spatial variation and soil parameters (N, P, soil moisture, soil texture and OM) in a small plot (5 ha) in 2004 and 2005. The maps produced from the study showed significant variability in the relationship between switchgrass yield and nearly all the soil parameters (Di Virgilio et al. 2007).

In the northern US, variation in switchgrass population for nine variables (biomass yield, survival, dry matter, lodging, maturity, plant height, holocellulose, lignin, and ash) was partly due to temperature and eco-region defined by soil type (Casler 2005). Likewise, switchgrass yield was found to vary across 10 locations in the Great Plains [North Dakota (Munich and Streeter), South Dakota (Bristol, Highmore, Huron and Ehtan) and Nebraska (Crofton, Atkinson, Douglas and Lawrence)] (Schmer et al. 2010). Kiniry et al. (2005) simulating switchgrass yield using the ALMANAC (Agricultural Land Management Alternatives with Numerical Assessment Criteria) model for locations in three southern states [Texas (Dallas, Stephenville, and College Station), Arkansas (Hope) and Louisiana (Clinton)] found that changing the runoff curve number used to determine potential runoff water from the soil by 15% changed the mean annual biomass from 1 to 31% depending on location.

A quantitative estimation of spatial variability of soil properties and crop yield can be obtained using semivariogram modeling (Di Virgilio et al. 2007; Huang et al. 2001; Reese and Moorhead 1996; Warrick et al. 1986). A semivariogram describes the relationship between spatially separated data points as a function of distance (Buchter et al. 1991; Isaaks and Srivastava 1989; Warrick et al. 1986). The relationship is described for each variable by the semivariogram parameters: nugget, sill (total semi-variance) and range. Nugget is the variance at distance of zero and represent inherent variability or experimental error; sill is the semi-variance value at which the semivariogram reaches the upper bound after its initial increase; range is the distance at which each variable becomes spatially independent (samples closer to the range are related , samples further apart are not). Traditionally, one of the main reasons for deriving a semivariogram is to use it to predict or estimates values at unsampled locations in kriging interpolation (Di Virgilio et al. 2007; Huang et al. 2001; Curran 1988). However, a semi-variograms can also be used to relate semivariance of spatial separation and provides concise and unbiased description of the scale and pattern of spatial variability (Curran 1988; Journel and Huijbregts 1978). For example, spatial distribution of soil properties, erosion and crop yield along a cultivated transect and an adjacent transect in virgin grassland was studied by Moulin et al (1994). The statistical distribution of soil properties and crop yield in the landscape was found to be affected by erosion that was a result of the interaction between elevation and surface curvature. Likewise, Huang et al. (2001) observed a periodic behavior for soil total carbon along transect that was mainly dependent on field topographic position and not on land use.

Site specific crop management using remote sensing and geographic information systems that make use of semivariogram modeling has been proposed as a means of managing the spatial and temporal variation of soil related, biological, landform and meteorological factors that influence crop yield (Corwin et al. 2008; Corwin and Lesch 2005; Reuter et al. 2005; Kitchen et al. 2003). Remote sensing is the process of acquiring information about an object by a device separate from it by some distance such as ground-based booms, aircraft, or satellite. Barnes et al. (1996) outlined three applications for using remote sensing data in site specific agriculture. In the first application, multispectral images are used for detection of plant stresses (such as, pest, water stress and nutrient deficiency). In the second application, variation in spectral responses is correlated to specific variables such as soil properties. Once these site-specific relationships are developed, multispectral images can be translated directly to maps of fertilizer applications and yield variability. In the third application, multispectral data is converted to quantitative units such as vegetative indices (VIs) with physical meaning. Vegetative indices can be integrated into physically based growth models used for assessing crop growth and development. Remotely sensed measurements through various VIs can assess crop yield potential for switchgrass production and can provide reliable and consistent information about spatial and temporal variability at regional production scale.

Characterizing of variation within a field is dependent on the sampling method used. The selection of the appropriate sampling approach is important to enable the calculation of means with the minimum variance. Curran and Williamson (1986) reported that systematic as opposed to random sampling offers the potential to increase the precision. Semivariogram analysis has demonstrated in a various studies that the proportion of nugget to sill or total semivariance is a strong indicator of whether the precision of a parameter can be increased with systematic as opposed to random sampling (Cambardella et al. 1994; Curran and Williamson 1986). Furthermore,Curran (1988) suggested that the semivariograms can be used for remote sensed and ground data to aid the choice of sample units and sample numbers. Thus the objective of this study was to describe the spatial patterns of fine and coarse scale sampling of OC, TN, NDVI and switchgrass yield to determine the appropriate sampling approach to enable the calculation of means with minimum variance.

MATERIALS AND METHODS

Experimental site

This study was conducted on an 8 ha switchgrass (Alamo) field established in 2010 at Chickasha, Oklahoma (35.042° N, -97.917°W). The field comprises of two soil types a Dale silt loam [Fine-silty, mixed, superactive, thermic Pachic Haplustolls] (~60%) and McLain silty clay loam [Fine, mixed, superactive, thermic Pachic Argiustolls] (~40 %). Soil P and K were maintained at the levels recommended by the Oklahoma State Soil testing laboratory for warm season grasses. Annual N fertilization (82 kg ha^{-1}) was applied in the second year after the establishment and each subsequent year. Table 1 describes the climatic condition of the site for the 2012 and 2013 growing seasons.

Yield and soil measurements

Each year 2012 and 2013, the field was sampled at fine and coarse scale to permit spatial modeling of biomass yield and soil properties. For coarse scale sampling, switchgrass biomass and soil samples will be collected within 0.5 m^2 area centered on geo-referenced-grid nodes spaced every 10 m. Fine scale sampling of feedstock biomass and soil samples will occur within 0.5 m^2 distributed every 2.5 m along the two 100 m transects spaced between grid nodes to capture spatial variability at short distances. After randomly establishing transects in 2012, it was later discovered that majority of transect 1 was located on the Dale silt loam and the entire transect 2 on the McLain silty clay loam. In 2013, transects were randomly established on each of the soil type (Fig 1). Subsamples of the switchgrass biomass yield [0.1 m^2 (0.5 m row at 0.20 m row spacing)] were hand-clipped and processed for determination of dry matter yield. Soil samples were collected in March of both years from 0-15 cm depth and analyzed for total organic carbon (OC) and total nitrogen (TN). Soil OC and TN concentrations were determined by dry combustion using LECO CN analyzer (LECO Corp., St. Joseph, MI).

Acquisition of Sensor Reflectance Measurements

Spectral data was collected from aerial photograph taken in August of 2012 and 2013. Imagery was converted into reflectance to compute the normalize difference vegetation index (NDVI).

Spatial analysis

Spatial variability of feedstock (NDVI and yield) and soil properties (TN and OC) at fine and course-scales was assessed through semivariogram modeling to quantify the spatial variation for each variable (Warrick et al. 1986). Traditionally, modeled semivariogram are used in kriging interpolation, but the parameters of a semivariogram can also be used to describe the spatial dependence (pattern) of a variable with distance (Huang et al. 2001). There are several models to describe semivariogram. However, in this study, spatial variation was characterized using circular and spherical models.

Calculating Semivariogram

For a transect running across the field of equally spaced samples and measurements of soil properties, NDVI (pixel) and biomass yield there will be *m* pairs of observations separated by the same lag (distance). Thus, the semivariance γ(h) is estimated as:

$$\gamma(h) = \frac{1}{2N(h)} \sum_{i=1}^{N(h)} [Z(x_i) - Z(x_i + h)]^2. \qquad (1)$$

Where $N(h)$ is the number of pairs separated by lag distance h; $Z(x_i)$ is measured sample value at point i; and $Z(x_i + h)$ is measured sample value at point i+h.

To obtain the best fitted model, the model data frequency distribution was compared to a normal distribution. The shape of the data distribution is often described by the skewness coefficient. An absolute value greater than 2, the distribution is considered as skewed (Huang et al. 2001). A significant positive value indicates a long right tail; a negative value indicates a long left tail.

Statistical Analysis

Data analysis for each transect dataset was done to determine normality, descriptive statistics (mean, standard deviation, maximum, minimum and CV) and semivarigorams were defined and differences in nugget and total semivariance and range examined for each of the variable. The ArcView software package (Arcmap) was used to analyze the spatial structure of the data and to define the semivariograms. Selection of the best fitting semivariogram model was based on the lowest RMSE (root mean square error) and confirmed by visual inspection. The lag-distance used was between 2 and 8 depending on the variable.

Spatial correlation with distance for each variable was assessed quantitatively by dividing the nugget by the sill. The classification classes describe by Cambardella et al. (1994) was used to describe the nugget/sill ratio: 1) < 25%, strong spatial dependence; 2) 25-75% moderate spatial dependence; 3) >75% spatially independent or pure nugget; and 4) Random when the slope of semivariogram is close to zero, regardless of nugget ratio.

RESULTS AND DISCUSSION

Descriptive Statistics

The descriptive statistics for TN, OC, NDVI and biomass yield for 2012 and 2013 at fine (2.5 m) and coarse (10 m) scale sampling distance for each transects were presented in Table 1. Mean TN was similar between soils, while higher OC and biomass yield was observed for the McLain silty clay loam for both years. Switchgrass yield increased for each soil from 2012 to 2013, while OC and NDVI value decreased. Distributions of TN, OC, NDVI and biomass yield were normally distributed for the fine scale sampling distance based on the skewness value (skewness Coefficient < 2). The McLain Silty Clay Loam NDVI was significantly negatively skewed at the coarse scale for both years of the study. Log transformation generally reduced skewness, but skewness values for NDVI increased after the log transformation. The standard deviation and CV were used as estimates of variability (Table 2). In general, greater variation for the soil parameters (OC and TN) were observed in the Dale silt loam, but the McLain silty clay loam reported greater variability for yield parameters (NDVI and switchgrass yield) based on the standard deviation and CV values. Switchgrass yield was highly variable with CV greater than 40% for Dale silt loam and 50% for McLain silty clay loam at fine and coarse scale. The yield ranges from 150 -816 g/0.10m^2 in 2012 and 260 – 1463 g/0.10m^2 in 2013 for the Dale silt loam at fine and coarse scale. Yield for the McLain silty clay loam ranges from 35 -1655 g/0.10m^2 and 55 -1498 g/0.10m^2 in 2012 and 360 -2670 g/0.10m^2 and 390 -2580 g/0.10m^2 in 2013 at the fine and coarse scale respectively. The variation observed between the soils for the soil parameters and yield parameters may be attributed to intrinsic characteristics related to each soil and extrinsic sources. Rao and Wagenet (1985) define intrinsic variation as the natural variations within a soil and extrinsic variation as the variations that imposed on a field as part of crop production practices. However, since the same production practice was imposed on the entire field, the variation in soil parameters can be considered to be more intrinsic, whereas variation in yield parameters maybe attributed to a combination of intrinsic and extrinsic sources.

Semivariogram Models

The geostatistical parameters describing the soil and yield parameters from the transect datasets were listed in Table 3. Spatial variation was characterized using spherical and circular models. For circular and spherical models, semivariance increases with distance between samples (lag distance) to a constant value (sill or total semivariance) at a given separation distance called the range of influence (Cambardella et al. 1994).   Samples separated by range distance are related spatially, and those separated by distance greater than the range are not spatially related. In other words, semivariogram models where the slope is not equal to zero describes samples that are spatially related, while models with slope that is close to zero (where the total variance equals the nugget variance) describes samples that are not related. The semivariogram for the McLain silty clay loam fine and coarse scale TN exhibits a slope close to zero in 2013, suggesting that TN was not related at either the fine or coarse scale sampling distance. Likewise, coarse scale TN and switchgrass yield also reported slope close to zero on the Dale silt loam and the McLain silty clay loam coarse scale NDVI for both 2012 and 2013. Semivariogram slope for OC was positive, except at the 2013 fine scale.   A positive slope means that samples within the distance of influence (range) were closely related. Positive slope was also observed for the fine scale NDVI and yield for both soils in 2012.

According to Webster, (1985) estimates of range tend to be landscape dependent that may be interpreted to indicate the distance across distinct soil type. However, in this study the estimate of range can be attributed to small landscape changes within a soil type (i.e. wet spots). Range values were considerable variable among the different parameters. There were some similarities in range values for OC, TN and NDVI for the Dale silt loam at the fine scale sampling distance across both years. While, greater variation in range values were observed for the McLain silty clay loam and at the coarse scale sampling distance.

The distinct classification of spatial dependence based on Cambardella et al.(1994) that uses a nugget ratio expressed as percentage of the total semivariance was used to determine the spatial dependence of fine and coarse scale TN, OC, NDVI and switchgrass yield of Dale silt loam and McLain silty clay loam soils within the same field for the 2012 and 2013 growing seasons. Semivariograms indicated strong spatial dependence for variables such as coarse scale OC for both soils in 2012 and 2013, McLain silty clay loam fine scale switchgrass yield in 2012 and 2013, and the Dale silt loam coarse scale NDVI in 2013 (Table 3). Strong spatial dependence of OC was also reported for several other studies under different production practices. For example, Cambardella and Karlen (1999) reported strong spatial dependence of OC under conventional and organic field in Iowa, Huang et al. (2001) for soils under conservation reserve program land for 10 years and partially continuously crop land, and Cambardella et al. (1994) under tillage and no-till fields. All these studies reported sampling distance greater than 10 m separating each sampling points. Therefore, the strong spatial dependence of the coarse scale OC reported in this study is a strong indication that the coarse scale sampling (10 m) was appropriate for determining the spatial dependence of OC. Moreover, the variations of spatial dependence for the fine scale OC. Whereby, strong and close to a weak spatial dependence was observed for the Dale silt loam in 2012 and 2013 respectively, and weak and no spatial dependence for the McLain silty clay loam in 2012 and 2013 respectively, suggest that the fine scale sampling was not the most appropriate. Considering that the transects location differed each year of the study (Fig 1), the results of this study and others mention above are strong indication that spatial distribution of OC can be determined systematically from samples collected at distance greater than 10 m apart.

Spatial dependence of fine scale NDVI did not change from 2012 to 2013, but switchgrass yield spatial dependence did for the Dale silt loam. In 2012 and 2013 growing seasons, fine scale NDVI was moderately correlated for both soils, but fine scale switchgrass yield was weak and moderately correlated in 2012 and 2013 for the Dale silt loam respectively, and strongly correlated for the McLain silty clay loam (Table 3). In contrast, spatial dependence was more variable at the coarse scale. The difference in the range distance was small from year to year. Similar range was observed for switchgrass yield at the fine scale for the McLain silty clay loam for both years, but differed for the Dale silt loam. The range of influence for the McLain silty clay loam was 5m for both years and the Dale silt loam was 36 and 5m in 2012 and 2013 respectively. The larger range of influence in 2012 for the Dale silt loam could be a result of the inclusion of a few samplings from the McLain silty clay loam (Fig 1). The small nugget ratio and small range values for the fine scale McLain silty clay loam switchgrass yield for both years (Table 3) is an indication of the high variable in stand density (Cambardella and Karlen 1999) that was observed within the field. Likewise, the small range for the Dale silt loam in 2013 is also an indication of a patchy distribution of switchgrass yield (Di Virgilio et al., 2007). The McLain silty clay loam high clay content resulted in an extended wet period during the early spring precipitation that impacted the germination and stand establishment. The average number of plants harvested per 0.1 m^2 was 2.3 for the Dale silt loam and 1.4 for the McLain silty clay loam. Therefore, the higher biomass yield observed on the McLain silty clay loam was a result of increased tillering as individual plants took advantage of the available space and less competition (Table 2). In addition, switchgrass stand established at row spacing of 0.2m have been observed to thin over time resulting in a more patchy distribution. This could very be the scenario with the Dale silt loam. Di Virgilio et al. (2007) also reported a smaller range in describing the spatial distribution of switchgrass in a field from 2004 to 2005. Spatial dependence at the coarse scale was inconsistent, thus a reliable spatial correlation could not be identified to describe the spatial patterns of NDVI and yield in this field.

There was a consistent pattern in the spatial correlation between NDVI and switchgrass yield. Moderate spatial correlation for fine scale Dale silt loam NDVI corresponds with a weak and a moderate spatial correlation for yield in 2012 and 2013 respectively. Similarly, a moderate spatial correlation for fine scale McLain silty clay loam NDVI corresponds with a strong spatial correlation for yield in 2012 and 2013. At the coarse scale, weak spatial dependence for the Dale silt loam NDVI correspond to a random distribution for the Dale silt loam yield in both years. The McLain silty clay loam coarse scale NDVI and yield were both randomly distributed in 2012, but NDVI was randomly distributed and yield was strongly spatial correlated within a distance of 65m in 2013. Curran (1986) pointed out that consideration of sample size is of particular importance when remotely sensed data are correlated to ground data or whenever ground data are being estimated from remotely sensed data. The sample size in this study was identical for ground and remotely sensed data. Therefore, the small variation was assumed to be a result of difference in sample area used to compute the NDVI (0.25 m^2) and sampling area (0.1 m^2) for the biomass. The computed NDVI is based on the extraction of a value for the transect point within a pixel in relation to the point location, while the actual sampling collection involve harvesting of a 0.5 m row within the location of each transect point. Based on the sampling approach, the consistency in the spatial pattern observed is a strong indication that remotely sensed data could be used to describe the spatial distribution of switchgrass yield across the two soil types within this field.

In general, remote sensing approach for determining the best sampling approach to enable the calculation of means with minimum variance offers numerous advantages over actual field samples, but should always be support by ground sampling data. For example, in this study a systematic sampling at distance of samples 2.5 m apart was found to be appropriate to describe the spatial distribution of NDVI for both soils. On the contrary, the actual ground sampling suggests that a random sampling approach might be appropriate for the Dale silt loam and systematic sampling at 2.5 m for the McLain silty clay loam. Sampling at 2.5m distance is impractical to most producers as it is labor intensive and time consuming. The use of remote sensing for the estimation of switchgrass yield can be done at this sampling distance inexpensively and with less labor and time. These results indicate that remote sensing measurements could be used to adequately describe the spatial distribution of switchgrass yield at fine scale.

To evaluate temporal variation from year to year, fine scale NDVI was computed for the 2012 and 2013 transect points using the aerial imagery of 2013 and 2012 respectively. The result shows similar spatial correlation for fine scale NDVI using the 2013 NDVI values and 2012 transects points for both soil types (Table 3). When NDVI was computed from the 2013 aerial image for the 2012 transect points the Dale silt loam fine scale NDVI was moderately correlated over a range of 39 m an increase of 10 m and the McLain silty clay loam was moderately correlated over a range of 5 m a decrease of 5m compared to the 2012 NDVI. Similarly, when 2012 NDVI was computed with the 2013 transects points the Dale silt loam was strongly correlated over a range of 9 m a decrease of 18m and the McLain silty clay loam strongly correlated over a range of 23 m a decrease of 1m compared to the 2013 NDVI. These results further suggest that variation was small from year to year for each of the soil type within the field and also illustrates the benefit of using remote sensed data for describing spatial distribution of switchgrass yield.

Spatial dependence of TN was ranked moderate, weak or random (no spatial dependence). Total N in 2012 was strong and moderate spatial dependence at the coarse scale over a distance of 54 and 66 m for the Dale silt loam and the McLain silty clay loam respectively. In 2013, randomness dominated at the coarse scale for both soil types. At the fine scale, weak spatial dependence was observed for both soils in 2012 and for the Dale silt loam in 2013, but was random for the McLain silty clay loam (Table 6.3). Spatial pattern of OC and biomass yield was in general somewhat stable within soil type for both years, but TN varied greatly. The variation of spatial dependence of TN is not surprising. It is well documented that soil nitrogen is influenced by environmental factors such as temperature and moisture. Therefore, the warmer temperature and wetter condition prior to sampling in 2012, opposed to cooler temperature and drier condition prior to sampling in 2013 could have attributed to differences in the spatial patterns observed.

Some researcher hypothesized that strongly spatially dependent properties may be controlled by intrinsic variations in soil characteristics such as texture and mineralogy and weak spatially dependence properties may be controlled by extrinsic variations such as fertilizer application and cropping practice (Rao and Wagenet, 1985; Cambardella et al., 1994). Therefore, the weak to random spatial correlation observed for TN at the fine and coarse scale could be seen as indicators of the influence of extrinsic variations, such as fertilizer application and cropping practice and the medium spatial dependence of NDVI controlled by the combined effect of the intrinsic and extrinsic factors. On the contrary, the consistent strong spatial dependence of coarse scale OC across the different soil type suggest that it may be controlled by extrinsic factors such as cropping system and residue removal. Whereas, the differences in spatial correlation for switchgrass yield between the two soils further suggest that soil surface texture was the dominant influence. Di Virgilio et al. (2007) study evaluated the spatial dependence of numerous soil characteristics (silt content, clay content, sand content, organic matter , soil strength, soil moisture, pH, P and N) based on nugget/ sill ratio (Cambardella et al., 1994) in a switchgrass field found only clay content to have strong spatial correlation with distance. The soils used in this study are almost identical with only difference is that the McLain silty clay loam contain 31% clay to 20 % of the Dale silt loam (Web Soil Survey, 2013).

CONCLUSIONS

Since most spatial analysis studies of a field involved multiple soil types. Similar spatial pattern of OC across soil type and variation in yield and TN could suggest that the best precision of OC maybe achieved by systematic sampling. While the best precision of switchgrass yield and TN could be achieved by random sampling. The coarse scale sampling was appropriate for determining the spatial variation of OC, while fine scale sampling was appropriate for switchgrass yield. The relationship between the spatial dependence of NDVI obtained from aerial imagery and the spatial dependence of switchgrass yield from ground sampling suggested that NDVI may be used to determine the appropriate sampling approach for measuring the switchgrass yield. Finally, spatial patterns described for the different parameters indicates that spatial dependence of coarse scale OC was independent of soil type, fine scale switchgrass yield was greatly influenced by the soil type (clay content) and spatial dependence of TN could not consistently be identified from year to year on the same soil type.

REFERENCES

Barnes, E. M., Moran, M. S., Pinter, J., P.J., & Clarke, T. R. Multispectral remote sensing and site-specific agriculture: Examples of current technology and future possibilities. In *International Conference on Precision Agriculture, Minneapolis, MN, 23 June 1996* (pp. 843-854): ASA

Buchter, B., Aina, P., Azari, A., & Nielsen, D. (1991). Soil spatial variability along transects. *Soil technology*, *4*(3), 297-314.

Cambardella, C., Moorman, T., Parkin, T., Karlen, D., Novak, J., Turco, R., et al. (1994). Field-scale variability of soil properties in central Iowa soils. *Soil Science Society of America Journal*, *58*(5), 1501-1511.

Cambardella, C. A., & Karlen, D. L. (1999). Spatial Analysis of Soil Fertility Parameters. *Precision Agriculture*, *1*(1), 5-14, doi:10.1023/a:1009925919134.

Casler, M. (2005). Ecotypic variation among switchgrass populations from the northern USA. *Crop Science*, *45*(1), 388-398.

Corwin, D., & Lesch, S. (2005). Characterizing soil spatial variability with apparent soil electrical conductivity: I. Survey protocols. *Computers and Electronics in Agriculture, 46*(1), 103-133.

Corwin, D. L., Lesch, S. M., Shouse, P. J., Soppe, R., & Ayars, J. E. (2008). 16 Delineating Site-Specific Management Units Using Geospatial ECa Measurements. *Handbook of agricultural geophysics*, 247.

Curran, P., & Williamson, H. (1986). Sample size for ground and remotely sensed data. *Remote Sensing of Environment, 20*(1), 31-41.

Curran, P. J. (1988). The semivariogram in remote sensing: an introduction. *Remote Sensing of Environment, 24*(3), 493-507.

Di Virgilio, N., Monti, A., & Venturi, G. (2007). Spatial variability of switchgrass (< i> Panicum virgatum</i> L.) yield as related to soil parameters in a small field. *Field Crops Research, 101*(2), 232-239.

Huang, X., Skidmore, E., & Tibke, G. (2001). Spatial Variability of soil properties along a transect of CRP and continuously cropped land. *Sustaining the Global Farm*, 24-29.

Isaaks, E. H., & Srivastava, R. M. (1989). *Applied geostatistics*: Oxford University Press.

Journel, A. G., & Huijbregts, C. J. (1978). *Mining geostatistics* (Vol. 600): Academic press London.

Kiniry, J., Cassida, K., Hussey, M., Muir, J., Ocumpaugh, W., Read, J., et al. (2005). Switchgrass simulation by the ALMANAC model at diverse sites in the southern US. *Biomass and Bioenergy, 29*(6), 419-425.

Kitchen, N., Drummond, S., Lund, E., Sudduth, K., & Buchleiter, G. (2003). Soil electrical conductivity and topography related to yield for three contrasting soil–crop systems. *Agronomy Journal, 95*(3), 483-495.

Larscheid, G., & Blackmore, B. (1996). Interactions between farm managers and information systems with respect to yield mapping. *Precision Agriculture*(precisionagricu3), 1153-1163.

Moulin, A., Anderson, D., & Mellinger, M. (1994). Spatial variability of wheat yield, soil properties and erosion in hummocky terrain. *Canadian journal of soil science, 74*(2), 219-228.

Rao, P., & Wagenet, R. (1985). Spatial variability of pesticides in field soils: methods for data analysis and consequences. *Weed Science, 33*.

Reese, R. E., & Moorhead, K. K. (1996). Spatial characteristics of soil properties along an elevational gradient in a Carolina bay wetland. *Soil Science Society of America Journal, 60*(4), 1273-1277.

Reuter, H., Giebel, A., & Wendroth, O. (2005). Can landform stratification improve our understanding of crop yield variability? *Precision Agriculture, 6*(6), 521-537.

Schmer, M. R., Mitchell, R. B., Vogel, K. P., Schacht, W. H., & Marx, D. B. (2010). Spatial and temporal effects on switchgrass stands and yield in the Great Plains. *BioEnergy research, 3*(2), 159-171.

Soil Survey Staff, Natural Resources Conservation Service, United States Department of Agriculture. Web Soil Survey. Available online at http://websoilsurvey.nrcs.usda.gov/. Accessed [September/17/2013].

Warrick, A., Myers, D., & Nielsen, D. (1986). Geostatistical methods applied to soil science. *Methods of Soil Analysis: Part 1—Physical and Mineralogical Methods*(methodsofsoilan1), 53-82.

Webster, R. (1985). Quantitative spatial analysis of soil in the field. *Advances in soil Sciences, 3*.

Wullschleger, S. D., Davis, E. B., Borsuk, M. E., Gunderson, C. A., & Lynd, L. R. (2010). Biomass Production in Switchgrass across the United States: Database Description and Determinants of Yield. *Agronomy Journal*, *102*(4), 1158-1168, doi:DOI 10.2134/agronj2010.0087.

Table 6.1 Precipitation (mm) and temperature (^{o}C) at Chickasha, Oklahoma during 2012 and 2013.

Months	Rainfall (mm)		Temperature (^{o}C)	
	2012	2013	2012	2013
Jan	50	38	5	4
Feb	16	73	7	6
Mar	113	27	15	9
Apr	79	269	18	13
May	150	76	22	20
Jun	71	113	26	26
Jul	48	145	30	27
Aug	43	24	28	27
Sep	117	49	24	28
Oct	14	58	16	16
Mean/ Total	701	872	19	18

Table 6.2. Statistical parameters of selected soil properties, NDVI and switchgrass yield along two 100 m transects at two sampling distance over two growing seasons.

Parameter	Transect and Sampling distance	Sample No.	Mean	Stand. Dev	Minimum	Maximum	Skewness	Coeff. Var.
				2012				
TN (g kg^{-1})	T1@2.5 m	40	1.10	0.20	0.70	1.60	0.29	19
	T1@10 m	9	1.10	0.20	0.70	1.40	-1.01	20
	T2@2.5 m	40	1.30	0.20	0.90	1.60	-0.01	14
	T2@10 m	9	1.30	0.20	1.00	1.40	-1.01	13
OC (g kg^{-1})	T1@2.5 m	40	11.2	2.60	7.80	20.7	1.26	23
	T1@10 m	9	13.0	2.40	8.10	15.30	-0.61	18
	T2@2.5 m	40	14.9	1.40	12.20	18.70	0.72	9
	T2@10 m	9	14.7	1.50	12.60	16.90	0.45	10
NDVI	T1@2.5 m	40	0.491	0.03	0.416	0.545	-0.45	7
	T1@10 m	9	0.492	0.02	0.464	0.519	-0.68	4
	T2@2.5 m	40	0.488	0.08	0.153	0.611	-1.85	16
	T2@10 m	9	0.470	0.13	0.150	0.610	-2.10	28
BM (g 0.1 m^{-2})	T1@2.5 m	40	403	185	150	816	0.66	46
	T1@10 m	9	385	238	150	816	0.94	62
	T2@2.5 m	40	619	383	35	1655	0.72	62
	T2@10 m	9	720	505	55	1498	0.47	70
				2013				
TN (g kg^{-1})	T1@2.5 m	40	1.10	0.10	0.90	1.30	-0.15	8
	T1@10 m	9	1.10	0.10	1.00	1.20	-0.18	7
	T2@2.5 m	40	1.20	0.10	1.10	1.30	-0.07	6
	T2@10 m	9	1.20	0.00	1.20	1.30	1.33	0.3
OC (g kg^{-1})	T1@2.5 m	40	11.0	1.10	9.00	13.7	0.29	10
	T1@10 m	9	11.1	1.20	9.50	13.7	0.88	11
	T2@2.5 m	40	13.4	0.60	12.4	15.5	0.98	4
	T2@10 m	9	13.3	0.20	12.4	14.0	-0.39	5
NDVI	T1@2.5 m	40	0.358	0.05	0.267	0.455	0.04	13
	T1@10 m	9	0.348	0.04	0.267	0.401	-0.72	12
	T2@2.5 m	40	0.444	0.07	0.267	0.600	-0.24	17
	T2@10 m	9	0.437	0.01	0.267	0.497	-1.97	2
BM (g 0.1 m^{-2})	T1@2.5 m	40	538	228	260	1463	1.80	42
	T1@10 m	9	712	342	260	1463	1.04	48
	T2@2.5 m	40	1051	515	360	2670	1.28	49
	T2@10 m	9	1087	681	390	2580	1.20	63

Transects (T1 and T2) were 100 m long with sample points every 2.5 and 10 m apart, T1 was located on a Dale silt loam and T2 on a McLain silty clay loam within the same switchgrass field in Chickasha Oklahoma.

Table 6.3. Semivariogram models and spatial distribution parameters of switchgrass yield, total nitrogen and organic carbon collected across two seasons (2012 and 2013) at different sampling distance (2.5m and 10m) along two 100 m transects on different soil types (Dale silt loam and McLain silty clay loam) within the same field.

Parameter	Transect and Sampling distance	Model	Range (m)	Nugget Ratio†	Class‡	RMSE
			2012			
TN (g kg^{-1})	T1@2.5 m	Spherical	35	75	W	0.02
	T1@10 m		0	100	R	0.02
	T2@2.5 m	Spherical	56	80	W	0.02
	T2@10 m	Spherical	66	49	M	0.02
OC (g kg^{-1})	T1@2.5 m	Spherical	90	20	S	0.13
	T1@10 m	Spherical	56	22	S	0.17
	T2@2.5 m	Spherical	8	80	W	0.15
	T2@10 m	Spherical	65	0	S	0.07
NDVI	T1@2.5 m	Spherical	29	48	M	0.03
	T1@10 m	Spherical	56	76	W	0.03
	T2@2.5 m	Spherical	10	38	M	0.07
	T2@10 m		0	100	R	0.14
	T1-NDVI13[1]	Spherical	39	70	M	0.04
	T2-NDVI13[2]	Spherical	5	63	M	0.07
BM (g 0.1 m^{-2})	T1@2.5 m	Spherical	36	87	W	191
	T1@10 m		0	100	R	258
	T2@2.5 m	Spherical	5	11	S	366
	T2@10 m		0	100	R	524
			2013			
TN (g kg^{-1})	T1@2.5 m	Spherical	52	75	W	0.01
	T1@10 m		0	100	R	0.01
	T2@2.5 m		0	100	R	0.01
	T2@10 m		0	100	R	0.01
OC (g kg^{-1})	T1@2.5 m	Circular	5	74	M	0.08
	T1@10 m	Spherical	78	5	S	0.08
	T2@2.5 m		0	100	R	0.05
	T2@10 m	Circular	54	9	S	0.03
NDVI	T1@2.5 m	Spherical	27	64	M	0.05
	T1@10 m	Spherical	65	2	S	0.03
	T2@2.5 m	Circular	24	70	M	0.07
	T2@10 m		0	100	R	0.08
	T1-NDVI12[3]	Spherical	9	0	S	0.03
	T2-NDVI12[4]	Spherical	23	25	S	0.04
BM (g 0.1 m^{-2})	T1@2.5 m	Spherical	5	60	M	244
	T1@10 m		0	100	R	391
	T2@2.5 m	Spherical	5	32	M	534
	T2@10 m	Spherical	65	6	S	468

†Nugget ratio = (Nugget semivariance/sill)*100 , [1] NDVI computed for T1@2.5m using 2013 aerial image, [2]NDVI computed for T2@2.5m using 2013 aerial image, [3]NDVI computed for T1@2.5m using 2012 aerial image, and [4]NDVI computed for T2@2.5m using 2012 aerial image. ‡Spatial Class: S= strong spatial dependence (% Nugget ratio <25); M = moderate spatial dependence (% Nugget ratio between 25 and 75); W= weak spatial dependence (% Nugget ratio >75); R = random (slope of semivariogram close to zero, regardless of nugget ratio).

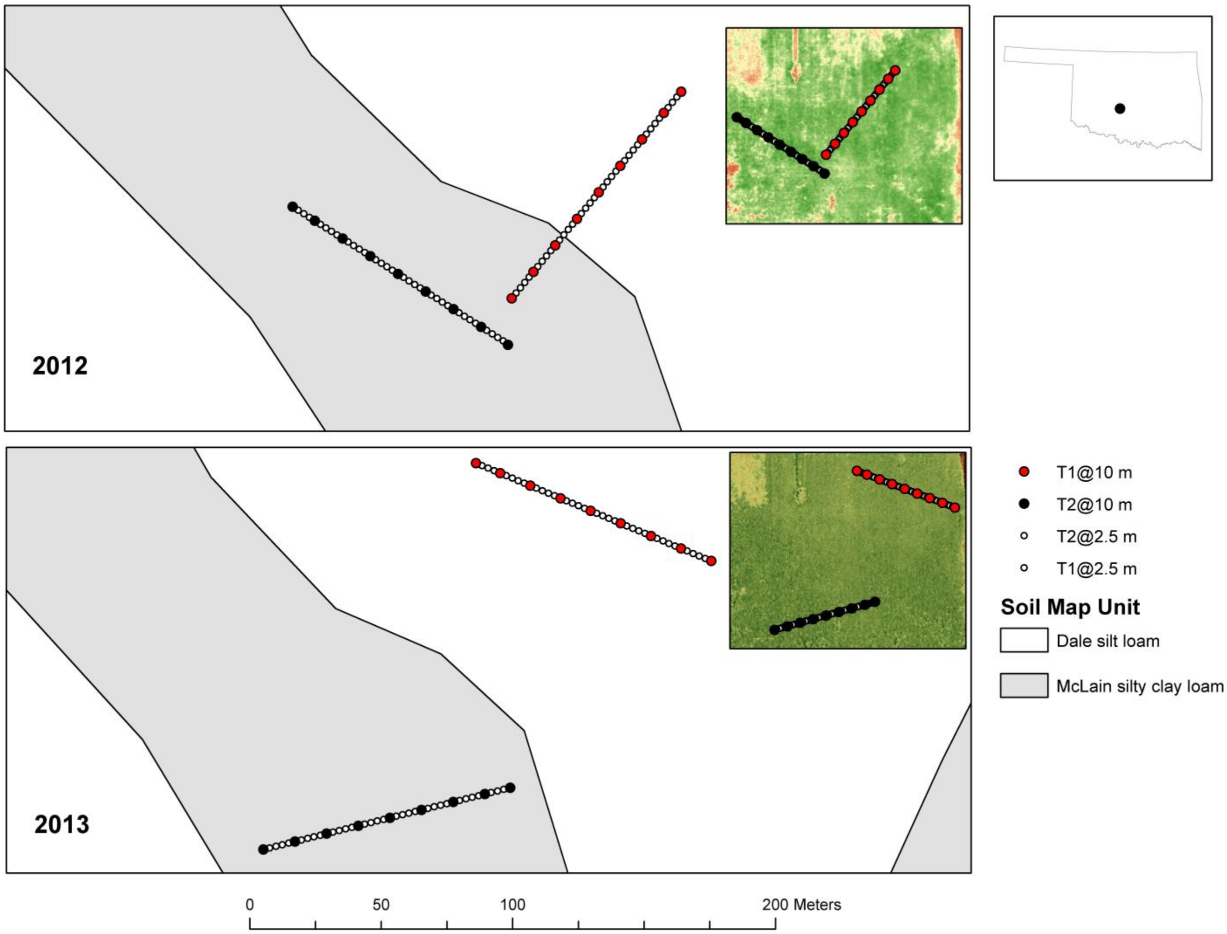

Figure 6.1. Site map with location of sampling transects in relation to soil map units for the 2012 and 2013 growing seasons. Transect 1 (T1) was located on a Dale silt loam (Fine-silty, mixed, superactive, thermic Pachic Haplustolls) and transect 2 (T2) on a McLain silty clay loam (Fine, mixed, superactive, thermic Pachic Argiustolls). Sample data was collected at points 2.5 m apart (fine scale) and 10 m apart (coarse scale).

CHAPTER VII

GENERAL CONCLUSIONS

High biomass yield, acceptable quality and reliable supply of feedstock material are three important components for the success of a bioenergy industry. However, for profitability of the industry production cost need to be low. Bioenergy crop production systems and nitrogen management was the central focus of this project. Nitrogen is one of the major players in limiting biomass yield , as well as nitrogen concentration in the biomass can affect the efficiency of the biomass conversion into biofuel. Evaluating nitrogen management on biomass yield and quality was the ultimate goal of this project. Remote sensing technique which has shown potential in crop management for number of years was employed as a major tool for monitoring crop N status, predicting biomass yield and N concentration within the plant and biomass material and describing the spatial variability of biomass yield within a switchgrass field.

In terms of high biomass yield, minimal amount of N fertilizer < 84 kg ha-1 was required to produce maximum biomass yield. The amount of biomass produced was directly related to the amount of rainfall received. For example, Woodward reached less rainfall than Stillwater and consistently produced less biomass yield and above normal rainfall in 2013 result in high biomass yield at both locations. Several researchers across the USA have already concluded that rainfall is the major driver for biomass yield. Crop species have different yield potential and is also important in the puzzle of achieving high biomass yield. High biomass sorghum produced significantly higher biomass yield (24Mg ha-1) than the perennial grass systems of monoculture switchgrass (13 Mg ha-1) and switchgrass within a mixture (16 Mg ha-1) under normal condition with adequate rainfall at Stillwater. At Woodward in 2013, no yield was available for the high biomass sorghum due to severe lodging, but switchgrass (7 Mg ha-1) and mixed grass (7 Mg ha-1) yields were about 50% lower than that of Stillwater. High biomass sorghum also failed in Woodward in 2011 and 2012 due to dry condition during the growing season. In Stillwater, high biomass sorghum produced yields similar to the perennial grasses during the dry period of 2011 and 2012. Clearly, high biomass sorghum has the potential to produce high yields, while the perennial grasses are a more reliable source of biomass yield that has a wider adaptability to extreme conditions.

Biomass yield of the high biomass sorghum and the perennial grasses could be successfully predicted using canopy spectral reflectance collected in the months of June and July. However, identification of the optimal wavebands that are more strongly related to the biomass in the different species could significantly improve prediction models. The use of partial least square regression (PLSR) models that make use of the entire spectra also improve biomass estimation significantly over the use of the best narrowband indices, but the narrowband indices were more stable and reliable in estimating biomass across growing seasons. The most useful prediction model can be achieved by identifying the optimal wavebands that is strongly related to the biomass yield of the specific crop.

Nitrogen concentration in biomass is critical with regards to the crop productivity, but can also affect the efficiency of the conversion process into biofuel. While high N concentration (>3%) is desirable for the enzymatic conversion process, low N (< 3%) is more suitable for the thermochemical conversion process. Biomass quality (hemicellulose, cellulose, and lignin) was affected by the species, but not N management and environmental condition. High biomass sorghum had lower hemicellulose, cellulose and lignin than the perennial grasses. These components also showed little variation (< 10%) across the years and locations. The greatest variation occurred in the extreme dry condition of 2011. Nitrogen concentration as expected was influenced by N application, as application of N increased N concentration compared to unfertilized. However, increasing N application rate beyond the 84 kg ha-1 did not significantly increase N concentration in the biomass. Most importantly, N concentration at final harvest was below 3% throughout the entirety of this study, indicating that these feedstock materials can be efficiently converted into biofuel by the thermochemical conversion process with minimal environmental concern.

Simple ratios R2080 /R2190 for TN and R2190/R2230 for ADF, NDF and ADL were similar to the full spectra calibration in estimating the feedstock composition in grounded samples. Likewise at canopy level NNVI computed with R400 and R510 for high biomass sorghum and R1500 and R2260 for perennial grasses were similar to the full spectra calibration in estimating N concentration. Therefore, identification of the optimal wavebands is essential in developing vegetation indices and simple ratios for estimating of biochemical components within a plant. These results suggested that the full spectra do not provide more information, because only a few of the wavebands are actually useful as the majority is redundant. This study has identified optimal wavebands that are strongly associated with estimating N concentration and biomass yield in high biomass sorghum and perennial grass systems of monoculture switchgrass and mixed grasses. The results of this study agree with other researchers that the focus should be on the design of optimal sensors for specific application rather than having a continuous spectral coverage. Knowledge of these optimal wavebands can save time and resources in future studies of these cropping systems.

VITA

Anserd Julius Foster

Candidate for the Degree of

Doctor of Philosophy

Thesis: REMOTE SENSING APPLICATION IN BIOMASS CROP PRODUCTION SYSTEMS IN OKLAHOMA

Major Field: Crop Science

Biographical:

Education:

Completed the requirements for the Doctor of Philosophy in Crop Science at Oklahoma State University, Stillwater, Oklahoma in December, 2013.Completed the requirements for the Master of Science in Agronomy at Louisiana State University, Baton Rouge, Louisiana, USA in 2003. Completed the requirements for the Bachelor of Science in Environmental Management Systems at Louisiana State University, Baton Rouge, Louisiana, USA in 2002.

Experience:

- Graduate Research Assistant, Department of Plant Sciences
  Oklahoma State University, Stillwater, Oklahoma 2010- 2013
- Graduate Research Assistant, Department of Plant Sciences
  Mississippi State University, Starkville, Mississippi 2005- 2009
- Graduate Research Assistant, School of Plant, Environmental and Soil Science
  Louisiana State University, Baton Rouge, Louisiana 2002- 2003
- Regional Agronomy Specialist, University of Missouri Extension
  Columbia, Missouri 2004-2005

Professional Memberships:

- Member- The American Association for the Advancement of Science 2012
- Member-Soil and Water Conservation Society 2006
- Member-ASA-CSSA-SSSA 2003
- Member-Gamma Sigma Delta Honor Society of Agriculture 2001
- Member-Golden key Honor Society 2001